PALAIOS
Emphasizing the impact of life on Earth's history

PALAIOS, 2019, v. 34, 542–561
Research Article
DOI: http://dx.doi.org/10.2110/palo.2019.019

TESTING THE *DAPTOCEPHALUS* AND *LYSTROSAURUS* ASSEMBLAGE ZONES IN A LITHOSTRATOGRAPHIC, MAGNETOSTRATIGRAPHIC, AND PALYNOLOGICAL FRAMEWORK IN THE FREE STATE, SOUTH AFRICA

ROBERT A. GASTALDO,[1] JOHANN NEVELING,[2] JOHN W. GEISSMAN,[3] AND CINDY V. LOOY[4]
[1]*Department of Geology, Colby College, Waterville, Maine 04901 USA*
[2]*Council for Geosciences, Private Bag x112, Silverton, Pretoria, South Africa 0001*
[3]*The University of Texas at Dallas, Richardson, Texas 75080-3021 USA*
[4]*Department of Integrative Biology, Museum of Paleontology, University and Jepson Herbaria, University of California–Berkeley, 3060 Valley Life Sciences Building #3140, Berkeley, California 94720-3140 USA*
email: robert.gastaldo@colby.edu

ABSTRACT: **The vertebrate-fossil record in the Karoo Basin has served as the accepted model for how terrestrial ecosystems responded to the end-Permian extinction event. A database of several hundred specimens, placed into generalized stratigraphies, has formed the basis of a step-wise extinction scenario interpreted by other workers as spanning the upper *Daptocephalus* (=*Dicynodon*) to *Lystrosaurus* Assemblage Zones (AZ). Seventy-three percent of specimens used to construct the published model originate from three farms in the Free State: Bethel, Heldenmoed, and Donald 207 (Fairydale). The current contribution empirically tests: (1) the stratigraphic resolution of the vertebrate record on these farms; (2) whether a sharp boundary exists that delimits the vertebrate assemblage zones in these classic localities; and (3) if the *Lystrosaurus* AZ is of early Triassic age. We have used a multi-disciplinary approach, combining lithostratigraphy, magnetostratigraphy, vertebrate biostratigraphy, and palynology, to test these long-held assumptions.**

Previously reported vertebrate-collection sites have been physically placed into a litho- and magnetostratigraphic framework on the Bethel and Heldenmoed farms. The reported assemblage-zone boundary is used as the datum against which the stratigraphic position of vertebrates is compared and a preliminary magnetostratigraphy constructed. We find specimens of the *Daptocephalus* AZ originate in the *Lystrosaurus* AZ (as currently defined) and vice versa, and discrepancies between reported and field-checked stratigraphic positions below or above the assemblage-zone boundary often exceed 30 m. Hence, the utility of the data set in defining a sharp or abrupt biozone boundary is questionable. We further demonstrate the presence of a stratigraphically thick reverse polarity magnetozone that encompasses the reported assemblage-zone boundary, implying that these rocks are not correlative with the end-Permian event, which is reported to lie in a normal polarity chron. A latest Permian age is supported by palynological data from the *Lystrosaurus* AZ on the Donald 207 (Fairydale) farm, with equivalence to Australian (APP602) and Eastern Cape Province assemblages. We conclude that the turnover from the *Daptocephalus* to *Lystrosaurus* Assemblage Zones is more protracted than envisioned, it is not coincident with the end-Permian event as recognized in the marine realm, and little evidence exists in support of a three-phased extinction model based on vertebrate assemblages in the Karoo Basin.

INTRODUCTION

Turnover in the terrestrial fossil record from the *Daptocephalus* to *Lystrosaurus* Assemblage Zones in the Karoo Basin, South Africa, continues to be equated by many workers to the end-Permian extinction event (Ward et al. 2005; Smith and Botha-Brink 2014; Rubidge et al. 2016; Viglietti et al. 2016, 2018; MacLeod et al. 2017). This continental extinction model, which has been applied globally (Benton and Newell 2014), is based on vertebrate biostratigraphic trends placed in a generalized lithostratigraphic and environmental context from a limited number of localities in the basin (Smith and Botha-Brink 2014; Viglietti et al. 2016, 2018). The vertebrate biostratigraphy is reported to be augmented by both a magnetostratigraphic (DeKock and Kirschvink 2004; Ward et al. 2005) and a chemostratigraphic (MacLeod et al. 2000, 2017; Ward et al. 2005) record which, in combination, have been used as the basis for correlation with the end-Permian marine event at the Meishan section, Zhejiang Province, South China (Shen et al. 2011). All four independent data sets in the Karoo Basin, however, are not without their limitations.

Limitations of Previous Studies

The fully continental succession in the Karoo Basin begins with deposition of the Beaufort Group, following deglaciation of the Gondwanan continent in the Middle Permian (Johnson et al. 2006; Fig. 1). These landscapes are characterized by sandstone channels of various fluvial architectures (Wilson et al. 2014) draining provenance areas in the Cape Fold Belt, located to the east-southeast. Fine- to very fine siliciclastic sediments were deposited in bedload barforms, abandoned channels, and overbank fines, wherein interfluvial areas were colonized by a glossopterid-dominated flora (Gastaldo et al. 2005, 2014; Prevec et al. 2010). Various workers identify both a change in fluvial architecture and siltstone color in

Published Online: November 2019
 0883-1351/19/034-542

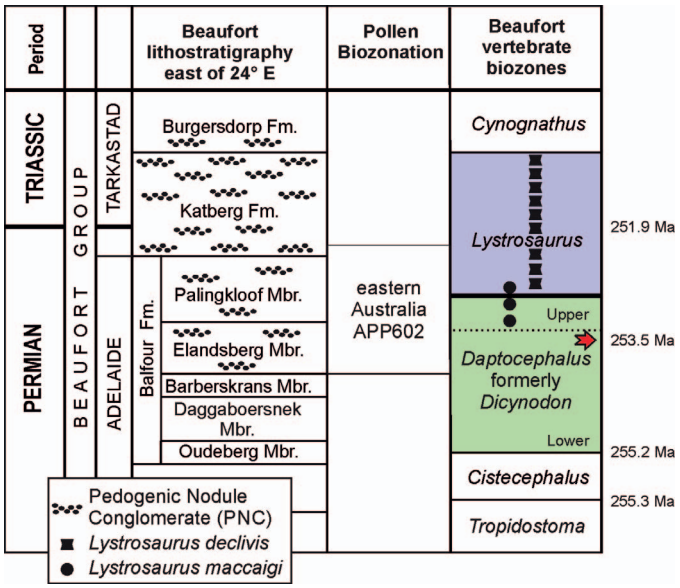

FIG. 1.—Litho- and vertebrate bio-stratigraphy of the Beaufort Group in the Karoo Basin, South Africa. Biostratigraphic ranges of *L. mccaigi* and *L. murrayi* follow Botha and Smith (2007), which are used by Viglietti et al. (2016) to delimit the Upper *Daptocephalus* Assemblage Zone (in green) from the overlying *Lystrosaurus* Assemblage Zone (in purple). The biozone boundary is considered by many workers (e.g., Ward et al. 2005; Smith and Botha-Brink 2014; Rubidge et al. 2016) as coincident with the Permian–Triassic Boundary (PTB) as recognized in the marine record. The placement of the PTB in the Katberg Formation follows the conclusions of Gastaldo et al. (2015, 2018) based on a U-Pb ID-TIMS age date of 253.48 ± 0.15 in the Elandsberg Member of the Balfour Formation (red arrow). Dates for the boundaries between the *Tropidostoma* and *Cistecephalus* AZs come from Rubidge et al. (2013); the boundary date for the Permian–Triassic is from Burgess et al. (2014). The assignment of palynological assemblages in the *Daptocephalus* and *Lystrosaurus* Assemblage Zones to the eastern Australian APP602 palynological zone of late Changhsingian age is based on Prevec et al. (2010), Gastaldo et al. (2015, 2017), and data from the current study.

the rocks of the Balfour Formation, in which they have placed the vertebrate-defined Permian–Triassic boundary (PTB; Smith 1995; Ward et al. 2000; Smith and Ward 2001; Smith and Botha-Brink 2014; Botha-Brink et al. 2014). River systems are reported to have shifted from meandering to low-sinuosity to braided channel architectures over a very short stratigraphic distance as a consequence of an aridification trend. This trend is interpreted based on: (1) a reported absence of lacustrine deposits in the uppermost exposures of the Ripplemead (recently proposed), Elandsberg, and Palingkloof members of the Balfour Formation (Upper *Daptocephalus* Assemblage Zone; Viglietti et al. 2018), and (2) a change in siltstone color (Smith and Ward 2001) which, more recently, has been interpreted as wind-blown contribution of oxidized silt (Smith and Botha-Brink 2014). Smith and Botha-Brink (2014) and other workers state that gray mudrock, illustrated as green and described as olive (Ward et al. 2000; Smith and Botha 2005; Botha and Smith 2006) to dark gray (5Y4/1 [olive gray, Goddard et al. 1975]; Smith and Botha 2005; Botha and Smith 2006), transitions to mottled maroon/gray mudrock, which is overlain by laminated pale-gray and reddish-brown mudrock couplets marking the vertebrate-biozone boundary. Siltstone in the overlying strata is reported to be rubified and appearing "maroon" (Ward et al. 2000; Smith and Ward 2001) to red (2.5YR4/6; Smith and Botha 2005; Botha and Smith 2006), and dominating the succession. That color changeover is attributed to aridification, irrespective of whether of pedogenic or loessic origin (Smith 1995; Smith and Ward 2001; Smith and Botha 2005; Smith and Botha-Brink 2014). Yet, geochemical data from greenish-and-reddish gray siltstone from this interval indicate that no significant differences exist between these lithologies, and there is no evidence for either an aridification trend (Li et al. 2017) or the presence of playa lake deposits (Gastaldo et al. 2019). Similarly, empirical observations have demonstrated that greenish-gray siltstone is a lateral facies equivalent of reddish-gray siltstone at numerous stratigraphic positions in these sections, negating a proposed eolian origin for the color change (Neveling et al. 2016a, 2016b; Gastaldo et al. 2017, 2018, 2019).

Limitations also exist with respect to the published magnetostratigraphy and chemostratigraphy for the Karoo succession. Gastaldo et al. (2015, 2018) published a high-resolution magnetostratigraphy from Old Lootsberg Pass (= West Lootsberg; Ward et al. 2005), constrained by an early Changhsingian U-Pb ID-TIMS age of 253.48 ± 0.15 Ma, where they were unable to duplicate the previously published polarity record for that locality. Here, three long normal polarity chrons, two of which are punctuated by reverse polarity chrons of short stratigraphic duration, represent hiatuses in the stratigraphic section as a consequence of landscape degradation and erosion (Gastaldo and Demko 2011; Gastaldo et al. 2018). Gastaldo et al. (2015, 2018) conclude that the observed magnetic polarity stratigraphy is more compatible with that of the early Changhsingian, as it is recorded elsewhere during the same chronostratigraphic succession, and conforms to the U-Pb ID-TIMS age assignment.

The published chemostratigraphy in support of the traditional model used two different stable-isotope proxies: $\delta^{13}C$ and $\delta^{18}O$ derived from carbonate-cemented concretions and vertebrate tusks (MacLeod et al. 2000, 2017; Ward et al. 2005). No trend was recognized in $\delta^{18}O$ values from concretions. The trends reported for $\delta^{13}C$ analyses originated from paleosol concretions where carbonate cements precipitated under a closed system, in response to methanogenesis (Tabor et al. 2007; DeWit 2016), rather than from calcite precipitated under an open system where the soil was in equilibrium with atmospheric CO_2 (Gastaldo et al. 2014). Hence, MacLeod et al.'s (2000) $\delta^{13}C$ stratigraphic pattern of carbonate nodule data is incompatible with other latest Permian trends, and cannot be used for correlative purposes. Recently, MacLeod et al. (2017) republished their earlier $\delta^{18}O$ stable-isotope data derived from therapsid tusks (MacLeod et al. 2000) and concluded that a trend of increasing and marked aridity occurred over the vertebrate-defined PTB (see Gastaldo et al. 2017 and below about the reliability of the vertebrate biostratigraphy). That boundary was, and continues to be, identified on the position of a reported biostratigraphic sharp turnover from the *Daptocephalus* (previously *Dicynodon*; Viglietti et al. 2016; but see Lucas 2017, 2018) to *Lystrosaurus* Assemblage Zone taxa (AZ; Fig. 1; although see Viglietti et al. 2018). That turnover is reported to be coupled with the presence of a lithostratigraphic "event" bed (Smith and Botha-Brink 2014; Botha-Brink et al. 2014; Day et al. 2015; Viglietti et al. 2016, 2018) of purported playa-lake origin (but see Gastaldo et al. 2019). Ward et al. (2012) acknowledge that the heterolithic, laminated horizon, reported to be a discrete mappable unit by Smith and Botha-Brink (2014), can be found at several different stratigraphic positions in the upper Balfour Formation, negating its utility as recognized by our previous studies (Gastaldo et al. 2009; Gastaldo and Neveling 2012, 2016).

The vertebrate-turnover and vertebrate-extinction event are identified by both Smith and Botha-Brink (2014, p. 100) and Viglietti et al. (2016, p. 4) on a data set that was reported by the authors to be more accurate in the locality and stratigraphic position of vertebrate fossils than locality data found in older literature. The GPS coordinates of specimens in the Smith and Botha-Brink (2014) database were used to position individuals on generalized measured sections from which reportedly reliable Lowest Occurrence (LO) and Highest Occurrence (HO; in some cases also interpreted at the Last Appearance Datum) are determined. As a consequence, it should be possible to assess the stratigraphic distance of any vertebrate fossil relative to the biozone (= PTB) boundary (Smith and Botha-Brink 2014, their supplemental data table) in localities or exposures

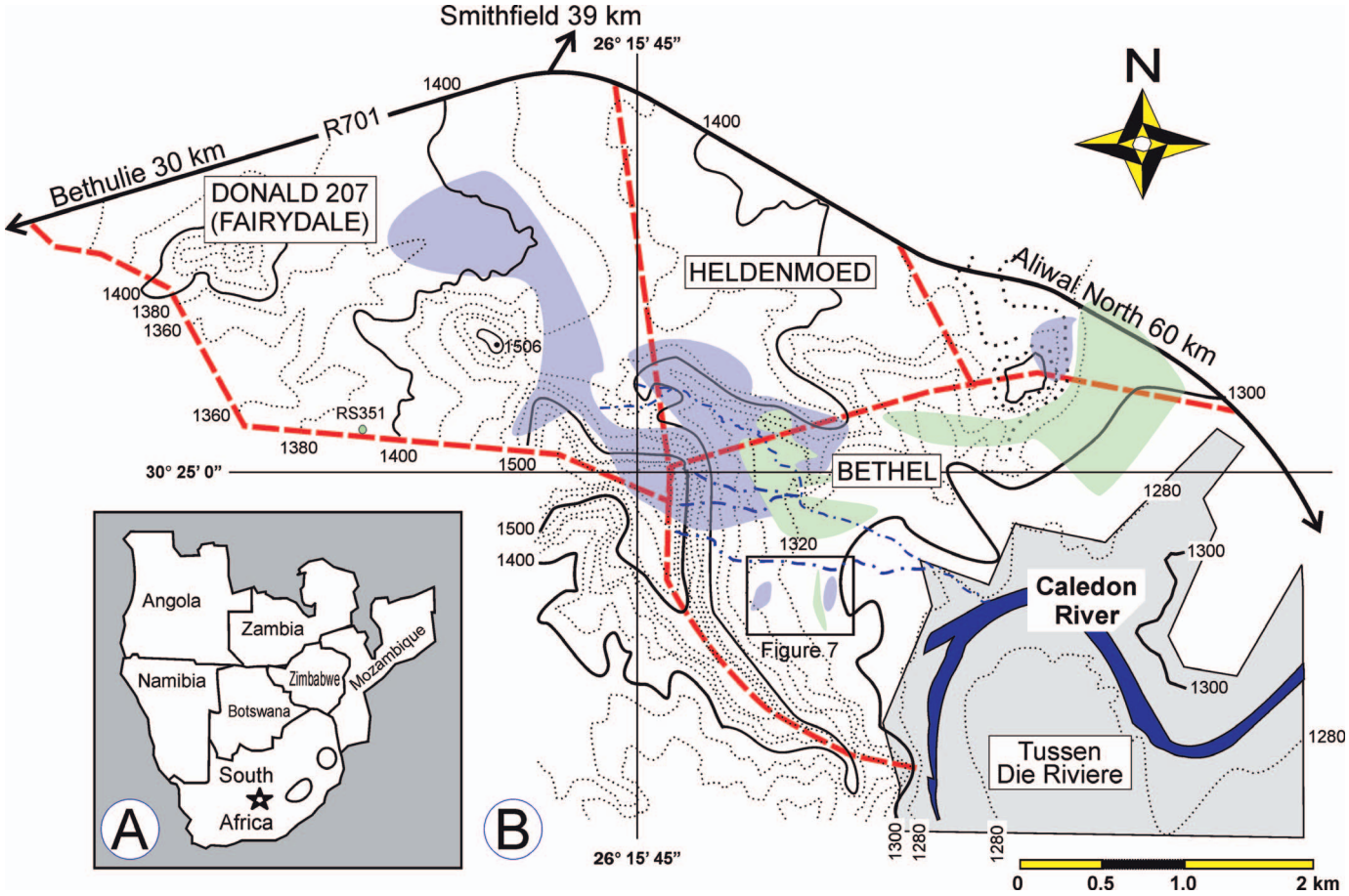

FIG. 2.—Locality maps. **A**) Generalized map of southern Africa on which the Bethel farm is located with a star. **B**) Map showing the geographic relationship between the Bethel, Heldenmoed and Donald 207 (Fairydale) farms relative to the R701 roadway. Areas in light green bound collection sites from which *Daptocephalus* (*Dicynodon*) Assemblage Zone specimens were collected; areas in light purple bound collection sites from which *Lystrosaurus* Assemblage Zone specimens were collected, both as reported by Smith and Botha-Brink (2014). Black box outlines geographic position of vertebrate sites in Figure 7. Contour intervals in 20 m, and scale in kilometers. Note discrepancies in the elevational differences in specimens reported from each assemblage zone.

where the lateral stratigraphic relationships are well understood. Using this data set, Smith and Botha-Brink (2014, fig. 12) proposed a three-phased extinction pattern, followed by a rapid recovery phase over a short stratigraphic distance of 60 m. This pattern spans part of the Elandsberg and Palingkloof members of the Balfour Formation and the lower part of the Katberg Formation. Using the same data set, augmented by the vertebrate database curated at the Evolutionary Science Institute, Viglietti et al. (2016) subdivided the *Daptocephalus* AZ into a lower and upper part, where the latter is defined by the LAD of the genus *Dicynodon* and the FAD of *Lystrosaurus maccaigi* (Fig. 1). Yet, when this biozone boundary model was tested with Smith and Botha-Brink's (2014) raw-data set at Old Lootsberg Pass, Gastaldo et al. (2017) were unable to replicate or identify a single stratigraphic horizon at which the vertebrate data converged to pinpoint the turnover. It was not possible to identify any vertebrate-biozone boundary because the raw data revealed four different stratigraphic positions, spanning a stratigraphic distance of nearly 75 m, at which the biozone boundary could be drawn as defined in the literature. It was concluded (Gastaldo et al. 2017) that the empirical field test raised serious questions about the reliability of the expanded Smith and Botha-Brink (2014) data set used to support what many have, over several decades in various iterations, considered to be the terrestrial response to the end-Permian extinction event (Smith 1995; Ward et al. 2000, 2005; Smith and Ward 2001; Smith and Botha 2005; Botha and Smith 2006; Botha-Brink et al. 2014; Rubidge et al. 2016; Rey et al. 2016; Viglietti et al. 2016, 2018). Yet, the total number of vertebrate specimens reported by Smith and Botha-Brink (2014) from the Blaauwater farm at Old Lootsberg Pass, Eastern Cape Province, is limited (N = 14) when compared with other biozone-boundary localities, such as in those in the Free State Province.

Present Study

The localities in the Free State Province from which vertebrates assigned to either the *Daptocephalus* (*Dicynodon*) or *Lystrosaurus* AZs include Bethel and Heldenmoed farms (Fig. 2; Smith 1995; Ward et al. 2000, 2005; Smith and Botha-Brink 2014), Fairydale farm (Donald 207 farm, Fig. 3; Abdala et al. 2006; Botha and Smith 2006, 2007; Smith and Botha-Brink 2014), Tussen Die Riviere (Retallack et al. 2003; Smith and Botha-Brink 2014), and Nooitgedacht (Botha-Brink et al. 2014). In fact, 73% of the specimens used in the published database as the basis for the extinction-and-recovery model originate from Bethel and Heldenmoed (N = 120), and Fairydale (N = 139) farms (Smith and Botha-Brink 2014), whereas an additional 13% (N = 46) originate from Tussen Die Riviere. Hence, 86% of specimens on which the model is based originate from this area.

Concerns have been raised about the quality of the vertebrate data set used to interpret both extinction and turnover in the Karoo stratigraphic record by several workers (Marshall 2005; Lucas 2009, 2017; Gastaldo et al. 2017, 2018). It was Marshall (2005, p. 1413b) who noted that the

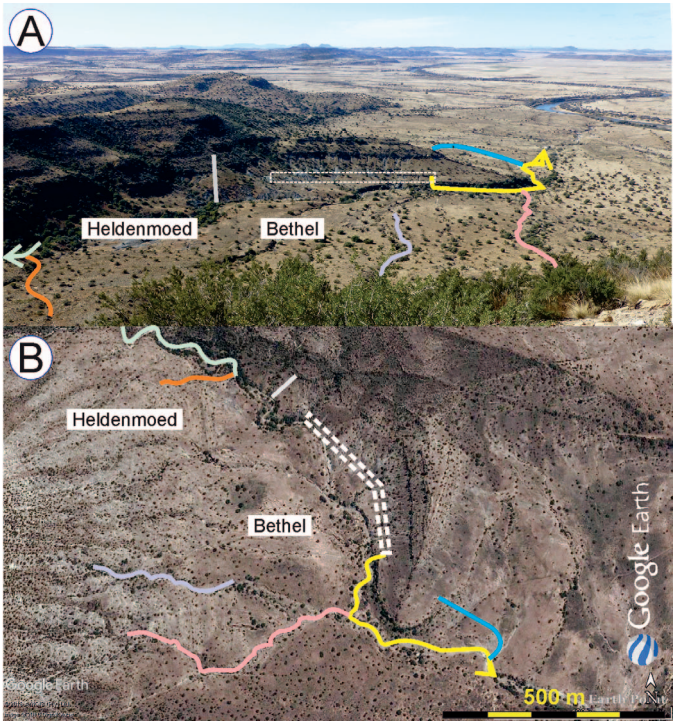

FIG. 3.—Images of the Heldenmoed and Bethel farms on which measured stratigraphic sections used in the current study are shown. **A**) Oblique overview of "Bethulie Valley" taken from the mountain to the west (see Fig. 2), showing the general landscape and erosional gullies in which stratigraphic sections were measured (see Fig. 5). **B**) Orthogonal GoogleEarth image on which measured stratigraphic sections are placed. The white-dashed polygon represents the stratigraphic position of Smith and Botha-Brink's (2014) proposed assemblage-zone boundary. Details of this interval can be found in Gastaldo et al. (2019).

"…accuracy of the relative positions of the fossil horizons depicted in the composite section…" ultimately would control the validity of the paleontological patterns in the basin, and whether a continental extinction event is recorded in these rocks. Hence, this current contribution provides an empirical test (similar to that of Gastaldo et al. [2017] at Old Lootsberg Pass) to evaluate the vertebrate patterns in the Free State localities of Bethel, Heldenmoed, and Fairydale farms where a correlative stratigraphic framework is constructed into which vertebrate collection sites can be placed. We are unable to place vertebrates from Tussen Die Riviere Nature Reserve into a stratigraphic framework because many of these originated from pavement outcrop in a low-relief terrain where it is not possible to measure and correlate stratigraphic sections using traceable sandstone bodies. To date, unlike the study at Old Lootsberg Pass, we have been unable to recognize any silicified volcanic ash-fall or reworked deposit (Gastaldo et al. 2017, 2018), or devitrified claystone (Gastaldo et al. 2014), from which a numerical age estimate could be obtained to provide a constraint on either vertebrate biozone in the Bethel-farm area. As such, we will necessarily rely on the magnetostratigraphic and palynologic record of this succession, as first reported in Neveling et al. (2016a), compared with that published for Old Lootsberg Pass (Gastaldo et al. 2015, 2018), for some temporal context.

KAROO BASIN GENERAL LITHO- AND BIOSTRATIGRAPHY

The Karoo Basin formed ahead of the rising Cape Fold Belt (Lindeque et al. 2011; Viglietti et al. 2017), and the basin began to fill after continental deglaciation in the Late Carboniferous (Johnson et al. 2006). This succession, known as the Karoo Supergroup, comprises the basal Dwyka (Upper Carboniferous) and Ecca (Lower–Middle Permian) groups, the Beaufort (Middle Permian–Middle Triassic) and Stormberg (Upper Triassic–Lower Jurassic; Catuneau et al. 2005) groups, and culminates in the basaltic lavas of the Drakensberg Group (Lower Jurassic). Dwyka and Ecca diamictite and turbidite deposits, respectively, filled a deep basin open to marine influence, whereas all subsequent sedimentation occurred exclusively in a closed interior continental setting. The Beaufort Group is subdivided into the lower Adelaide and upper Tarkastad subgroups (Fig. 1). The Balfour Formation is assigned to the Upper Permian to Lower Triassic and the Katberg Formation to the Lower Triassic by the South African Committee for Stratigraphy (1980; Johnson et al. 2006) based on vertebrate biostratigraphy. The discovery of a vertebrate skull of Permian systematic affinity led Gastaldo et al. (2017) to move the biozone boundary into the Katberg Formation (Fig. 1).

Six basic lithologies can be described in the upper Balfour Formation as being vertically and laterally arranged in a seemingly monotonous succession (Gastaldo et al. 2018). Fluvial bedload deposits are comprised of fine- to very-fine grained, yellowish-gray wacke that are enveloped in coarse-to-fine siltstone. Siltstone varies in color from greenish, olive, or light-olive gray to reddish gray (Li et al. 2017; Gastaldo et al. 2018, 2019). Very rarely are: (1) fine-to-medium grained sandstone; (2) very light gray to white silicified (porcellanite) siltstone; (3) light-gray to olive-gray devitrified claystone; and (4) intraformational conglomerate encountered (Gastaldo et al. 2018). The intraformational conglomerate is the coarsest lithology consisting of calcite-cemented pedogenic glaebules/nodules, disarticulated vertebrates (skull and bone, or fragments, thereof), and mud-clast aggregates as framework grains in either a fine/very fine sand, sandy silt, or coarse silt matrix (Pace et al. 2009; Gastaldo et al. 2013). Long associated with the Katberg Formation (Visser and Dukas 1979), this latter lithofacies was considered at one stage to be a diagnostic character of the *Lystrosaurus* AZ (Smith and Botha 2005; Smith and Botha-Brink 2014). More recently, it is shown to be a component of sandstone bodies in the Elandsberg Member of the Balfour Formation at least 100 m below the base of the Katberg Formation (Fig. 1; Viglietti et al. 2017; Gastaldo et al. 2018). Traditionally, lithostratigraphic units in this part of the section have been delimited on the appearance of a change in character including siltstone color (e.g., reddish-gray and/or mottling of this color with greenish-gray) or a perceived increase of sandstone relative to siltstone (South African Committee for Stratigraphy 1980). Greenish-gray siltstone has been demonstrated empirically to be a lateral facies equivalent of reddish-gray siltstone in these rocks (Neveling et al. 2016a, 2016b; Li et al. 2017; Gastaldo et al. 2017, 2018, 2019), reducing the utility of this criterion. Similarly, changes in the sandstone:siltstone ratio up section appear to be more of a function as to where sections were measured and described along roadcuts ascending escarpments. The limited variation of Beaufort Group lithologies required a means by which to subdivide the succession into quasi-chronostratigraphic units. The paucity of fossil plants (macrofossils and palynomorphs; Gastaldo et al. 2005) and the abundance of vertebrate skeletons and skeletal elements (Rubidge 1995) allowed for age assignments to be placed on the strata following the early assumptions of Broom (1906, 1911) on vertebrate biostratigraphy.

In the early part of the twentieth century, Broom (1906) was the first to establish a six-part biostratigraphic subdivision of the Karoo Basin rocks using fossil-vertebrate assemblages. He placed specimens of *Lystrosaurus* into the Triassic, and the underlying biozones, including the interval now encompassing the *Daptocephalus* AZ (Viglietti et al. 2016), into the Late Permian. Broom (1907, 1909, 1911) reinforced these age assignments over the next several years, although the logic and reasoning are unstated and may have reflected the prevailing assumption at the time. This six-fold biozonation was the standard for nearly 75 years until revisions by Kitching (1971, 1977) were published, with subsequent modification by Keyser and Smith (1978). The biostratigraphic systems of Keyser and Smith (1978) and Keyser (1979) were accepted by the South African

Committee for Stratigraphy (1980) as formal nomenclature. After a comprehensive revision in the 1990s, Rubidge (1995) provided diagnostic criteria for the recognition of vertebrate-assemblage zones, and also added a new biozone at the base of the Beaufort Group.

Broom's Permian age for the *Daptocephalus* AZ continued to be accepted for more than a century, based on strong biostratigraphic correlation of the underlying *Cistecephalus* AZ (Smith and Kitching 1995) with better-dated sequences in India (Kutty 1972), South America (Keyser 1981), and Russia (Boonstra 1969). Its age was confirmed by geochronometric data earlier this century. Rubidge et al. (2013) were the first to publish Guadalupian to Lopingian U-Pb ID-TIMS age estimates for the lower part of the Adelaide Subgroup (Fig. 1). These were supplemented by age estimates of the Teekloof Formation by Day et al. (2015). Subsequently, the first high resolution U-Pb ID-TIMS ages on zircons from two horizons in the upper part of the Balfour Formation were reported, and placed in a tightly constrained litho- and magnetostratigraphic framework at Old Lootsberg Pass (Gastaldo et al. 2015, 2018). One horizon, interpreted as a synsedimentary ashfall accumulation (Gastaldo et al. 2015, 2018), is positioned ~60 m below the purported biozone boundary identified by Smith and Botha-Brink (2014), and has yielded an early Changhsingian age (253.48 ± 0.15 Ma; Gastaldo et al. 2015). The second horizon is a well-silicified siltstone-trough fill, probably in the Elandsberg Member, although possibly in the lower Palingkloof Member, ~40 m below the biozone boundary of Smith and Botha-Brink (2014). This deposit yields a detrital zircon population of Wuchiapingian age (256.8 ± 0.6 Ma; Gastaldo et al. 2018), indicating reworking of an older ashfall deposit in response to landscape degradation (Gastaldo and Demko 2011) and redeposition into a younger landform. The question remained as to whether the base of the *Lystrosaurus* AZ, as circumscribed by the LAD of *L. maccaigi* below and the FAD of *L. declivis* and *L. murrayi* (Botha and Smith 2007; Fig. 1) above a reportedly distinctive and mappable bed (Smith and Botha-Brink 2014 and others; but see Gastaldo et al. 2009, 2018), was earliest Triassic in age (<251.9 Ma; e.g., Rey et al. 2016; Viglietti et al. 2017, 2018; MacLeod et al. 2017).

The Triassic age assignment of the *Lystrosaurus* AZ is not universally accepted. For example, Lucas (2009) noted that neither the $\delta^{13}C$ chemostratigraphic nor the magnetostratigraphic trends reported across *Daptocephalus* and *Lystrosaurus* AZ rocks in the Karoo Basin (MacLeod et al. 2000; DeKock and Kirschvink 2004; Ward et al. 2005) conform to the trend reported in the marine record. Lucas (2009) concluded that the biozone boundary predated the end-Permian extinction event, and indicated that the *Lystrosaurus* zone could be subdivided into three stages of his Lootsbergian Land-Vertebrate Faunachron (Lucas 2010). Assemblages in which both *Lystrosaurus* and *Dicynodon* (=*Daptocephalus*; see systematic discussion in Lucas 2009, 2017) co-occur are considered indicative of a Permian-aged cohort. In contrast, a Triassic age assignment is ascribed to assemblages where *Lystrosaurus* and *Procolophon*, in the absence of *Dicynodon*, are found (Lucas 2010). More recently, Lucas (2017, 2018) placed the lowest appearance of *Lystrosaurus* in the early Changhsingian, decoupling the Permian–Triassic Boundary from his Platbergian–Lootsbergian boundary, and continued the taxon's range into the Triassic. Using a combination of paleontologic, geochronometric, and magnetostratigraphic data, Gastaldo et al. (2015, 2017, 2018, 2019) and Neveling et al. (2016a, 2016b) challenged the Triassic-age assignment of the lowermost part of the *Lystrosaurus* AZ. They suggested that Lopingian rocks extend into the Katberg Formation of the Tarkastad subgroup (Fig. 1).

LOCALITIES AND METHODS

The Bethel, Heldenmoed, and Fairydale localities are located on adjacent farm properties in the Free State Province (Figs. 2–4), 30 kilometers to the east of the town of Bethulie, South Africa. There is little topographic relief where the Bethel farm lies next to the Caledon River and Tussen-die-Riviere Nature Reserve, with the area gaining in elevation westward, within 2 kilometers of the river, to a small valley between escarpments (Figs. 2, 3; see Smith and Botha-Brink 2014, fig. 4). Exposures on the Heldenmoed farm are along the northern slopes of the valley's walls. Elevations across these two farms range from 1243 m at the edge of the Caledon River (S30.4275°, E26.27950°; 13 June 2015 WP176, Garmin 62S GPS with barometric altimeter) to 1580 m atop the exposure of Katberg Formation (elevation recorded from drone data and beacon benchmark [1584 m]). *Dicynodon* AZ taxa (Fig. 2, green pattern) are reported as having been collected at lower elevations (Smith and Botha-Brink 2014; raw data, see below), whereas *Lystrosaurus* AZ taxa are reported from higher elevations up to an altitude of 1420 m and 1520 m on the eastern and western slopes, respectively (Fig. 2, purple pattern). Smith and Botha-Brink (2014) report 120 vertebrate fossils as part of their data set from these farms including *Dicynodon* (=*Daptocephalus*; N = 12), *Lystrosaurus* (N = 86), *Moschorhiinus* (N = 4), *Prolacerta* (N = 2), *Tetracynodon* (N = 2), *Dicynodontoides* (N = 1), *Micropholis* (N = 1), *Promoschorhynus* (N = 1), *Regiasaurus* (N = 1), *Scaloposaurus* (N = 1), and *Thrinaxodon* (N = 1). The proposed boundary between the *Daptocephalus (Dicynodon)* and *Lystrosaurus* AZs (Smith and Botha-Brink 2014, fig. 5) is placed at ~1335 m (Gastaldo et al. 2019), whereas the base of the Katberg Formation is placed by Smith and Botha-Brink (2014) at an elevation of 1355 m on the northeast side of the Bethel valley. On the opposite side of the valley, Smith and Botha-Brink (2014, fig. 4 at white arrow) place the base of the Katberg Formation at an elevation of ~1450 m (Fig. 2). There is no fault that offsets the strata across the area.

The Fairydale locality (= Donald 207 farm; Figs. 2, 4) is situated to the southeast of the R701, which runs from Bethulie to Smithfield. Fairydale is the farm locality name used by Smith and Botha-Brink (2014) and others (e.g., Abdala et al. 2006; Botha and Smith 2007) although the collection site is actually on Donald 207 farm. Hence, we will refer to the area as Donald 207 using its designation on the 1:50000 3026AC Dupleston and 3026AD Tampasfontein topographic maps. There is less topographic relief here as it is located on a relatively flat plain at higher elevation, with low-lying escarpments bordering the plain to the northeast and southwest. A large number of *Lystrosaurus* (Botha and Smith 2006; Viglietti et al. 2013)—mainly *L. declivis* (N = 38), *L. murrayi* (N = 25), and *L.* indet. (N = 18)–along with other taxa (*Prolacerta,* N = 9; *Galesaurus,* N = 8; *Procolophon,* N = 6; *Thrinaxodon,* N = 6; *Micropholis,* N = 3; *Scaloposaurus,* N = 2; *Tetracynodon,* N = 1; *Owenetta,* N = 1; and *Myosaurus,* N = 1) are reported from this low-relief area (Fig. 4). Elevations over which these vertebrate collections originated range from ~1385 m (RS 407) to ~1430 m (Sam-pk-k10456; Smith and Botha-Brink 2014). Barbolini (2014, table 3.1, p. 102) reports a palynological sample from the *Dicynodon* AZ on "Farm Fairydale, Permo–Triassic boundary". That exposure (S30.407°, E26.23771°; 20 January 2018 WP926; Fig. 4 yellow arrow; see Online Supplemental File) is in a shallow donga at an elevation of 1384 m (Fig. 3) and ~70 m laterally from a specimen of *Thrinaxodon* (Sam-pk-k10615) in the *Lystrosaurus* AZ.

The spatial positions of vertebrate specimens on the Bethel, Heldenmoed, and Donald 207 farms, identified by Smith and Botha-Brink (2014, supplemental table 1), were located using GPS coordinates supplied by R.H.M. Smith (email dated 19 February 2014). Hence, these GPS coordinates include the raw data used by Ward et al. (2005), Botha and Smith (2006, 2007), and Smith and Botha-Brink (2014), and subsequently incorporated into Viglietti et al.'s (2016, 2018) database and others, to develop their assemblage zones and high, stratigraphic-resolution models of turnover, extinction, and recovery. The recovery of vertebrate specimens in the area, based on collection dates and acquisition numbers in the Iziko Museum database, spans the last decade of the twentieth century and first few years of the twenty-first century. During that time, two different GPS coordinate systems were in use in the country.

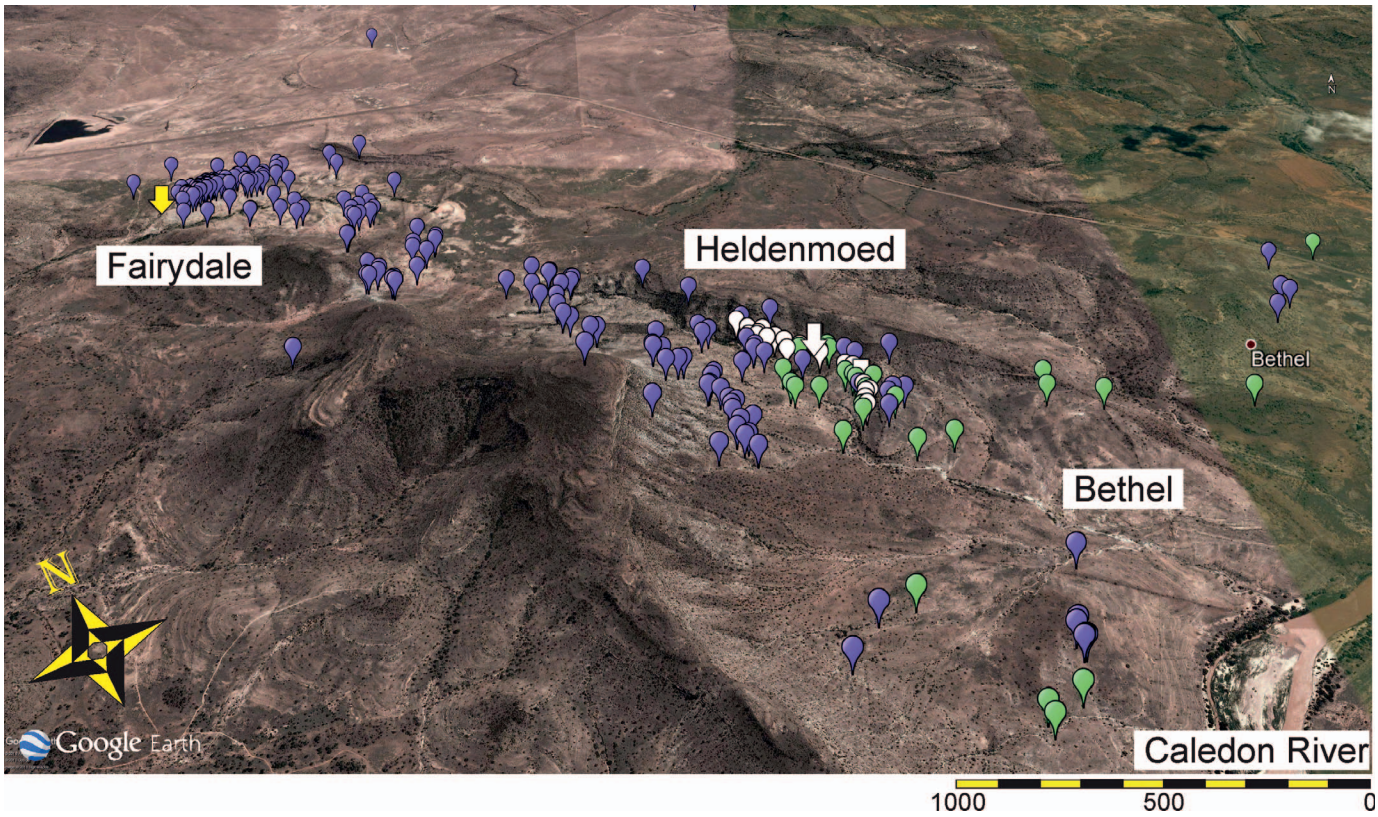

FIG. 4.—Oblique GoogleEarth aerial view of the relationship between the Bethel, Heldenmoed, and Donald 207 (Fairydale) farms on which all GPS coordinates of reported vertebrate fossils used by Smith and Botha-Brink (2014) to develop their extinction-and-recovery model are plotted. Green balloons mark sites of vertebrate fossils assigned to the *Daptocephalus* Assemblage Zone; purple balloons mark sites of specimens assigned to the *Lystrosaurus* Assemblage Zone. White balloons on the Bethel and Heldenmoed farms plot the GPS coordinates of the proposed *Daptocephalus–Lystrosaurus* assemblage-zone boundary physically traced along the northeast side of the valley. The white arrow on the Bethel farm marks the position of the assemblage-zone boundary as illustrated by Smith and Botha-Brink (2014), Gastaldo et al. (2009, 2019) and Neveling et al. (2016a). The yellow arrow on the Donald 207 farm marks the assemblage zone boundary as reported by Barbolini (2014) in the *Lystrosaurus* AZ (also see supplemental information). Scale in meters.

Prior to 1 January 1999, the Cape Datum was routinely used to record locations whereas South Africa adopted the WGS84 standard at the beginning of 1999; Selective Availability was terminated in 2000. Vertebrates with RS collection numbers lower than RS 78, with a catalog acquisition number of SAM-PK-K09958, were collected as late as 1998. Vertebrates with RS collection numbers beginning with RS 78, with a catalog acquisition number of SAM-PK-K09956, were collected beginning in 1999 (see Online Supplemental File Table 1). The collection date is important although, notably, there is no information in queried data from the museum collections about which coordinate system was in use at the time of field work. When comparing the geographic position of a specimen recorded under the Cape Datum standard with its location under the WGS84 system, Cape-Datum points shift ~55 m to the southwest of their WGS84 equivalents (see Online Supplemental File Fig. 1 for a comparative test). Hence, the current analysis is based mainly on vertebrates collected after 1 January 1999 and, presumably, all recorded using WGS84 coordinates.

Our analysis also recognizes the fact that GPS coordinates, acquired using hand-held devices since 2000 when the United States terminated its use of Selective Availability, are of higher geographic resolution (± a few m) since this filter was discontinued. Prior to 2000, GPS coordinates from hand-held devices may have recorded slightly wider variance in positioning data, and coordinates acquired under Selective Availability may have been up to 50 m displaced horizontally in *any* direction. The exact date and method of data acquisition are unrecorded fields in the supplemental data set of Smith and Botha-Brink (2014) and no metadata for any vertebrate specimen were provided to us. Hence, we have taken the following approach to this problem in our analysis. Vertebrate fossils reported from GPS coordinates in low-lying terrain versus those collected from sites on steeper terrain may differ in their stratigraphic position when plotted against stratigraphic sections. Where specimens were collected from low-relief sites and elevational differences are minimal (Fig. 2), our field checks of a subset of these specimens demonstrate that they originated from either rock pavement or shallow donga exposures. The GPS coordinates of these specimens are considered more highly reliable and are placed into sections measured either through, or within meters of, these collection sites (e.g., RS 356; Fig. 5). In fact, our stratigraphic placement of these specimens, relative to the *Daptocephalus/Lystrosaurus* biozone contact on the northeast face of the escarpment, conforms to within a few meters to their reported positions (see Online Supplemental File Fig. 2). Field checks of vertebrate-fossil sites located on steeper gradients also indicate that collections originated from deeper donga exposures or adjacent weathered siltstone surfaces. We recognize that a few meters of coordinate variance in these terrains would place the collection site either higher *or* lower on the slope, changing its stratigraphic position relative to the biozone contact. Hence, our analysis accepts the fact that there may be up to a 10-m variance in stratigraphic position of any specimen (based on our own field-based tests), and eliminates these taxa from the discussion where the field-checked versus reported horizon discrepancy is <10 m.

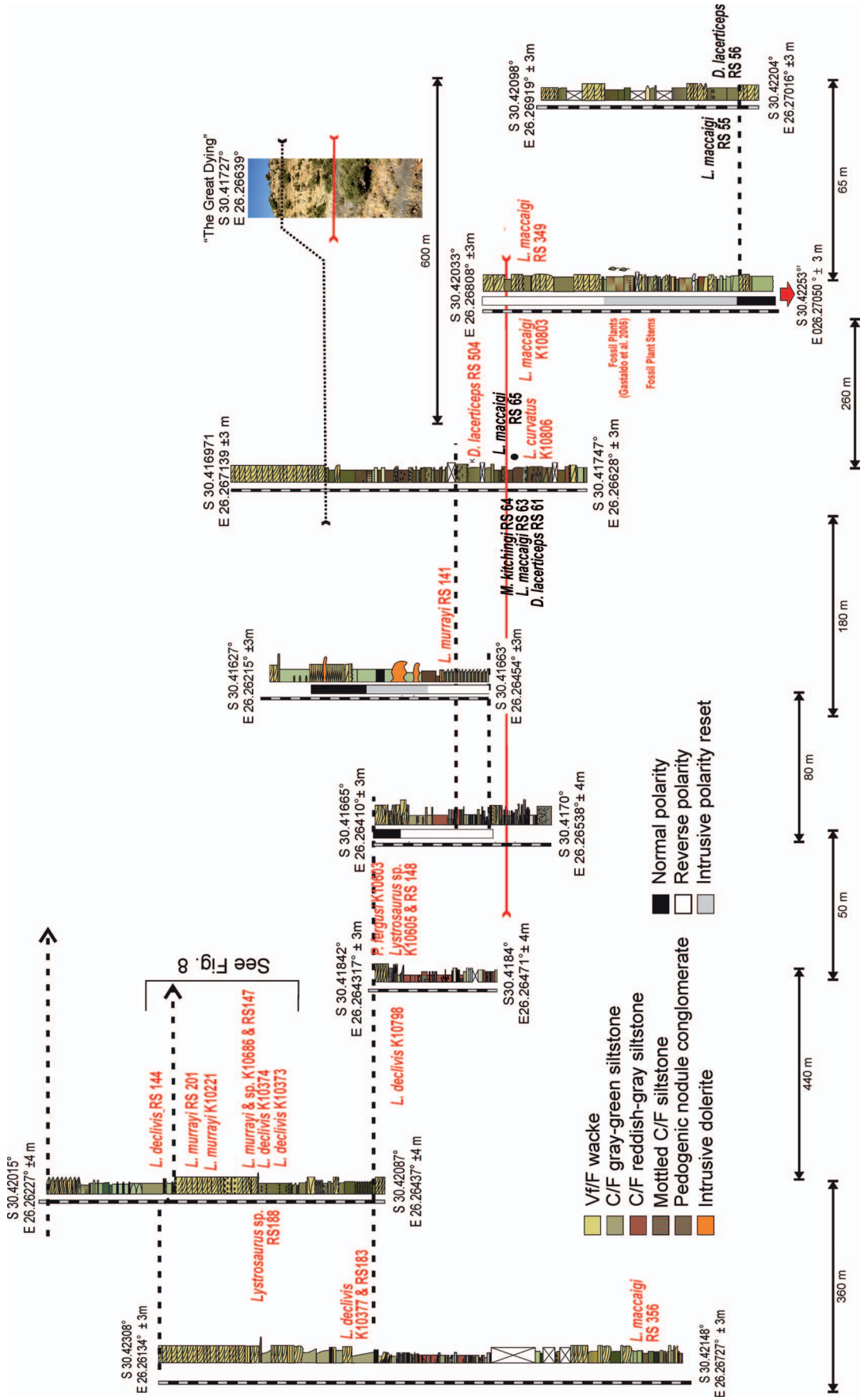

FIG. 5.—Eight measured stratigraphic sections, correlated across a ~750 m, east-to-west transect using physically traced upper bounding contacts of sandstone bodies (black dashed lines). A subset of *Daptocephalus* and *Lystrosaurus* AZ specimens from Smith and Botha-Brink's (2014) data set have been placed in the stratigraphic positions from which they were collected. Vertebrate collection numbers in black are presumed to have been recorded using Cape Datum coordinates (with Selective Availability), as their collection dates precede 1 January 1999; collection numbers in red are presumed to have been recorded using WGS84 coordinates, having been collected after 1 January 1999 (see Online Supplemental File). The solid red line represents direct stratigraphic correlation with the top of Facies C of Smith and Botha-Brink (2014), reported to be the contact between assemblage zones. Dotted black line represents base of Facies E of Smith and Botha-Brink (2014). Vertical bars adjacent to measured sections indicate normal (black) and reverse (white) polarity magnetozones as reported by Neveling et al. (2016a) and this contribution (see Online Supplemental File for composite magnetostratigraphy). Vertical scale in meters; distance between measured sections in meters.

The collection sites of a subset of vertebrate specimens were located using hand-held GPS units including a Garmin 62S with barometric altimeter, GPSMap 64S, Montana 650, and eTrex Legend, all of which were set to the WGS84 standard. Thirty percent of post-2000 specimens in the vertebrate database recorded on the Bethel and Heldenmoed farms (40/120), and 13% of vertebrate-collection sites on Donald 207 (15/118) have been field checked. Individual hand-held GPS units were cross-checked on a daily basis. Once the location of the vertebrate sample was obtained, it was correlated physically on the same day into one or more of our measured sections using standard field methods and elevation data. This is the same method used by Gastaldo et al. (2017) at the Old Lootsberg Pass and Tweefontein sites in the Eastern Cape Province.

Rocks exposed on the Bethel, Heldenmoed, and Donald 207 farms are essentially flat lying, with a strike that runs northwest-southeast or north-south, depending on which side of the valley is examined, and a gentle dip of one degree to the southwest. There is no evidence of fault displacement and little evidence of localized stratigraphic displacement due to the emplacement of Early Jurassic mafic dikes of the Karoo large igneous province in the area. Eight stratigraphic sections, totaling >280 m, were measured at either centimeter or decimeter scale resolution (depending on the lithology) using a leveling Jacob's staff and Abney level along the valley slopes on the Bethel and Heldenmoed farms (Fig. 3). These are supplemented with shorter stratigraphic sections (Gastaldo et al. 2009, unpublished) through, or adjacent to, GPS coordinates of collected vertebrate fossils. Measured sections were correlated over a total distance of 1.0 km using the upper bounding surfaces of sandstone bodies that were physically walked for more than 0.5 kilometers laterally. Upper bounding surfaces of these sandstone bodies were waypointed every 40 to 80 m (50 to 100 paces) using the Garmin Map62S with barometric altimeter, and serve as correlation datums (Fig. 5, dashed black lines). The biozone boundary figured by Smith and Botha-Brink (2014) also was physically traced using the same field technique across the northeastern escarpment (Gastaldo et al. 2009, 2019; Figs. 5, 6).

Samples for magnetic polarity stratigraphy were collected by drilling oriented cores using a portable field drill with a non-magnetic diamond drill bit as reported by Gastaldo et al. (2015, 2018, 2019) and Neveling et al. (2016a). Typically, seven to 12+ independently-oriented core samples were obtained from each competent bed (independent sampling site). In some cases (e.g., for paleomagnetic contact tests with Karoo dikes), a considerably larger number of independently oriented samples were obtained. Most beds sampled are exposed in the dongas (Figs. 3, 5) with samples designated Bt (see Online Supplemental File Fig. 4). Sampled lithologies consist of medium- to coarse-grained siltstone and very fine wacke, in addition to some nodular (concretions) horizons in fine siltstone/mudstone. Details on sample preparation, remanence measurements, thermal and AF demagnetization, acquisition of rock magnetic data, and data analysis can be found in the Online Supplemental File.

Siltstone samples for palynological preparation were collected on both the Bethel and Donald 207 farms. The Bethel farm samples came from the interval encompassing Smith and Botha-Brink's (2014, fig. 5) biozone boundary and include six samples beginning 7 m below the reported boundary contact (WP907, S30.41916°, E26.266935°) and extending to the base of the Katberg Formation (WP912, S30.418281°, E26.268485°). A sample suite was collected on the Donald 207 farm from the biozone boundary of Barbolini (2014; see Online Supplemental File). Here, seven siltstone samples cover a stratigraphic interval of 2.3 m (WP926, S30.406952°, E26.23771°). Palynological preparations were undertaken by RPS Ichron, Northwich, Cheshire.

RESULTS

Vertebrate specimens placed by Smith and Botha-Brink (2014) in the *Daptocephalus* AZ are restricted to collection sites on the Bethel and Heldenmoed farms, whereas vertebrate fossils assigned to the *Lystrosaurus* AZ are reported across a geographic distance of ~4.5 kilometers distributed across the three farms (Figs. 2, 4; see Smith and Botha-Brink 2014, their supplementary table 1). The majority of outcrop exposure is confined to erosional gullies (dongas) and resistant-sandstone benches, whereas pavement surfaces are limited to small areas of exposed siltstone with limited vegetation. Most of the ground is covered with rock debris and vegetated by low-growing cover and small, thorny shrubs. No data are provided by Smith and Botha-Brink (2014) on the entombing lithology for any specimen in their data set. Field checks of vertebrate-collection sites, regardless of the biozone assignment, indicate that most specimens were preserved in either greenish-, olive-, or light olive-gray siltstone or very fine sandstone units (Fig. 5). We acknowledge the possibility that skeletal elements may have originated from siltstone trough fills between trough cross-bedded intervals units, or in intraformational conglomerate lags, rather than in sandstone bedsets as a consequence of GPS coordinate variance. But, without the original metadata associated with each collection, along with the taphonomic characterization of each vertebrate remain, it is impossible for us to discriminate whether the specimen was penecontemporaneous with deposition or reworked from underlying strata into lag or sandstone bedload deposits. Skeletal material also is preserved in large, calcite-cemented nodules weathered brownish-gray which, primarily, formed in the greenish-gray siltstone lithology and are considered as preserved *in situ*. Very few of the vertebrate-collection sites are located in reddish-gray siltstone. And, these sites are found limited to ~25 m of stratigraphic section below and above the position of the reported biozone boundary on the Bethel and Heldenmoed farms (Fig. 5).

The stratigraphic position of the proposed biozone boundary, also termed "the Great Dying" as figured by Smith and Botha-Brink (2014, fig. 5A), is easily identifiable in the field at the contact between two siltstone units on the northeast wall of Bethel valley (see Gastaldo et al. 2009, 2019; Neveling et al. 2016a), trending towards the northwest. The horizon separating these siltstones is easily traced physically for a few hundred meters across the hill (Figs. 3, 5, 6; Gastaldo et al. 2019). To the northwest along the escarpment and into the donga on the Heldenmoed farm, lithologies below the "contact" have a reddish-gray appearance due to a veneer of weathered siltstone. But, upon closer examination, these are mainly a greenish-gray siltstone with decimeter-scale intervals of reddish-gray siltstone to mudstone, displaying a homogenous and massive character (see Gastaldo et al. 2019, fig. 5). Here, there is little evidence of primary structures in either outcrop or thin section (see Gastaldo et al. 2019, fig. 5A). To the northwest, the interval transitions to an interlaminated heterolithic succession, whereas to the south and around the nose of the escarpment (ridge shown in Fig. 6B), siltstone coloration grades to a mottled reddish-gray to a greenish- and light olive-gray siltstone, as previously documented (Gastaldo et al. 2009, 2019; Neveling et al. 2016b). The interval becomes covered in the Heldenmoed-farm donga at an elevation of 1339 m (WP890; 13 January 2018; Fig. 5). Greenish-gray siltstone dominates the succession at higher stratigraphic positions, above the proposed biozone contact of Smith and Botha-Brink (2014), with subordinate intervals of reddish-gray concretion-bearing siltstone, both of which preserve the ichnofossil *Katbergia* (Gastaldo and Rolerson 2008). Thin, planar and lenticular beds of very fine to fine wacke, in which there are cross bedding and ripple structures, occur encased in massive siltstone (Fig. 5). When vertebrate fossils collected in this area are field checked (Fig. 5), specimens assigned to the *Daptocephalus* AZ originate not only from stratigraphic positions below the proposed biozone boundary, but at least one specimen appears to have been collected above it. These relationships are well illustrated when plotted on GoogleEarth (Fig. 6A, 6B).

Of the limited number of *Daptocephalus* AZ specimens collected close to the boundary horizon, several do conform to their published stratigraphic position below the biozone boundary (e.g., *L. maccaigi* [RS

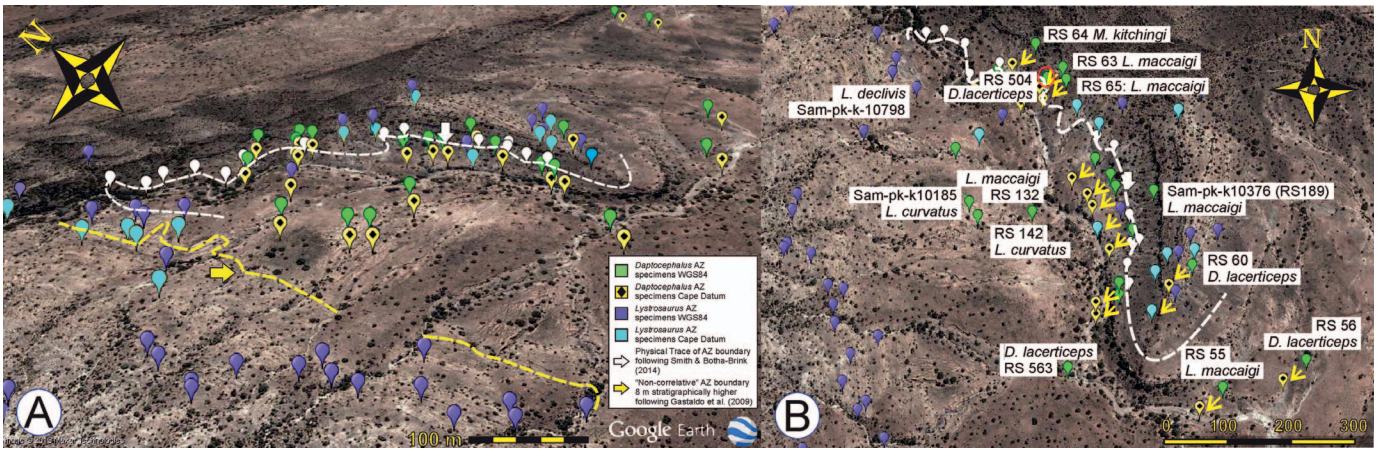

FIG. 6.—GoogleEarth images on which reported *Daptocephalus* AZ (green balloons WGS 84; yellow balloons Cape Datum) and *Lystrosaurus* (purple balloons WGS84; light blue Cape Datum) taxa are plotted using GPS coordinates provided by R.H.M Smith (see text and supplemental information). **A**) Plot with area oriented from southwest to northeast across the Bethel farm where white arrow and white balloons atop dashed white line mark the biozone contact, as illustrated by Smith and Botha-Brink (2014), physically traced across the Bethel to Heldenmoed farms (Gastaldo et al. 2009, 2019; Neveling et al. 2016a) northwestward into the donga where it is covered. Horizontal yellow arrow marks the upper contact of the heterolithic (laminated) interval, figured by Gastaldo et al. (2009, fig. 2A) and reported by Smith and Botha-Brink (2014, p. 103) to illustrate the unique character of their Facies C, the event bed. Dashed yellow line represents physical trace of that contact on western side of Bethulie Valley. Gastaldo et al. (2009, fig. 3) have demonstrated that this interval lies 8 m above the stratigraphic position of the biozone boundary marked by the white arrow and dashed white line (see Fig. 5). Scale equals 100 m. **B**) Northeastern side of Bethulie farm valley on which reported *Daptocephalus* AZ (green balloons WGS84; yellow balloons Cape Datum) and *Lystrosaurus* (purple balloons; light blue Cape Datum) taxa are plotted using GPS coordinates provided by R.H.M Smith (see text and Online Supplemental File). White arrow indicates the position of the assemblage-zone boundary as figured by Smith and Botha-Brink (2014, fig. 5), Gastaldo et al. (2009, 2019), and Neveling et al. (2016a), and white balloons show the waypoints taken while physically tracing the upper boundary contact across the Bethel and Heldenmoed farms. Yellow arrows show the shift in geographic position of specimens when Cape Datum coordinates are plotted for vertebrates collected prior to 1 January 1999. *Daptocephalus lacerticeps* (RS 504) is green balloon inside red circle. Scale in meters.

349, SAM-P-PK-10803]). But, at least two specimens do not conform to their reported stratigraphic position below the boundary. For example, specimens of *L. maccaigi* (RS 351; SAM-P-PK-10376) are positioned above the biozone boundary of Ward et al. (2000, 2005), Smith and Ward (2001), Botha and Smith (2006, 2007), and Smith and Botha-Brink (2014; Figs. 2, 6). SAM-P-PK-10376 (*L. maccaigi*; Fig. 6B) is reported by Smith and Botha-Brink (2014) in a stratigraphic position 15 m *below* the biozone boundary; its field-checked site lies ~17 m above the proposed boundary. RS 351 (*L. maccaigi*) is a lower jaw and skull, preserved in a "red laminated event bed" reported from Bethel farm. Yet, the GPS coordinates of the collection site plot 3.2 km to the west atop the escarpment at an elevation of 1390 m on the Donald 207 farm (Fig. 2); all vertebrates from the Donald 207 farm at this elevation are assigned to the *Lystrosaurus* AZ. SAM-PK-K-10805, noted to be 8 m below the boundary, originates from a farm 15 km to the east where there is neither outcrop or a measured section reported, illustrated, or figured. The site's elevation is 1435 m. All other specimens assigned to the *Lystrosaurus* AZ on the Bethel and Heldenmoed farms are reported to lie above the biozone boundary, as defined on the eastern slopes of the valley (see Discussion). But, stratigraphic discrepancies exist relative to where each lies relative to the proposed biozone boundary on both of these farms.

A subset of *Lystrosaurus* AZ specimens are outliers and occur toward the southwest of Bethel valley (lower purple ellipse on Fig. 2). Here, the terrain is of relatively low relief. All vertebrates assigned to the *Lystrosaurus* AZ lie between an elevation of 1290–1310 m and are associated with vertebrates assigned to the *Daptocephalus* AZ. At an elevation of 1310 m, SAM-PK-K-10015 (*M. kitchingi*) and RS 126 (Dicynodontia indet.) are reported to occur -5 and -20 m below the biozone contact, respectively. At the same elevation, five specimens are assigned to the *Lystrosaurus* AZ and placed up to 7 m above the biozone boundary. For example, RS 131 *(L. curvatus*) is reported 7 m above the assemblage-zone boundary, but lies beneath at least two sandstone bodies which, themselves, lie below a cluster of *Lystrosaurus* (RS 127, 128, 130), *Moschorhiinus* (RS 139), and *Prolacerta* (SAM-PK-P-10014). These vertebrates are reported to range from 1–7 m above the boundary. Our field check of these sites indicates that they originated on a boulder-covered, low-relief ridge formed by a dolerite dike (our field notes, 14 June 2015). There is no exposure, let alone outcropping of a purported "event bed" against which the original authors may have fixed a stratigraphic position for these vertebrates. Hence, we cannot explain how any placement relative to any horizon for these specimens was determined. Many other discrepancies exist in the reported stratigraphic positions of *Lystrosaurus* AZ vertebrates.

Eighteen specimens assigned to the *Lystrosaurus* AZ (mainly *L. murrayi*, *L. declivis*, and *L.* sp.) occur over an area of 0.1 km^2 between the 1300 and 1400 m contour lines on the western side of the valley (Fig. 8; see Online Supplemental File Fig. 2). Specimens SAM-P-PK10686, SAM-P-PK10221, assigned to *L. murrayi*, and RS 144, *L. declivis*, are reported 20, 20, and 17 m above the biozone boundary, respectively (Figs. 5, 8; Table 1). Specimen RS147, an unidentified *Lystrosaurus* sp., also occurring at the same stratigraphic position as SAM-P-PK10686 is recorded as 21 m above the boundary. Yet, within that same stratigraphic interval, and field-checked at essentially the same elevation on the mountainside, are specimens RS 188, RS 201, SAM-P-PK10373 and SAM-P-PK10374. According to the data set of Smith and Botha-Brink (2014), these *Lystrosaurus* specimens were collected 160 m (RS 188; *L.* sp.), 120 m (RS 201; *L. murrayi*), 90 m (SAM-P-PK10373; *L. declivis*), and 125 m (SAM-P-PK10374; *L. declivis*), respectively, above the biozone boundary (Figs. 5, 8; see Online Supplemental File Fig. 2). These are not the only examples where the reported stratigraphic position of taxa in the *Lystrosaurus* AZ are incongruent on the Bethel and Heldenmoed farms. For example, the stratigraphic positions of specimens RS 183 (*L. declivis*) and SAM-P-PK-10377 (*L. declivis)* lie ~16 m above the proposed biozone boundary (Fig. 5). Yet, Smith and Botha-Brink (2014) report their positions as being 92 and 105 m above the boundary, respectively. Similar wide discrepancies

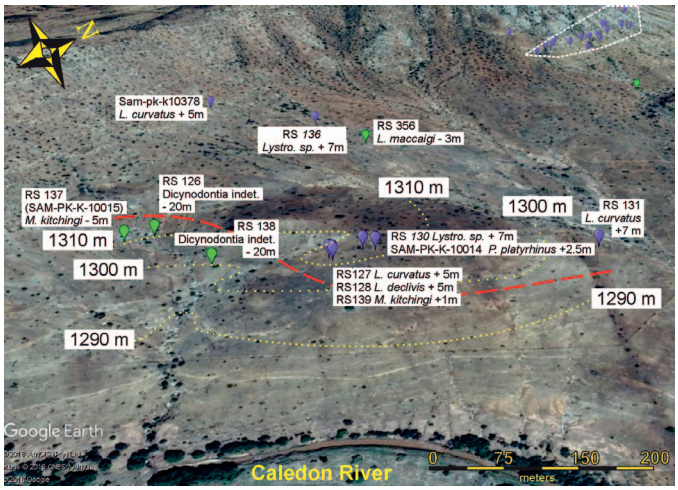

FIG. 7.—Plot of vertebrate-collection sites reported in the *Daptocephalus* (green balloon) and *Lystrosaurus* (purple balloon) Assemblage Zones in close geographic proximity in an area of relatively low relief to the southwest. Contour intervals drawn based on GoogleEarth Digital Elevation Model. GPS coordinates of specimens from Smith and Botha-Brink (2014) plotted using WGS84 system as explained in the supplemental text based on collection number. Red dashed line is the Permian–Triassic Boundary as illustrated by Marchetti et al. (in press) also using GPS coordinates of these samples. Field relationships indicate an overlap of vertebrate ranges of assemblage-zone taxa as identified by Smith and Botha-Brink (2014) to one of the two vertebrate assemblage zones. Dashed white polygon is discussed in Fig. 8. Contour interval equals 10 m; scale bar equals 150 m.

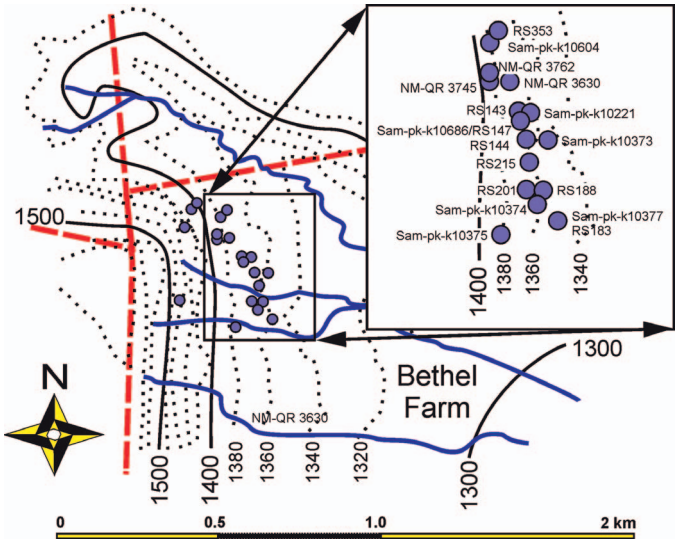

FIG. 8.—Map plotting vertebrate fossils placed in the *Lystrosaurus* AZ from the southwestern side of Bethel valley as reported by Smith and Botha-Brink (2014, supplemental data table), with GPS coordinates of each specimen provided by R.H.M. Smith (see text). See Table 1 and Figure 13 for systematic assignment of specimens, the reported position of each above the biozone boundary, and discrepancy in meters between a specimen's field-verified versus reported position. Contour intervals are 20 m; scale in kilometers.

abound on the Donald 207 farm for collection sites within a small geographic area.

Vertebrate fossils collected within 150 m east/northeast of Barbolini's (2014) palynological site exhibit a wide variance in their reported position above the *Daptocephalus-Lystrosaurus* biozone boundary (Fig. 9) which, here, must be considered in the context of the Bethel farm locality (Figs. 5, 6). A subset of eight vertebrates, which are part of the Smith and Botha-Brink (2014) database, all originate within a small, 0.5 hectare area with an elevational difference of only 5 m from the top of the Donald 207 donga. Yet, the stratigraphic positions of these fossils are reported to vary from 39 m to 89 m above the Bethel biozone boundary. RS 501 (*Prolcerta* sp.) was recovered at an elevation of 1390 m and reported with a stratigraphic position 39 m above the proposed boundary. In contrast, RS408, an unidentified *Lystrosaurus* sp., also collected at an elevation of 1390 m, is reported with a stratigraphic position 89 m above the biozone boundary as identified on the Bethel farm (Table 2). Such discrepancies are found throughout Donald 207 farm (Fig. 10).

Magnetostratigraphy

Any efforts to develop a magnetic polarity stratigraphy framework for any stratigraphic section in the Karoo Basin must take into consideration the thermal history of the basin. The early syn-burial history of the basin is quite varied across the region, as studies have demonstrated a general north to south/southwest increase in burial diagenesis during early stages of metamorphism attending Cape Fold Belt tectonism (Jourdan et al. 2005). This pattern is further complicated by both regional and local effects of widespread mafic magmatism associated with emplacement of the volumetrically enormous (greater than 106 km^3) Karoo Large Igneous Province of Early Jurassic (ca. 184 to 182 Ma) age. Here, mafic sills and dikes of a wide range of dimensions were emplaced into Karoo Basin strata across the Eastern Cape Province and Free State (e.g., Duncan et al. 1997; Jourdan et al. 2005; Svenson et al. 2012) and elsewhere in southern Africa. Thus, the thermal history of Karoo Supergroup strata, as influenced by both tectonic and magmatic processes, bears on the ability to extract primary, or very early acquired magnetizations from these strata and provide meaningful magnetic polarity stratigraphic records. The field relations exposed in the area of the Bethel section, which involve at least six thin (less than 2 m thick) Karoo dikes that cross-cut the section (see Online Supplemental File), afford key opportunities to examine the local effects of small-volume Karoo magmatism through paleomagnetic contact tests involving sampling of the Karoo intrusions and host strata, as a function of distance away from dike contacts.

The scope of this paper does not permit detailed presentation of all of the paleomagnetic data obtained from the Bethulie stratigraphic section, which includes over 75 discrete sampling sites, most of which are in separate, distinct beds. Response to progressive demagnetization (either thermal methods, or less common, alternating field methods) is typically quite well-defined in both the sedimentary rocks and the Karoo dikes sampled (Fig. 11). Most demagnetization results are fully interpretable, with principal components analysis (Kirschvink 1980) providing the resolution of magnetization vectors associated with maximum angular deviation (MAD) values well less than 10°. Several directional responses to progressive demagnetization are recognized and, on this basis, we tentatively define a magnetic polarity stratigraphy for the Bethel farm section. This polarity stratigraphy consists of: a lower magnetozone of normal polarity (north-northwest directed, moderate to steep negative inclination remanence dominates); an interval that has been influenced by Karoo intrusions; a middle magnetozone of reverse polarity (south-southeast directed, moderate to steep positive inclination remanence dominates); an overlying interval that also has been influenced by Karoo dikes; and an upper magnetozone of normal polarity (see Online Supplemental File Fig. 4). Notably, for the sites providing data interpreted to be of reverse polarity, it is always the case that a north-northwest directed, moderate to steep negative inclination remanence (normal polarity) is superimposed on this magnetization. This "overprint" remanence is typically unblocked in the laboratory by about 400°C. The magnetization record of most of the Karoo dikes is, with minor exceptions,

TABLE 1.—*Reported, field-verified, and estimated positions in meters of Lystrosaurus, Prolocerta, Regiosaurus, Scaloposaurus, and Tetracynodon specimens reported by Smith and Botha-Brink (2014) from the Lystrosaurus Assemblage Zone above their biozone boundary on the Bethel Farm, Free State. All vertebrate fossils were collected from a 6.7 hectare area shown in Figure 8.*

Vertebrate sample number	Systematic affinity	Reported position in meters	Field verified position in meters	GPSwaypoint date and time	EstimatedPosition in meters	Difference in reported vs. **verified** or *estimated*
SAM-PK-K10737	*Prolocerta* sp.	67			75	*+12*
SAM-PK-K10793	*Lystrosaurus declivis*	41			85	*+44*
RS353	*Lystrosaurus murrayi*	45			45	*0*
SAM-PK-K10604	*Scaloposau* sp.	50			50	*0*
NM-QR 3762	*Lystrosaurus murrayi*	51			55	*+4*
NM-QR 3630	*Regiasaurus* sp.	50			45	*-5*
NM-QR 3745	*Tetracynodon darti*	76			55	*-19*
RS147	*Lystrosaurus* sp.	21	32	2015-06-20 10:08:54		**+11**
RS143	*Lystrosaurus murrayi*	19.5	42	2015-06-20 10:24:46		**+22**
SAM-PK-K10221	*Lystrosaurus murrayi*	19.5	35	2015-06-20 10:33:00		**+15**
SAM-PK-K10686	*Lystrosaurus murrayi*	20			35	*+15*
SAM-PK-K10373	*Lystrosaurus declivis*	90	24	2015-06-20 11:00:11		**-66**
RS144	*Lystrosaurus declivis*	17	38	2015-06-20 09:58:27		**+21**
RS215	unidentified gen. and sp.	90			25	*-65*
RS201	*Lystrosaurus murrayi*	120	36	2015-06-20 09:49:15		**-84**
RS188	*Lystrosaurus* sp.	160	29	2015-06-20 09:38:49		**-131**
SAM-PK-P10374	*Lystrosaurus declivis*	120	29	2015-06-20 08:56:03		**-96**
SAM-PK-K10377	*Lystrosaurus declivis*	105	25	2015-06-20 08:01:53		**-80**
RS183	*Lystrosaurus declivis*	92	22	2015-06-20 08:01:53		**-70**
SAM-PK-K10375	*Lystrosaurus murrayi*	180			50	*-130*
RS152	*Lystrosaurus* sp.	42			100	*+58*

very uniform. The magnetization characteristic (ChRM) of the Karoo dikes being of east-southeast declination and shallow positive inclination (Fig. 11A). The direction of this ChRM in the Karoo dikes is considerably shallower in inclination than and, in fact, statistically distinguishable from that recovered from the sites that define the middle stratigraphic interval of interpreted reverse polarity (Fig. 11A). Host strata in immediate contact with Karoo dikes typically yield a magnetization similar in direction to the ChRM of the Karoo dike (e.g., compare results from site Bt29 [Karoo dike] and Bt35 [host strata immediately adjacent and up to about 2 m distant from the southeast contact with the dike]; Fig. 11), indicating that the host strata adjacent to the dike have been pervasively remagnetized due to dike intrusion. All specimens from all samples of this Karoo dike (site Bt29) and the host rock in contact (site Bt29) show the first removal, in either progressive thermal or alternating field demagnetization, of a north-northwest directed, moderate to steep negative inclination magnetization. This "overprint" magnetization is, here, demonstrably younger than the Early Jurassic Karoo dike. Sites Bt31, Bt32, and Bt33, some 12 m farther to the northwest up the donga and stratigraphically above host strata at site

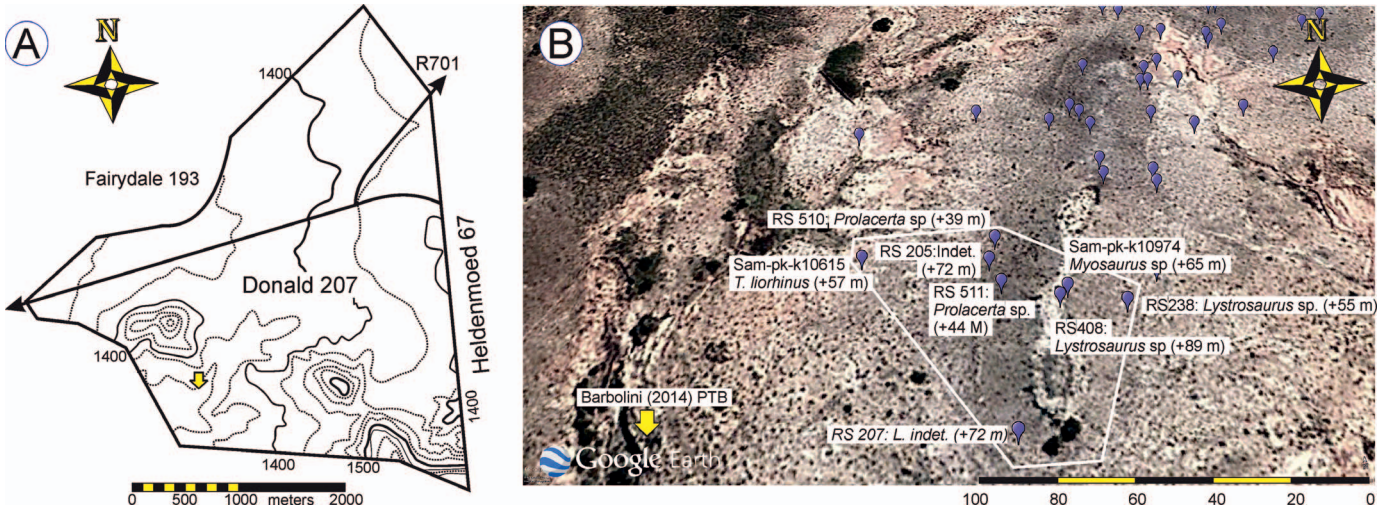

FIG. 9.—Map and plot of *Lystrosaurus* AZ fossils on the Donald 207 farm. **A**) Topographic map showing the relatively flat and gentle land surface from which the majority of *Lystrosaurus* AZ fossils were reported. Yellow arrow marks the location of the Permian–Triassic boundary as reported by Barbolini (2014). **B**) GoogleEarth image of *Lystrosaurus*-AZ fossils (purple balloons), the systematic affinity of a subset, and the stratigraphic position reported above the biozone boundary for this subset, as reported by Smith and Botha-Brink (2014) over an area of 0.5 hectares on the Donald 207 Farm. These specimens are in close proximity to the sample site from which a Permian-aged palynoflora is preserved. Scale in meters; elevational difference between top of donga in which Barbolini's (2014) palynological samples originate and RS 510 is 5 m (see Table 2).

TABLE 2.—*Reported and field-verified positions in meters of Lystrosaurus, Micropholis, Myosaurus, Prolacerta, and Thrinaxodon specimens reported by Smith and Botha-Brink (2014) from the Lystrosaurus Assemblage Zone on the Donald 207 (Fairydale) farm, Free State. All vertebrate fossils are reported from within a 0.5 hectare area shown in Figure 9.*

Vertebrate sample number	Systematic affinity	Reported position in meters above biozone boundary	Field verified elevation in meters	Date and time	GPS waypoint
RS 408	*Lystrosaurus* sp.	+89	1390	6/13/2018 13:35	WP 979
RS 204	*Micropholis stowi*	+72	1388	6/13/2018 13:55	WP 984
RS 205	Indeterminate	+72	1389	6/13/2018 13:59	WP 985
RS 207	*Lystrosaurus* indet.	+72	1386	6/13/2018 13:40	WP 980
RS 404	*Lystrosaurus* sp.	+69	1389	6/13/2018 13:53	WP 983
SAM-PK-K10974	*Myosaurus* sp.	+65	1391	6/13/2018 13:44	WP 981
RS 409	*Lystrosaurus* sp.	+63	1383	6/13/2018 14:24	WP 989
RS 403	*Lystrosaurus murrayi*	+62	1388	6/13/2018 14:17	WP 988
SAM-PK-K10615	*Thrinaxodon liorhinus*	+57	1383	6/13/2018 13:47	WP 982
RS 238	*Lystrosaurus* sp.	+55	1385	6/13/2018 13:30	WP 978
RS 511	*Prolacerta* sp.	+44	1386	6/13/2018 13:26	WP 977
RS 510	*Prolacerta* sp.	+39	1386	6/13/2018 14:12	WP 987

Bt35, show no evidence of a thermal remagnetization by the dike (Fig. 11). Taken together, these kinds of paleomagnetic observations lead us to construct the preliminary magnetic polarity stratigraphy reported here for the Bethulie section (Fig. 3; Online Supplemental File Fig. 4).

Donald 207 (Fairydale) Farm Palynology

The Donald 207 palynological assemblage is characterized by taeniate asaccate and bisaccate pollen, alete non- and bisaccate pollen, as well as simple spores and cavate/cingulate spores, with the latter being the most abundant group (Fig. 12). Most multitaeniate bisaccate grains are damaged but can be identified as *Protohaploxypinus* sp., *Lunatisporites pellucidus*, and *Hamiapollenites insolitus*. Other common taeniate forms are the bisaccates *Lueckisporites virkkiae*, *Corisaccites alutas*, and *Guttulapollenites hannonicus*. Alete, non-taeniate bisaccates and non-saccate pollen include *Scheuringipollenites ovatus* (= *Alisporites ovatus*), *Alisporites tenuicorpus*, *Falcisporites australis*, *Pteruchipllenites cf. gracilis*, and *Inaperturopollenites nebulosus*. Polyplicate and monosulcate pollen are represented by *Marsupipollenites striatus*, *M. Triradiatus*, *Weylandites lucifer*, *Cycadopites cymbatus*, and *C. follicularis*. *Densoisporites playfordii*, *D. nejburgii*, *Playfordiaspora crenulata*, *Limatulasporites fossulatus*, and *L. limatulus* are among the cavate and cingulate spore taxa. Simple spore taxa include *Cyclogranisporites gondwanensis*, *Brevitriletes hennellyi (= bulliensis)*, *Deltoidospora* sp., cf. *Camptotriletes warchianus*, *Verrucosisporites*, and *Calamaspora*. In addition to the pollen and spores, palynomorphs that represent either fungal (*Reduviasporonites*) or algal remains *(Leiosphaeridia* spp., *Quadrisporites horridus*, *Micrhystridium*, and cf. *Brazilea*) are present. Of these, *Leiosphaeridia* spp. and an unidentified palynomoroph are very abundant.

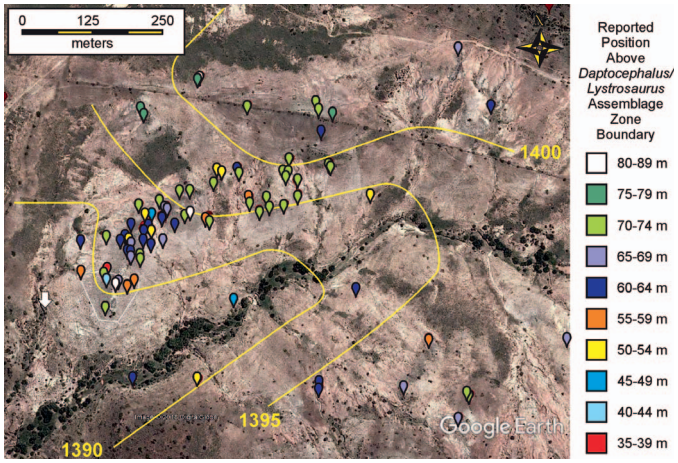

FIG. 10.—*Lystrosaurus* AZ specimens on Donald 207 farm expanded beyond the 0.5 hectare plot in Figure 9. Note that over a gentle topography of only 10 m relief, adjacent specimens are reported to be positioned over a wide range of levels above the *Daptocephalus–Lystrosaurus* AZ boundary, as recognized on the Bethel farm (Smith and Botha-Brink 2014). Contour intervals drawn using GoogleEarth DEM onto which elevations of field-checked specimens act as a reference. See supplemental information for an additional plot of the *Lystrosaurus* AZ collection sites not included, herein.

DISCUSSION

The terrestrial response to the end-Permian extinction event long has centered on the vertebrate-fossil record of the Karoo Basin (e.g., Smith 1995; Retallack et al. 2003; Ward et al. 2005; Day et al. 2015; Rey et al. 2016; Rubidge et al. 2016; Viglietti et al. 2018). The traditional model of a phased turnover in vertebrates over a short stratigraphic interval, with the abrupt loss of taxa immediately at the top of the *Daptocephalus* AZ followed by a rapid expansion of *Lystrosaurus* species and the appearance of other genera (Smith and Botha-Brink 2014), is: (1) accepted widely; (2) applied to other continental successions (Benton and Newell 2014; Rey et al. 2016); and (3) used to interpret paleogeographic and global ecologic patterns of extinction and recovery (e.g., Sidor et al. 2013; Roopnarine et al. 2017, 2018). These models are predicated on the accuracy and reliability of the reported stratigraphic position of vertebrate specimens relative to a single datum identified as a contact between assemblage zones across the basin. The current study, in conjunction with a field test of vertebrates at Old Lootsberg Pass (Gastaldo et al. 2017), continues to document significant discrepancies between the reported and recorded stratigraphic positions on which these extinction-and-recovery models have been based.

Smith and Botha-Brink (2014, p. 100) unequivocally state that the data set they used to refine previous end-Permian model of continental ecosystem turnover and recovery (Smith 1995; Ward et al. 2000, 2005; Smith and Ward 2001) is highly accurate. In turn, it is maintained that this level of accuracy allowed them to develop a high-resolution record of the biostratigraphic ranges of vertebrate taxa, such that individual specimens could be placed to within a few meters below or above the biozone contact (as defined on the northeast side of Bethel valley; Figs. 4–6). The majority of fossil vertebrates comprising that data set originate from the Free State

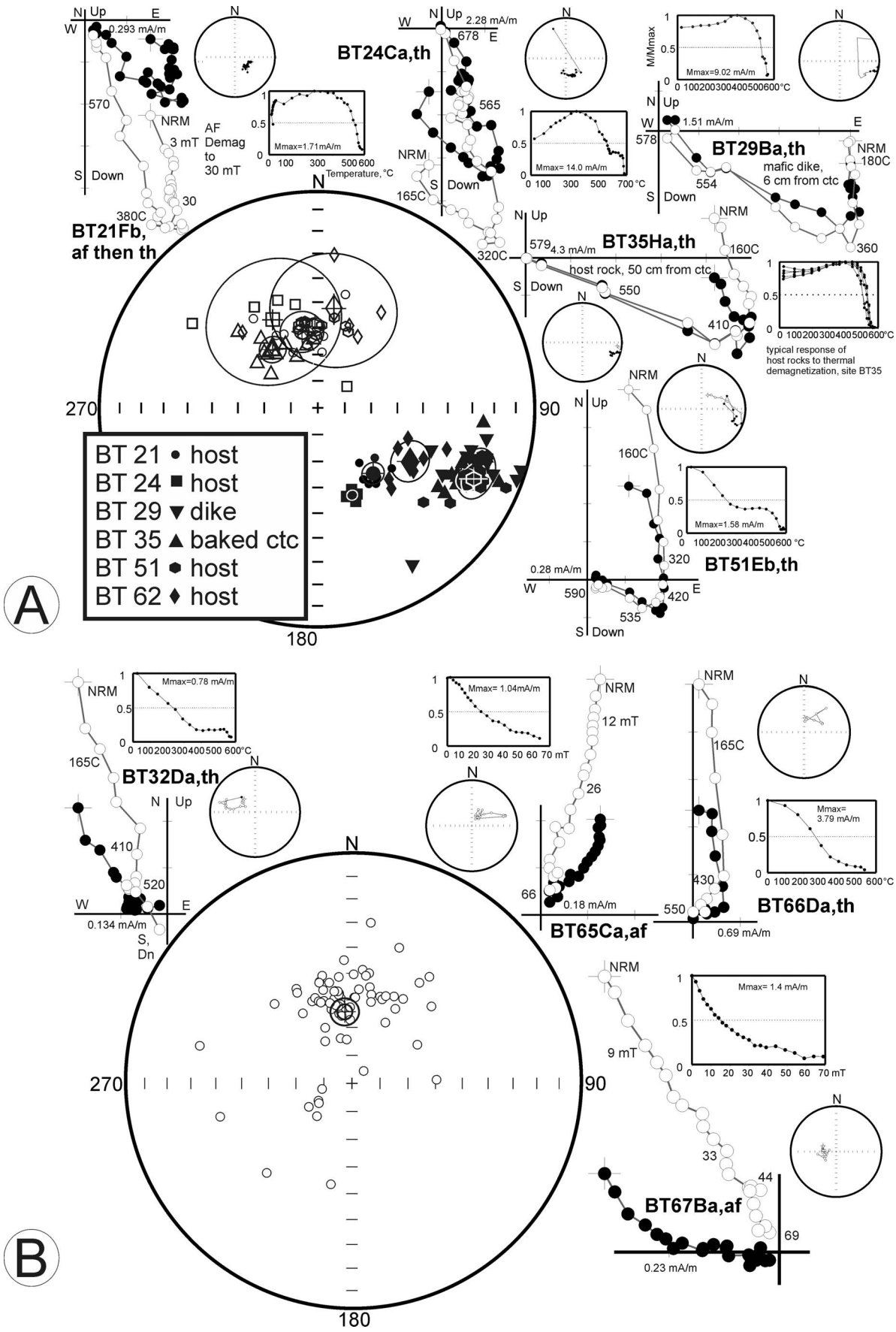

localities of Bethel, Heldenmoed, and Donald 207 farms, where the stratigraphic section is known to be condensed relative to locations in the Eastern Cape Province (e.g., Lootsberg Pass; Viglietti et al. 2017). An assessment of these specimens, using the raw-collection data with specimen-GPS coordinates provided by Smith (personal communication 2014), raises serious questions about the quality of that data set and, thus, its utility.

Our empirical field test of a subset of the most critical taxa used to define the relationship of vertebrate assemblages across the biozone boundary (Ward et al. 2005; Botha and Smith 2007; Smith and Botha-Brink 2014; Viglietti et al. 2016) demonstrates many inconsistencies in the data (Figs. 7–10, 13). There is a wide disparity in the reported and field-checked stratigraphic positions of *Daptocephalus* and *Lystrosaurus* AZ specimens on the Bethel and Heldenmoed farms. Collection sites of the 12 *Dicynodon* (presumably *Daptocephalus*) specimens are located both below and, at least one above the biozone boundary of Smith and Botha-Brink (2014). For example, RS 504 and SAM-PK-K-10600 are reported to be positioned -7 and -4 m below the contact, respectively, and conform to these levels based on our criteria. One curious specimen of *D. laceriteps*, SAM-PK-K-10811, is reported as -21 m below the boundary and reportedly was recovered on the Bethel farm; that collection site is ∼18 km to the southwest on the Tussen-die-Riviere game reserve where its GPS coordinates plot. Its actual stratigraphic position cannot be checked because there is no laterally continuous sandstone body that exists between Bethel farm and the game reserve that can be used as a datum upon which to base a correlation. In addition, Gastaldo et al. (2009) report the presence of small faults on the game reserve that inhibit correlation there. RS 60 is reported to be positioned -7 m below the biozone contact although our field check places it >10 m above boundary irrespective of whether the WGS84 or Cape Datum coordinate system is employed (Fig. 6B). But, we acknowledge that the enforcement of selective availability on all GPS data at this time may be responsible for the discrepancy we observe for this specimen. Yet, spatial discrepancies hold true for *L. maccaigi*, another diagnostic taxon of the upper *Daptocephalus* AZ (Viglietti et al. 2016). Twenty-two specimens of *L. maccaigi* originate from the Bethel farm, most of which conform to a position below the boundary contact. For example, SAM-PK-K-10803 and RS 356 are reported to be positioned -5 and -3 m below the biozone contact, respectively, and their positions conform to our criteria. In contrast, specimens SAM-PK-K-10376 and RS 351 (Fig. 2), reported in a position -9 and -3 m below the boundary, respectively, occur in the *Lystrosaurus* AZ. We conclude that ∼42% (5/12) of *D. laceriteps* and ∼27% (6/22) of *L. maccaigi* collection sites on these farms cannot be placed with any confidence into a stratigraphic context. What are even more enigmatic concerns are the positions of *Lystrosaurus* AZ taxa, the GPS coordinates of which are in close geographic proximity (Fig. 8), that are reported to be at various stratigraphic positions that range over more than 50 m (Fig. 10).

Diagnostic *Lystrosaurus* AZ taxa, *L. declivis* and *L. murrayi* (Botha and Smith 2007), are commonly reported from the western side of the valley (Fig. 8; see Online Supplemental File Fig. 3) with disparate assignments of their stratigraphic position relative to the biozone boundary (Figs. 5–7). The lowest occurrence of *L. declivis* (SAM-K-PK10376) is reported as 5 m above the proposed biozone boundary. Yet, the site from which the specimen originates is a small depression that is stratigraphically above the horizon figured by Smith and Botha-Brink (2014, fig. 5) but stratigraphically below the interlaminated interval figured by Gastaldo et al. (2009) to which Smith and Botha-Brink (2014, p. 103) refer readers as illustrative of the boundary facies. Neveling et al. (2016a, fig. 30) note and illustrate the problem in higher detail. SAM-K-PK10373 (*L. declivis*) is positioned along the valley wall and reported ∼90 m above the proposed biozone boundary. Its field-checked stratigraphic position lies ∼25 m above the biozone boundary (Fig. 8; Table 1). These are not the only two specimens where the reported and field-checked positions of adjacent lystrosaurid specimens range from <10 to >100 m. Such variance clearly cannot be a consequence of GPS coordinates acquired by hand-held devices nor attributed to selective availability, because specimen numbers suggest collection dates following its termination. Similar discrepancies exist with the reported stratigraphic position of lystrosaurid and other taxa on the Donald 207 farm, relative to the proposed biozone boundary on the Bethel farm (Figs. 9, 10). Hence, we conclude that 52% (45/82) of the reported positions above the proposed biozone boundary of *Lystrosaurus* AZ specimens are problematic and the existence of a definitive, single horizon on which two biozones can be separated appears unreliable.

The cluster of outlier *Lystrosaurus* AZ taxa, all reported within 10 m of the boundary, occur over a stratigraphic interval that includes at least three, if not four, laterally traceable sandstones (Fig. 7). In fact, RS 131 (*L. curvatus*), reported as occurring above the assemblage-zone boundary, is almost 20 m below RS 137 *(M. kitchingi*), a specimen assigned to the *Daptocephalus* AZ. Similarly, RS 131 is reported at approximately the same stratigraphic position as the other vertebrates assigned to the *Lystrosaurus* AZ. Recently, Marchetti et al. (in press, their figure 1C) provide a spatial plot of these taxa through which the PTB of Smith and Botha-Brink (2014) is illustrated. That horizon is illustrated here (Fig. 7) and would require the PTB to ascend the stratigraphy and cross cut laterally continuous, and flat-lying, sandstone bodies. This relationship indicates that no single stratigraphic horizon has been used to separate

←

FIG. 11.— Summary of examples of paleomagnetic data from the Bethulie section that have been used to develop a tentative composite magnetic polarity stratigraphy for the stratigraphic section (Fig. 5; see Online Supplemental File). Both (A, B) include examples of orthogonal demagnetization diagrams showing the response of individual specimens to progressive thermal or alternating field demagnetization, or a combination of both. In these diagrams, the end point of the magnetization vector is projected simultaneously onto the horizontal (solid symbols) and vertical (open symbols) plane. Several demagnetization steps are identified along the vertical projections. Both (A, B) also include an equal area projection showing directions of magnetization resolved using principal components analysis on demagnetization data from specific specimens (typically one specimen per independent sample analyzed), the estimated site-mean direction (larger symbol) based on the specimen directions from that site, and the projected cone of 95 percent confidence (heavy line) about the estimated mean direction. Open (closed) symbols refer to upper (lower) hemisphere directions. In (A), are shown data from several horizons (sites, #'s 21, 24, and 62) where a southeast-directed, relatively steep positive inclination remanence (interpreted to be of reverse polarity) is isolated in progressive demagnetization after the first removal of north-northwest-directed, relatively steep negative inclination ("overprint") magnetization. In addition, data from several locations in the Bethulie section are shown that reveal the effects of emplacement of Early Jurassic Karoo dolerite dikes. Site BT29 is in a 2 m wide Karoo dike and progressive demagnetization isolates an east-southeast directed magnetization of shallow positive inclination. Site BT35 is in gray-green siltstone in immediate contact with the site BT29 dike, on the southeast margin of the dike. Specimens from all samples in the host-rock contact zone reveal the isolation of a magnetization similar to that of the dike at site BT29, of east-southeast declination and shallow positive inclination. Notably, all specimens, as well as those from samples of the BT29 dike, also show the initial removal of a magnetization of north to north-northwest declination and relatively steep negative inclination. This first-removed magnetization (interpreted to be of normal polarity) was clearly acquired after the emplacement of the Karoo dike. Site BT51 is in a light gray-green siltstone, some 45 m to the east of the eastern margin of another (∼1.25 m wide) Karoo dike (sampled repeatedly as sites BT3, BT30, BT52). Specimens from samples from site BT51 exhibit a behavior similar to that at site BT35, and show the first removal of a normal polarity (north-northwest and steep negative) magnetization and then the isolation of an east-southeast and shallow positive inclination magnetization. In (B), are shown data from specimens from samples from sites that predominantly yield only a north-northwest and relatively steep negative inclination magnetization, interpreted to be of normal polarity. All data are show in geographic (*in situ*) coordinates.

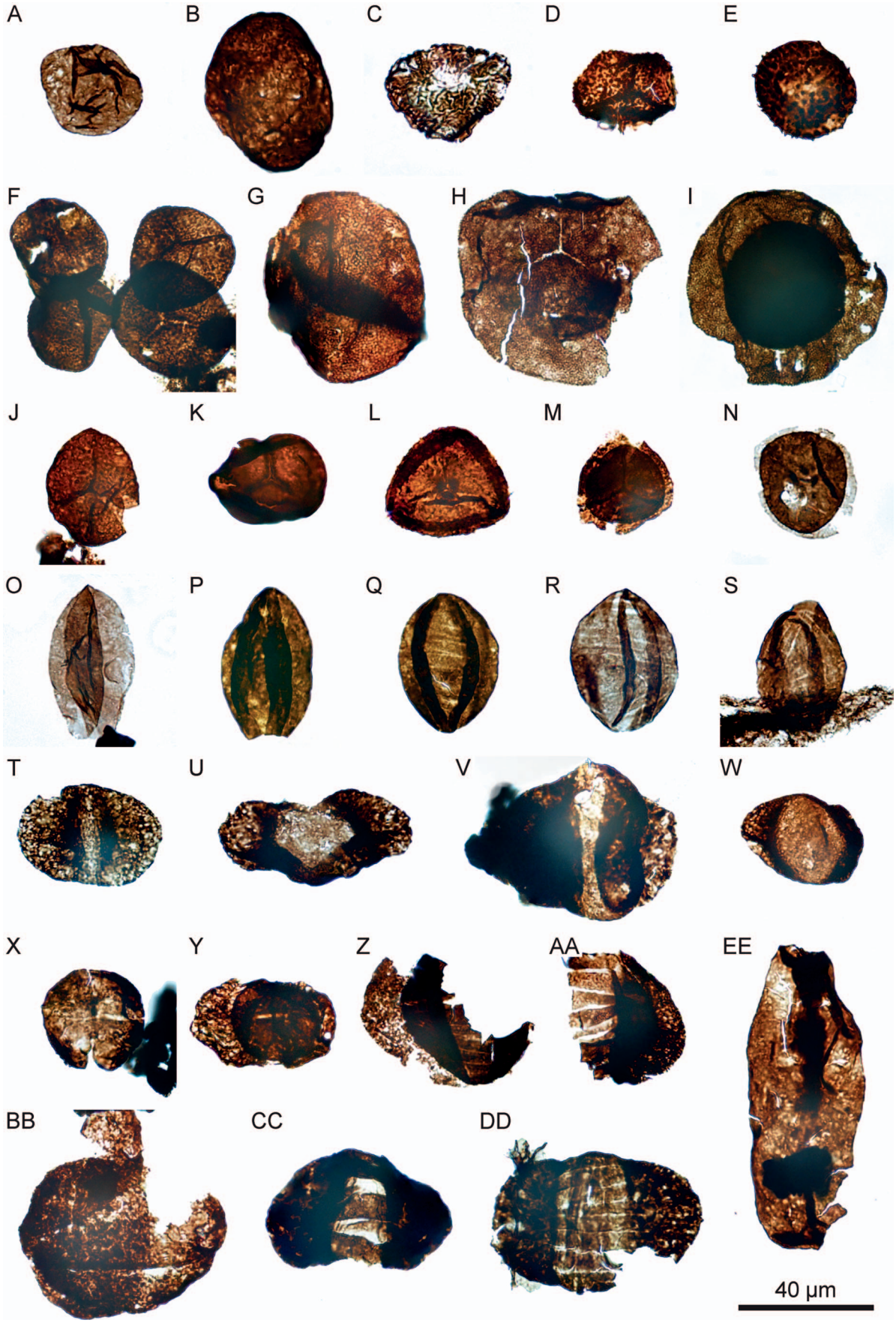

assemblage zones in this area. Rather, it appears that the assemblage-zone boundary is a function of the spatial distribution of taxa traditionally assigned to either the *Daptocephalus* (= *Dicynodon*) or *Lystrosaurus* Assemblage according to the prevailing paradigm. Hence, based on the original raw data, there appears to be overlap in the ranges of vertebrate taxa used to separate two distinctive assemblage zones (Fig. 13).

Palynological Age Assignment

Barbolini (2014, p. 102; Barbolini et al. 2018) reports recovering two palynomorph assemblages from the Elandsberg and Palingkloof members of the Balfour Formation (Fig. 1). One locality is in the Eastern Cape Province, whereas the other is located in the Free State (see discussion in Online Supplemental File). The first locality is from a roadside outcrop along the R390 from Steynsburg to Venterstad (Barbolini 2014; sample 14, see Online Supplemental File Fig. 9), in the vicinity of Bethulie, that is reported to be at the biozone contact; the second is on the Donald 207 farm reported as the "Permian–Triassic boundary" (Barbolini 2014; sample 15, see Online Supplemental File Fig. 10). The GPS coordinates published for sample 15 site lie in the *Lystrosaurus* AZ (Figs. 5, 9; see Online Supplemental File), ~50 m in elevation above the "classic" Bethel farm horizon used as reference in the current contribution (Smith and Botha-Brink 2014, fig. 4; Gastaldo et al. 2017, their figs. 3–6). The Donald 207 exposure is 2.3 m-thick and is located in a shallow erosional gully. The succession consists of: (1) a 50-cm thick interval of 11 cycles of light olive gray, sandy coarse siltstone, each of which fine upward to siltstone of the same color; and (2) a 1-m thick interval of interbedded poorly sorted, fining up successions of very fine-to-medium, yellowish-gray wacke. *Katbergia* burrows (Gastaldo and Rolerson 2008) are preserved in a basal olive-gray siltstone and overlying reddish-gray siltstone, whereas vertebrate burrows are found in siltstone mottled olive- and reddish-gray. Barbolini (2014) interprets the palynological assemblage recovered from these rocks as Permian, with some elements that are dominant in late Permian assemblages and taxa that became dominant in the early Triassic. Barbolini et al. (2018) suggest a Wuchiapingian–Changhsingian age for their palynological interval zone (K11; FAD of *Dictyophyllidites mortonii* and/or *Aratrisporites* sp.) based on this assemblage.

The Australian palynostratigraphic zones are among the very few in the southern hemisphere that have been calibrated against well-dated marine invertebrate zones (Foster and Archbold 2001) and, more recently, U–Pb zircon dates (Metcalfe et al. 2015; Laurie et al. 2016; Fielding et al. 2019). As such, these Australian biozones are considered to be the palynological standard for Gondwana. Each biozone is based largely on the first, or consistent, occurrence of indicator taxa in western (e.g., Mory and Backhouse 1997) and eastern Australian basins (e.g., Price 1997). Several of these indicator taxa either are rare, do not occur in the Karoo Basin, or appear in a different stratigraphic order (suggesting diachrony across Gondwana; Barbolini et al. 2016). Hence, our comparisons rely on relative proportions of major spore-and-pollen categories with Australia and the overall species associations as reported by Barbolini et al. (2016).

The eastern Australian APP6 zone (Price 1997) and the western Australian *Protohaploxypinus microcorpus* Zone (Mory and Backhouse 1997) are the youngest zones with their upper boundaries placed in the Changhsingian. It is within these biozones that a major floral change is recorded; assemblages dominated by taeniate bisaccates are replaced by assemblages rich in non-taeniate alete bisaccates and cavate spores. This palynofloral change occurs at the transition of the APP601–APP602 subzones and the basal part of the *P. microcorpus* zone; it coincides with the negative excursion in $\delta^{13}C$ of organic matter that is associated with the end-Permian biotic crisis (Metcalfe et al. 2008, 2015). The diversity and abundance of both taeniate and non-teaniate bisaccates is still relatively high in the APP601 and basal *P. microcorpus* zones. In both Australia and Antarctica, these assemblages are associated with the last occurrences of characteristic Permian *Glossopteris* megafloras (e.g., Foster 1982; Collinson et al. 2006; Fielding et al. 2019). During the transition between zones, there is a decline in the proportion of multitaeniate bisaccate taxa while, at the same time, simple and cavate spores (e.g., *Densoisporites* and *Lundbladispora*) and specific taeniate taxa (e.g., *Lueckisporites*, *P. microcorpus*, and *Lunatisporites noviaulensis*) become dominant. A similar change in floral composition has been recorded from high-resolution records from the central Transantarctic and Prince Charles Mountains in Antarctica, and shows a stepwise disappearance of characteristic late Permian taxa (Lindström et al. 1997; Collinson et al. 2006; Vajda and McLoughlin 2007).

The Donald 207 palynological assemblage is considered to be contemporaneous and equivalent to those of the subzone APP602 of Price (1997), and the non-basal part of the *Protohaploxypinus microcorpus* Zone (Mory and Backhouse 1997). This assignment is based on: (1) the low abundance and diversity of characteristic late Permian multitaeniate pollen taxa (e.g., *Protohaploxypinus*); (2) the presence of pollen taxa that become dominant in latest Permian and Triassic palynofloras (*Falcisporites* and *Lunatisporites*); (3) on a relatively high abundance and diversity of cavate/cingulate spores *(Densoisporites*, *Playfordiaspora*, *Limatulasporites*) and acavate spores (*Cyclogranisporites* and *Brevitriletes*); and (4) the presence of fungal remains of *Reduviasporonites*. Similar assemblages were described by Steiner et al. (2003) as the *Klausipollenites schaubergeri* zone from the southern Karoo Basin at Carlton Heights. Although originally interpreted as part of the Katberg Formation, this section is considered as part of the Balfour Formation (see Prevec et al. 2010; Barbolini et al. 2018). The assemblages from both Donald 207 and the Carlton Heights' *K. schaubergeri* zone conform with Barbolini et al.'s (2018) *Dictyophyllidites mortonii* Interval Zone and, based on comparison with the Australian and Antarctica sections, are considered late Changhsingian in age.

These biostratigraphic assignments conform with the palynological conclusions published by Prevec et al. (2010) at Wapadsberg Pass, and Gastaldo et al. (2015, 2017) at Old Lootsberg Pass. Yet, the collection site is identified as representing the PTB (see Online Supplemental File), ~50 m above the base of the *Lystrosaurus* AZ. Its recognition as the PTB, presumably, is based on a lithologic succession that mimics the "unique" heterolithic unit of previous end-Permian models (Smith and Ward 2001; Ward et al. 2000, 2005; Smith and Botha-Brink 2014; Botha-Brink et al.

←

FIG. 12.—Representative palynomorphs recovered from Donald 207 farm at the location reported by Barbolini (2014; see Online Supplemental File). Scale bar = 40 μm. Taxonomic names are followed by a UCMP collection locality number code (i.e., LN1 for UCMP PA1351.1, or LN2 for UCMP PA1351.2), the UCMP specimen number, and England Finder graticule coordinates. **A**) *Leiosphaeridia* sp. (LN2, 398634, V50-3). **B**) indet. palynomorph (LN1, 398635, E43-3/4). **C**) cf. *Camptotriletes warchianus* (LN2, 398636, S39-2). **D**) *Brevitriletes bulliensis* (LN1, 398637, E53-3). **E**) *Brevitriletes bulliensis* (LN2, 398638, P62-2). **F**) *Cyclogranisporites gondwanensis* (LN1, 398639, O36-2). **G**) *Inaperturopollenites nebulosus* (LN2, 398640, T55-3). **H**) *Playfordiaspora crenulata* (LN1, 398641, Y41-1/2). **I**) *Playfordiaspora crenulata* (LN2, 398642, M49-3). J) *Cyclogranisporites gondwanensis* (LN2, 398643, P43-1). **K**) *Limatulasporites fossulatus* (LN2, 398644, N48-1). **L**) *Limatulasporites limatulus* (LN2, 398645, T62-3). **M**) *Densoisporites playfordii* (LN1, 398646, G65-4). **N**) *Densoisporites playfordii* (LN1, 398647, E44-2). **O**) *Cycadopites cymbatus* (LN1, 398648, L63-1). **P**) *Marsupipollenites triradiatus* (LN2, 398649, M49-4). **Q**) *Marsupipollenites striatus* (LN1, 398650, K61-2). **R**) *Marsupipollenites striatus* (LN2, 398651, K36-1). **S**) *Weylandites lucifer* (LN1, 398652, E42-4). **T**) *Scheuringipollenites ovatus* (LN2, 398653, H56-4). **U**) *Pteruchipollenites* cf. *gracilis* (LN1, 398654, L41-3). **V**) *Falcisporites australis* (LN2, 398655, G37-3/4). **W**) *Alisporites tenuicorpus* (LN1, 398656, J48-4). **X**) *Corisaccites alutas* (LN2, 398657, P45-4). **Y**) *Lueckisporites virkkiae* (LN2, 398658, S46-2). **Z**) *Protohaploxypinus* sp. (LN2, 398659, G36-1/2). **AA**) *Protohaploxypinus* sp. (LN1, 398660, F65-3). **BB**) *Guttulapollenites hannonicus* (LN1, 398661, M49-1). **CC**) *Lunatisporites pellucidus* (LN1, 398662, H55-3). **DD**) *Hamiapollenites insolitus* (LN2, 398663, T50-4). **EE**) *Reduviasporonites* sp. (LN1, 398664, M49-1).

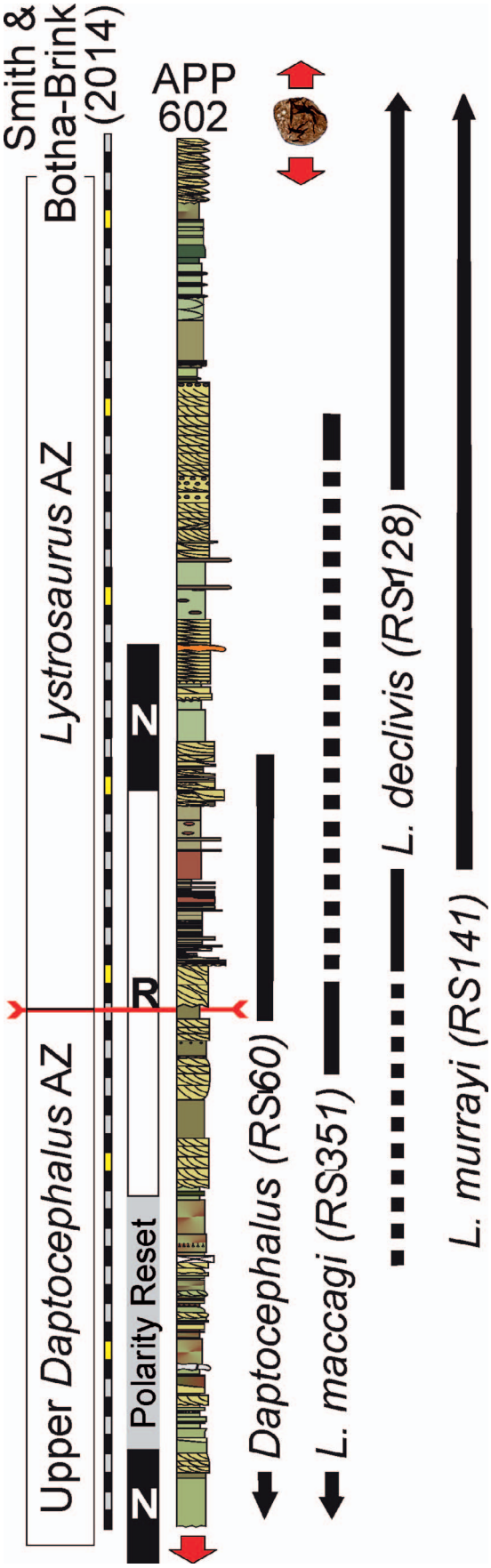

2014, and others). This, alone, demonstrates the ineffectiveness and lack of utility of any lithologic boundary criterion (Gastaldo et al. 2009; Gastaldo and Neveling 2012; Neveling et al. 2016a). Hence, currently there are three different stratigraphic positions reported in the literature, across the distance of 4.5 km from Bethulie to Donald 207 and at three different elevations, at which the purported biozone boundary (equated by other workers to represent the PTB) is reported to exist: two on the Bethel farm (Gastaldo et al. 2009) and one on Donald 207 (Barbolini 2014).

Magnetostratigraphic Implications and Correlation with Old Lootsberg Pass

The magnetostratigraphic record on the Bethel farm consists of two normal polarity magnetozones below and above a long reverse polarity magnetozone (Figs. 5, 13; see Online Supplemental File Fig. 4), based on analyses of 71 discrete, competent beds over a stratigraphic thickness of 94 m. Notably, neither the base nor the top of the reverse polarity magnetozone is well defined, as these intervals have been thermally affected by the emplacement of thin Karoo dikes. Nevertheless, our new results extend the stratigraphic interval of the reverse polarity magnetozone first reported by Neveling et al. (2016a) to encompass the interval below, across, and above the proposed *Daptocephalus–Lystrosaurus* AZ boundary of Smith and Botha-Brink (2014; Fig. 5). A similar magnetostratigraphy is documented for Old Lootsberg Pass, where the stratigraphic thickness of the interval across the biozone boundary is greater. Yet, the reverse polarity magnetozones identified at Old Lootsberg Pass are stratigraphically thinner due to hiatuses and the emplacement of erosive-based fluvial sandstone with intraformational pedogenic nodule conglomerate (Gastaldo et al. 2018).

Gastaldo et al. (2015, 2017) demonstrated the presence of both *Glossopteris* and *Daptocephalus* AZ taxa above the proposed biozone boundary, as circumscribed by Smith and Botha-Brink (2014) based on the reported stratigraphic positions of vertebrate taxa in their database at Old (West) Lootsberg Pass. These fossils are preserved in olive- and greenish-gray siltstone, and as components of channel-lag deposits of intraformational Pedogenic Nodule Conglomerate (PNC; Pace et al. 2009; Gastaldo et al. 2018), respectively. A dicynodontoid skull recovered from a PNC, above the proposed assemblage zone contact by Smith and Botha-Brink (2014), exhibits features consistent with the genera *Dicynodon*, *Daptocephalus*, and *Dinanomodon*, as well as *Lystrosaurus maccaigi* and *L. curvatus* (Gastaldo et al. 2017). The skull's stratigraphic position lies in a PNC directly above the erosional contact of a sandstone body in which a normal polarity chron is identified (Gastaldo et al. 2018). Directly beneath the erosional contact is a short, 1.5-m-thick siltstone in which a reverse polarity magnetozone is recorded. Subjacent rocks to this siltstone interval primarily record a normal polarity magnetozone.

The magnetostratigraphic pattern, in conjunction with the vertebrate paleontology at the Bethel farm, provides a basis on which to propose a correlation between the Free State succession and Old Lootsberg Pass. The presence of a *Glossopteris* flora and, possibly, vertebrate taxa of the

←

FIG. 13.—A summary diagram consisting of our composite measured stratigraphic section (see Fig. 5) against which are placed: results of our magnetostratigraphic analyses; the *Daptocephalus/Lystrosaurus* Assemblage Zone boundary as identified by Smith and Botha-Brink (2014) and others (e.g., Ward et al. 2005; Botha and Smith 2007); the stratigraphic range of three vertebrate taxa (*Daptocephalus*, formerly *Dicynodon* [but see Lucas 2017, 2018], *Lystrosaurus maccaigi*, and *L. declivis*) identified by other workers as being restricted to one assemblage zone but found to occur in a stratigraphic position either above (*Daptocephalus*, *L. maccaigi*) or below (*L. declivis*) the boundary; and the position of the latest Changhsingian palynoflora recovered from the *Lystrosaurus* Assemblage Zone, as currently accepted. Stippled parts of range represent uncertainty in lowest or highest taxon occurrence due to the absence of original metadata and request for GPS clarification from the original authors.

Daptocephalus AZ at both Bethel farm (Fig. 5) and Old Lootsberg Pass (Gastaldo et al. 2015), preserved in the upper normal polarity magnetozone, stratigraphically above the reverse polarity magnetozone, intimates the possibility that a temporal relationship exists between the two sections. We interpret that this relationship also is correlative. Gastaldo et al. (2015, 2018) report an early Changhsingian U-Pb ID-TIMS age for a synsedimentary ashfall deposit, ~80 m below the upper short, reverse polarity chron in the Old Lootsberg Pass section. Based on a combination of magnetostratigraphy and geochronometry, Gastaldo et al. (2015, 2017) concluded that the reported *Daptocephalus* to *Lystrosaurus* turnover, which they place above the stratigraphic position of the dicynodontoid skull preserved in a PNC lag deposit, is not latest Changhsingian (Gastaldo et al. 2018). And, that turnover is not coincident with the end-Permian extinction event as recognized in the marine record. This conclusion appears to be corroborated by the results of the current work demonstrating: (1) the presence of *Daptocephalus* AZ vertebrate taxa in the *Lystrosaurus* AZ (Figs. 5, 6, 13) on the Bethel farm; (2) a latest Permian-aged palynoflora (Barbolini 2014) in a stratigraphic position ~50 m above the assemblage zone contact; and (3) a long reverse polarity magnetozone that spans the stratigraphic interval in which vertebrate extinction, turnover, and rapid recovery are reported to have occurred. The end-Permian crisis in the marine realm is well-documented to lie in strata that define a normal polarity magnetozone. Furthermore, many relatively recent compilations of the geomagnetic polarity time scale across the Permian–Triassic boundary place the end-Permian crisis in a normal polarity chron of up to ~700 ka duration (e.g., Szurlies 2013).

CONCLUSIONS

The traditional, and currently accepted, model for the response of terrestrial ecosystems to the end-Permian extinction event relies on the high-resolution placement of vertebrates in generalized stratigraphies spanning the *Daptocephalus* and *Lystrosaurus* Assemblage Zones. Based on this claim of accuracy and resolution, a stepped (Ward et al. 2005) or three-phased turnover-and-extinction model (Smith and Botha-Brink 2014) was developed and has been equated with the step-wise extinction event in the marine realm. In an empirical test of the data on the Bethel, Heldenmoed, and Donald 207 farms in the Free State Province, where 73% of the vertebrates collected form the basis of the published terrestrial model, we have been unable to replicate many of the observations and conclusions drawn from these "classic" localities. Our data indicate that there is an overlap in biostratigraphic ranges of the critical taxa (i.e., *Dicynodon=Daptocephalus*; *Lystrosaurus maccaigi*, *L. declivis*; Fig. 13) used to define the three-phased model at these sites and, as such, no sharp or abrupt boundary can be identified across which vertebrate turnover is documented. Difference in the FAD (or LO) and LAD (or HO) of taxa and their reported transition at these, and other Karoo Basin localities, may be a consequence of both low numbers of critical specimens per any locality and taphonomic bias associated with the areas over which collections have been made. The pattern we document here, based on the original data used by Smith and Botha-Brink (2014), conforms to the interpretations of Sues and Frasier (2010) and Schneider et al. (in press, fig. 16) that there was no vertebrate-extinction crisis across the Permian–Triassic boundary.

We have recovered palynological assemblages from high in the *Lystrosaurus* AZ, ~ 50 m higher stratigraphically than the proposed biozone boundary, from where Barbolini (2014) identified another Permian–Triassic boundary interval (see Online Supplemental File). Our palynological data, conforming to Barbolini et al. (2018), indicate that at least the base of the *Lystrosaurus* AZ is of late Changhsingian age. The palynoflora, although containing typical early Triassic taxa, is characteristic of other palynological assemblages recovered from the interval across the vertebrate assemblage zone (Steiner et al. 2003) and are comparable to latest Permian, post-collapse assemblages in Australia (e.g., Fielding et al. 2019). The late Changhsingian age of the palynoflora accords well with the magnetostratigraphic record derived from 71 discrete beds on the Bethel and Heldenmoed farms. We document a long reverse polarity magnetozone that begins meters below the purported boundary, transitions the assemblage-zone contact, and extends into the base of the *Lystrosaurus* AZ as currently recognized. As recorded in the marine realm, however, the end-Permian event occurred during a normal polarity chron. The Bethel/Heldenmoed pattern is similar to that reported by Gastaldo et al. (2018) from Old Lootsberg Pass, which is geochronometrically age constrained, and interpreted to be early Changhsingian. The only data point missing to unequivocally demonstrate a late Permian age assignment for the *Lystrosaurus* AZ, if it exists as currently defined, is a high-resolution geochronometric age constraint.

ACKNOWLEDGMENTS

The authors appreciate the hospitality and kindness shown to them over past decade by: Pieter and Ansie Grobelaar, Bethel Farm; Pieter Steyn, Donald 207; and Anthony Hocking and the staff at the Bethulie Royal Hotel. Field assistance by S. Gray, D. Pace, K. Clark, S. Newberry, O. Battifarano, A. Churchill, and S. Harrison, Colby College, and S. Makubalo, Council for Geosciences, are acknowledged and appreciated. Dirk Grobbelaar, Council for Geoscience, is thanked for conversion of GPS coordinates to Cape Datum standards and providing us with the .kmz file for analysis, and Ivo Duijnstee, UC-Berkeley, is thanked for his palyno-plate assembling skills. Colby student participation was supported by the Selover Family student-research endowment and Barrett T. Dixon Geology Research and Internship Fund for undergraduate experiences in the Department of Geology. PIs research efforts were supported, in part, by: the Council for Geoscience (South Africa); JWG startup funds at the University of Texas–Dallas; and NSF EAR 0749895, 0934077, 1123570, and 1624302 to RAG. Comments by two anonymous reviewers, Dr. Spencer Lucas, and Dr. Patrick Orr strengthened the final manuscript draft.

SUPPLEMENTAL MATERIAL

Data are available from the PALAIOS Data Archive: https://www.sepm.org/supplemental-materials.

REFERENCES

Abdala, F., Cisneros J.C., and Smith, R.M.H., 2006, Faunal aggregation in the early Triassic Karoo Basin: earliest evidence of shelter-sharing behavior among tetrapods?: PALAIOS, v. 21, p. 507–512.

Barbolini, N., 2014. Palynostratigraphy of the South African Karoo Supergroup and Correlations with Coeval Gondwanan Successions: Unpublished Ph.D. Thesis, University of the Witwatersrand, Johannesburg, South Africa, 386 p.

Barbolini, N., Bamford M.K., and Rubidge B., 2016. Radiometric dating demonstrates that Permian spore pollen zones of Australia and South Africa are diachronous: Gondwana Research, v. 37, p. 241–251.

Barbolini, N., Rubidge, B., and Bamford, M.K., 2018, A new approach to biostratigraphy in the Karoo retroarc foreland system: utilizing restricted-range palynomorphs and their first appearance datums for correlation: Journal of African Earth Sciences, v. 140, p. 114–133.

Benton, M.J. and Newell, A.J., 2014, Impacts of global warming on Permo–Triassic terrestrial ecosystems: Gondwana Research, v. 25, p. 1308–1337, doi:10.1016/j.gr.2012.12.010.

Boonstra, L.D., 1969, The fauna of the Tapinocephalus Zone (Beaufort Beds of the Karoo): Annals of the South African Museum, v. 56, 73 p.

Botha, J. and Smith, R.M.H., 2006, Rapid vertebrate recuperation in the Karoo Basin of South Africa following the end-Permian extinction: Journal of African Earth Sciences, v. 45, p. 502–514, doi:10.1016/j.jafrearsci.2006.04.006.

Botha, J. and Smith, R.M.H., 2007, *Lystrosaurus* species composition across the Permo–Triassic boundary in the Karoo Basin of South Africa: Lethaia, v. 40, p. 125–137.

Botha-Brink, J., Huttenlocker, A.K., and Modesto, S.P., 2014, Vertebrate paleontology of Nooitgedacht 68: a *Lystrosaurus maccaigi*-rich Permo–Triassic boundary locality in South Africa, *in* C.F. Kammerer, K.D. Angielczyk, and J. Fröbisch (eds.), Early Evolutionary History of the Synapsida, Vertebrate Paleobiology and Paleoanthropology: Springer, Dordrecht, p. 289–304, doi: 10.1007/978-94-007-6841-3_17.

Broom, R., 1906, On the Permian and Triassic faunas of South Africa: Geological Magazine, Decade, v. 5, p. 29–30.

Broom, R., 1907, On the geological horizons of the vertebrate genera of the Karroo Formation: Records of the Albany Museum, v. 2, p. 156–163.

Broom, R., 1909, An attempt to determine the horizons of the fossil vertebrates of the Karroo: Annals of the South African Museum, v. 7, p. 285–289.

Broom, R., 1911, On some new South African Permian reptiles: Proceedings of The Zoological Society of London 1911, p. 1073–1082.

Burgess, S.D., Bowring, S., and Shen, S.Z., 2014, High-precision timeline for Earth's most severe extinction: Proceedings of the National Academy of Science, v. 111, p. 3316–3321, doi: 10.1073/pnas.1317692111.

Catuneanu, O., Wopfner, H., Eriksson, P.G., Cairncross, B., Rubidge, B.S., Smith, R.M.H., and Hancox, P.J., 2005, The Karoo basins of southcentral Africa: Journal of African Earth Sciences, v. 43, p. 211–253.

Collinson, J.W., Hammer, W.R., Askin, R.A., and Elliot, D.H., 2006, Permian–Triassic boundary in the central Transantarctic Mountains, Antarctica: Geological Society of America Bulletin, v. 118, p. 747–763.

Day, M.O., Ramezani, J., Bowring, S.A., Sadler, P.M., Erwin, D.H., Abdala, F., and Rubidge, B.S., 2015, When and how did the terrestrial mid-Permian mass extinction occur? Evidence from the tetrapod record of the Karoo basin, South Africa: Proceedings of the Royal Society of London, B, v. 282, 20150834.

De Kock, M.O. and Kirschvink, J.L., 2004, Paleomagnetic constraints on the Permian–Triassic boundary in terrestrial strata of the Karoo Supergroup, South Africa: implications for causes of the end-Permian extinction event: Gondwana Research, v. 7, p. 175–183.

De Wit, M.J., 2016, Organic Carbon Isotope Stratigraphy of the Karoo Supergroup, *in* M.J. de Wit and B. Linol (eds.), The Origin and Evolution of the Cape Mountains and Karoo Basin: Springer Publishing, New York, p. 161–182.

Duncan, R.A., Hooper, P.R., Rehacek, J., Marsh, J.S., and Duncan, A.R., 1997, the timing and duration of the Karoo igneous event, southern Gondwana: Journal of Geophysical Research, v. 102, p. 18,127–18,138.

Fielding, C.R., Frank, T.D., McLoughlin, S., Vajda, V., Mays, C., Tevyaw, A.P., Winguth, A., Winguth, C., Nicoll, R.S., Bocking, M., and Crowley, J.L., 2019, Age and pattern of the southern high-latitude continental end-Permian extinction constrained by multiproxy analysis: Nature Communications, v. 10, article 385, doi: 10.1038/s41 467-018-07934.

Foster, C.B., 1982, Spore-pollen assemblages of the Bowen Basin, Queensland (Australia): their relationship to the Permian/Triassic boundary: Review of Palaeobotany and Palynology, v. 36, p. 165–183.

Foster, C.B. and Archbold, N.W., 2001, Chronologic anchor points for the Permian and Early Triassic of the Eastern Australian Basins, *in* R.H. Weiss (ed.), Contributions to Geology and Palaeontology of Gondwana in Honour of Helmut Wopfner: Geological Institute, University of Cologne, Germany, p. 175–197.

Gastaldo, R.A., Adendorff, R., Bamford, M.K., Labandeira, C.C., Neveling, J., and Sims, H.J., 2005, Taphonomic trends of macrofloral assemblages across the Permian–Triassic boundary, Karoo Basin, South Africa: PALAIOS, v. 20, p. 479–497.

Gastaldo, R.A. and Demko, T.M., 2011, Long term hydrology controls the plant fossil record, *in* P.A. Allison and D.J. Bottjer (eds.), Taphonomy, second edition: Processes and Bias Through Time: Topics in Geobiology, v. 32, p. 249–286, doi 10.1007/978-90-481-8643-3_7.

Gastaldo, R.A. Kamo, S.L., Neveling, J., Geissman, J.W., Bamford, M., and Looy, C.V., 2015, Is the vertebrate defined Permian–Triassic boundary in the Karoo Basin, South Africa, the terrestrial expression of the End Permian marine event?: Geology, v. 43, p. 939–942, doi:10.1130/G37040.1.

Gastaldo, R.A., Knight, C.L., Neveling, J., and Tabor, N.J., 2014, Latest Permian paleosols from Wapadsberg Pass, South Africa: implications for Changhsingian climate: Geological Society of America Bulletin, v. 126, p. 665–679, doi: 10.1130/B30887.1.

Gastaldo, R.A. and Neveling, J., 2012, The terrestrial Permian–Triassic boundary event bed is a non-event, Comment and Reply: Geology, v. 37, p. 199 –202.

Gastaldo, R.A. and Neveling, J., 2016, Comment on: "Anatomy of a mass extinction: sedimentological and taphonomic evidence for drought-induced die-offs at the Permo–Triassic boundary in the main Karoo Basin, South Africa": Palaeogeography, Palaeoclimatology, Palaeoecology, v. 396, p. 99–118, doi: 10.1016 /j .palaeo .2014 .01.002.

Gastaldo, R.A., Neveling, J., Clark, C.K., and Newbury, S.S., 2009, The terrestrial Permian–Triassic boundary event bed is a non-event: Geology, v. 37, p. 199–202, doi:10.1130/G25255A.1.

Gastaldo, R.A., Neveling, J., Geissman, J.W., and Kamo, S.L., 2018, A lithostratigraphic and magnetostratigraphic framework in a geochronologic context for a purported Permian–Triassic boundary section at Old (West) Lootsberg Pass, Karoo Basin, South Africa: Geological Society of America Bulletin, v. 130, p. 1411–1438, doi: 10 .1130 / B31881.1.

Gastaldo, R.A., Neveling, J., Geissman, J.W., and Li., J.W., 2019, A multidisciplinary approach to review the vertical and lateral facies relationships of the purported vertebrate-defined terrestrial boundary interval at Bethulie, Karoo Basin, South Africa: Earth Science Reviews, v. 189, p. 220–243, doi: 10.1016/j.earscirev.2017.08.002.

Gastaldo, R.A., Neveling, J., Looy, C.V., Bamford, M.K., Kamo, S.L., and Geissman, J.W., 2017, Paleontology of the Blaauwater 67 Farm, South Africa: testing the *Daptocephalus/Lystrosaurus* Biozone boundary in a stratigraphic framework: PALAIOS, v. 34, p. 349–366, doi: 10.2110/palo.2016.106.

Gastaldo, R.A., Pludow, B.A., and Neveling, J., 2013, Mud aggregates from the Katberg Formation, South Africa: additional evidence for Early Triassic degradational landscapes: Journal of Sedimentary Research, v. 83, p. 531–540.

Gastaldo, R.A. and Rolerson, M.W., 2008, *Katbergia* gen. nov., a new trace fossil from the Upper Permian and Lower Triassic Rocks of the Karoo Basin: implications for paleoenvironmental conditions at the P/Tr extinction event: Palaeontology, v. 51, p. 215–229.

Goddard, E.N., Trask, P.D., De Ford, R.K., Rove, O.N., Singewald, J.T., and Overbeck, R.N., 1975, Rock color chart: The Geological Society of America, Boulder, Colorado, 11 p.

Johnson, M.R., Anhaeusser, C.R., and Thomas, R.J., Eds., 2006, The Geology of South Africa, second edition: The Geological Society of South Africa, Johannesburg and the Council for Geoscience, Pretoria, 691 p.

Jourdan, F., Feraud, G., Bertrand, H., Bashira Kampunzu, A., Tshoso, G., Watkeys, M.K., and Le Gall, B., 2005, Karoo large igneous province: brevity, origin, and relation to mass extinction questioned by new $^{40}Ar/^{39}Ar$ age data: Geology, v. 33, p. 745–748.

Keyser, A.W., 1981, The stratigraphic distribution of the Dicynodontia of Africa reviewed in a Gondwana context, *in* M.M. Creswell and P. Vella (eds.), Gondwana Five: A.A. Balkema, Rotterdam, p. 61–64.

Keyser, A.W., 1979, A review of the biostratigraphy of the Beaufort Group in the Karoo Basin of South Africa: Geological Society of South Africa, 15th Geocongress, Abstracts, Part 2, p. 13–31.

Keyser, A.W. and Smith, R.H.M., 1978, Vertebrate biozonation of the Beaufort Group with special reference to the Western Karoo Basin: Annals of the Geological Survey, v. 12(1977–1978), p. 1–35.

Kirschvink, J.L., 1980, The least squares line and plane and the analysis of paleomagnetic data: Geophysical Journal of the Royal Astronomical Society, v. 62, p. 699–718.

Kitching, J.W., 1971, A short review of the Beaufort zoning in South Africa, *in* S.H. Haughton (ed.), Second Gondwana Symposium, Proceedings and Papers, p. 309–312.

Kitching, J.W., 1977, The distribution of the Karoo vertebrate fauna: Memoir of the Bernard Price Institute for Palaeontological Research, University of the Witwatersrand, v. 1, p. 1–131.

Kutty, T.S., 1972, Permian reptilian fauna from India: Nature, v. 237, p. 462–463.

Laurie, J.R., Bodorkos, S., Nicoll, R.S., Crowley, J., Mantle, J.D., Mory, A.J., Wood, G.R., Backhouse, J., Holmes, E.K., Smith, T.E., and Champion, D.C., 2016, Calibrating the middle and late Permian palynostratigraphy of Australia to the geologic timescale via UePb zircon CA-IDTIMS dating: Australian Journal of Earth Science, v. 63, p. 701–730.

Li, J., Gastaldo, R.A., Neveling, J., and Geissman, J.W., 2017, Siltstones across the *Daptocephalus* (*Dicynodon*) and *Lystrosaurus* Assemblage zones, Karoo Basin, South Africa, show no evidence for aridification: Journal of Sedimentary Research, v. 87, p. 653–671, doi: 10.2110/jsr.2017.35.

Lindeque, A., de Wit, M.J., Ryberg, T., Weber, M., and Chevallier, I., 2011, Deep crustal profile across the southern Karoo Basin and Beattie magnetic anomaly, South Africa: an integrated interpretation with tectonic implications: South African Journal of Geology, v. 114, p. 265–292.

Lindström, S., McLoughlin, S., and Drinnan, A.N., 1997, Intraspecific variation of taeniate bisaccate pollen within Permian glossopterid sporangia, from the Prince Charles Mountains, Antarctica: International Journal of Plant Sciences, v. 158, p. 673–684.

Lucas, S.G., 2009, Timing and magnitude of tetrapod extinctions across the Permo–Triassic boundary: Journal of Asian Earth Sciences, v. 36, p. 491–502.

Lucas, S.G., 2010, The Triassic timescale based on nonmarine tetrapod biostratigraphy and biochronology: Geological Society of London, Special Publications, v. 334, p. 447–500.

Lucas, S.G., 2017, Permian tetrapod extinction events: Earth Science Reviews, v. 170, p. 31–60.

Lucas, S.G., 2018, Permian tetrapod biochronology, correlation and evolutionary events: *in* S.G. Lucas and S.Z. Shen (eds.), The Permian Timescale, Geological Society, London, Special Publications, v. 450, doi: 10.1144/SP450.

MacLeod, K.G., Smith, R.M., Koch, P.L., and Ward, P.D., 2000, Timing of mammal-like reptile extinctions across the Permian–Triassic boundary in South Africa: Geology, v. 28, p. 227–230.

MacLeod, K.G., Quinton, P.C., and Bassett, D.J., 2017, Warming and increased aridity during the earliest Triassic in the Karoo Basin, South Africa, Geology, v. 45, p. 483–486.

Marchetti, L., Klein, H., Buchwitz, M., Ronchi, A., Smith, R.M.H., De Klerk, W.J., Sciscio, L., and Groenewald, G.H., in press, Reply to discussion of ''Permian—Triassic vertebrate footprints from South Africa: Ichnotaxonomy, producers and biostratigraphy through two major faunal crises" by Marchetti, L., Klein, H., Buchwitz, M., Ronchi, A., Smith, R.M.H., DeKlerk, W.J., Sciscio, L., and Groenewald, G.H. (2019): Gondwana Research, doi: https://doi.org/10.1016/j.gr.2019.08.002.

Marshall, C., 2005, Comment on "Abrupt and Gradual Extinction Among Late Permian Land Vertebrates in the Karoo Basin, South Africa": Science, v. 308, p. 1413, doi: 10.1126/science.1110443.

McElwain, J.C. and Punyasena, S., 2007, Mass extinction events and the plant fossil record: Trends in Ecology and Evolution, v. 22, p. 548–557.

Metcalfe, I., Crowley, J.L., Nicoll, R.S., and Schmitz, M., 2015, High-precision U-Pb CATIMS calibration of middle Permian to lower Triassic sequences, mass extinction and extreme climate-change in eastern Australian Gondwana: Gondwana Research, v. 28, p. 61–81.

Metcalfe, I., Nicoll, R.S., and Willink, R.J., 2008, Conodonts from the Permian–Triassic transition in Australia and the position of the Permian–Triassic boundary: Australian Journal of Earth Science, v. 55, p. 365–377.

Mory, A.J. and Backhouse, J., 1997, Permian stratigraphy and palynology of the Carnarvon Basin, Western Australia: Geological Survey of Western Australia, Report 51, p. 1–101.

Neveling, J., Gastaldo, R.A., and Geissman, J.W., 2016a, Permo–Triassic boundary in the Karoo Basin: field trip guide Pre-3: Council for Geoscience, Pretoria, South Africa, 81 p., doi: 10.13140/RG.2.2.22414.15683.

Neveling, J., Gastaldo, R.A., Kamo, S.L., Geissman, J.W., Looy, C., and Bamford, M.K., 2016b, A review of stratigraphic, geochemical, and paleontologic correlation data of the terrestrial end-Permian record in South Africa, *in* M.J. de Wit and B. Linol (eds.), The Origin and Evolution of the Cape Mountains and Karoo Basin: Springer Publishing, New York, p. 151–157.

Pace, D.W., Gastaldo, R.A., and Neveling, J., 2009, Early Triassic aggradational and degradational landscapes of the Karoo basin and evidence for climate oscillation following the P-Tr Event: Journal of Sedimentary Research, v. 79, p. 316–331.

Prevec, R., Gastaldo, R.A., Neveling, J., Reid, S.B., and Looy, C.V., 2010, An autochthonous glossoperid flora with latest Permian palynomorphs from the *Dicynodon* Assemblage Zone of the southern Karoo Basin, South Africa: Palaeogeography, Palaeoclimatology, Palaeoecology, v. 292, p. 381–408.

Price, P.L., 1997, Permian to Jurassic palynostratigraphic nomenclature of the Bowen and Surat Basins, *in* P.M. Green (ed.), The Surat and Bowen Basins, South-East Queensland: Queensland Department of Mines and Energy, p. 137–178.

Retallack, G.J., Smith, R.M.H., and Ward, P.D., 2003, Vertebrate extinction across Permian–Triassic boundary in Karoo Basin, South Africa: Geological Society of America Bulletin, v. 115, p. 1133–1152.

Rey, K., Amiot, R., Fourel, F., Rigaudier, T., Abdala, F., Day, M.O., Fernandez, V., Fluteau, F., France-Lanord, C., Rubidge, B.S., Smith, R.M., Viglietti, P.A., Zipfel, B., and Lécuyer, C., 2016, Global climate perturbations during the Permo–Triassic mass extinctions recorded by continental tetrapods from South Africa: Gondwana Research, v. 37, p. 384–396, doi: 10.1016/j.gr.2015.09.008.

Roopnarine, P.D. and Angielczyk, K.D., 2015, Community stability and selective extinction during the Permian–Triassic mass extinction: Science, v. 350, p. 90–93, doi: 10.1126/science.aab1371.

Roopnarine, P.D., Angielczyk, K.D., Olroyd, S.L., Nesbitt, S.J., Botha-Brink, J., Peecook, B.R., Day, M.O., and Smith, R.M.H., 2017, Comparative ecological dynamics of Permian–Triassic communities from the Karoo, Luangwa, and Ruhuhu basins of southern Africa: Journal of Vertebrate Paleontology, v. 37, supplement 1, p. 254–272.

Roopnarine, P.D., Angielczyk, K.D., Weik, A., and Dineen, A., 2018, Ecological persistence, incumbency and reorganization in the Karoo Basin during the Permian–Triassic transition: Earth-Science Reviews, doi: 10.1016/j.earscirev.2018.10.014.

Rubidge, B.S., (ed.), 1995, Biostratigraphy of the Beaufort Group (Karoo Supergroup): Geological Survey of South Africa Biostratigraphic Series, no. 1, p. 1–46.

Rubidge B.S., Day M.O., Barbolini N., Hancox P.J., Choiniere J., Bamford M.K., Viglietti P.A., McPhee B., and Jirah S., 2016, Advances in nonmarine Karoo biostratigraphy: significance for understanding basin development, *in* M. de Wit and B. Linol (eds.), The Origin and Evolution of the Cape Mountains and Karoo Basin: Springer Publishing, New York, p. 141–149.

Rubidge, B.S., Erwin, D.H., Ramezani, J., Bowring, S.A., and de Klerk, W.J., 2013, High-precision temporal calibration of Late Permian vertebrate biostratigraphy: U-Pb zircon constraints from the Karoo Supergroup, South Africa: Geology, v. 41, p. 363–366.

Schneider, J.W., Lucas, S., Scholze, F., Voigt, S., Marchetti, L., Klein, H., Oplustil, S., Werneburg, R., Golubev, V.K., Barrick, J., Nemyrovska, T., Ronchi, A., Day, M., Silantiev, V., Rößler, R., Saber, H., Linnemann, U., Zharinova, V., and Shen, S., in Press, Late Paleozoic–early Mesozoic continental biostratigraphy: PalaeoWorld.

Shen, S.Z., Crowley, J.L., Wang, Y., Bowring, S.A., Erwin, D.H., Sadler, P.M., Cao, C.Q., Rothman, D.H., Henderson, C.M., Ramezani, J., Zhang, H., Shen, Y., Wang, X.D., Wang, W., Mu, L., Li, W.Z., Tang, Y.G., Liu, X.L., Liu, L.J., Zeng, Y., Jiang, Y.F., and Jin, Y.G., 2011, Calibrating the end-Permian mass extinction: Science, v. 334, p. 1367–1372.

Sidor, C.A., Vilhena, D.A., Angielczyk, K.D., Huttenlocker, A.K., Nesbitt, S.J., Peecook, B.R., Steyer, J.S., Smith, R.M.H., and Tsuji, L.A., 2013, Provincialization of terrestrial faunas following the end-Permian mass extinction: Proceedings of the National Academy of Sciences, v. 110, p. 8129–8133.

Smith, R.M.H., 1995, Changing fluvial environments across the Permian–Triassic boundary in the Karoo Basin, South Africa, and possible causes of tetrapod extinctions: Palaeogeography, Palaeoclimatology, Palaeoecology, v. 117, p. 81–104.

Smith, R.M.H. and Botha, J., 2005, The recovery of terrestrial vertebrate diversity in the South African Karoo Basin after the end-Permian Extinction: Compte Rendu Palevol, v. 4, p. 555–568.

Smith, R.M.H. and Botha-Brink, J., 2014, Anatomy of a mass extinction: sedimentological and taphonomic evidence for drought-induced die-offs at the Permo–Triassic boundary in the main Karoo Basin, South Africa: Palaeogeography, Palaeoclimatology, Palaeoecology, v. 396, p. 99–118.

Smith, R.M.H. and Kitching, J.W., 1995, Biostratigraphy of the Cistecephalus Assemblage Zone, *in* B.S. Rubidge (ed.), Reptilian Biostratigraphy of the Permian–Triassic Beaufort Group (Karoo Supergroup): South Africa Commission on Stratigraphy, Biostratigraphic Series 1, p. 23–28.

Smith, R.M.H. and Ward, P.D., 2001, Pattern of vertebrate extinctions across an event bed at the Permian–Triassic boundary in the Karoo Basin of South Africa: Geology, v. 29, p. 1147–1150.

South African Committee for Stratigraphy, 1980, Stratigraphy of South Africa, Part 1: Africa, South West Africa/Namibia, and the republics of Bophuthatswana, Transkei and Venda: Geological Survey of South Africa, Handbook 8, p. 535–548.

Steiner, M.B., Eshet, Y., Rampino, M.R., and Schwindt, D.M., 2003, Fungal abundance spike and the Permian–Triassic boundary in the Karoo Supergroup (South Africa): Palaeogeography, Palaeoclimatology, Palaeoecology, v. 194, p. 405–414.

Sues, H.D. and Fraser, N.C., 2010, Triassic Life on Land: The Great Transition: Columbia University Press, New York, 236 p.

Svensen, H., Corfu, F., Polteau, S., Hammer, Ø., and Planke, S., 2012, Rapid magma emplacement in the Karoo Large Igneous Province: Earth and Planetary Science Letters, v. 325–326, p. 1–9.

Szurlies, M., 2013, Late Permian (Zechstein) magnetostratigraphy in Western and Central Europe, *in* A. Gasiewicz and M. Stowakiewicz (eds.), Palaeozoic Climate Cycles: Their Evolutionary and Sedimentological Impact: Geological Society of London, Special Publication, v. 376, p.73–85, doi: 10.1144/SP376.7.

Tabor, N.J., Montañez, I.P., Steiner, M. and Schwindt, D., 2007, The d13C values of Permo–Triassic carbonates from South Africa reflect a stinking, sulfurous swamp, not atmospheric conditions: Palaeogeography, Palaeoclimatology, Palaeoecology, v. 225, p. 370–381.

Vajda, V. and McLoughlin, S., 2007, Extinction and recovery patterns of the vegetation across the Cretaceous–Palaeogene boundary— a tool for unravelling the causes of the end-Permian mass extinction: Review of Palaeobotany and Palynology, v. 144, p. 99–112.

Viglietti, P.A., Smith, R.M.H., Angielczyk, K.D., Kammerer, C.F., Frobisch, J., and Rubidge, B.S., 2016, The *Daptocephalus* Assemblage Zone (Lopingian), South Africa: a proposed biostratigraphy based on a new compilation of stratigraphic ranges: Journal of African Earth Sciences, v. 113, p. 153–164.

Viglietti, P.A., Smith, R.M.H., and Compton, S., 2013, Origin and palaeoenvironmental significance of Lystrosaurus bonebeds in the earliest Triassic Karoo Basin, South Africa: Palaeogeography, Palaeoclimatology, Palaeoecology, v. 392, p. 9–21.

Viglietti, P.A., Rubidge, B.S., and Smith, R.M.H., 2017, New Late Permian tectonic model for South Africa's Karoo Basin: foreland tectonics and climate change before the end-Permian crisis: Scientific Reports, 10861, 10.1038/s41598-017-09853-3.

Viglietti, P.A., Smith, R.M.H., and Rubidge, B.S., 2018, Changing palaeoenvironments and tetrapod populations in the *Daptocephalus* Assemblage Zone (Karoo Basin, South Africa) indicate early onset of the Permo–Triassic mass extinction: Journal of African Earth Science, v. 138, p. 102–111.

Visser, J.N.J. and Dukas, B.A., 1979, Upward-fining fluviatile megacycles in the Beaufort Group, north of Graaff-Reinet, Cape Province: Transactions of the Geological Society of South Africa, v. 82, p. 149–154.

Ward, P.D., Botha, J., Buick, R., DeKock, M.O., Erwin, D.H., Garrison, G., Kirschvink, J., and Smith, R.M.H., 2005, Abrupt and gradual extinction among Late Permian land vertebrates in the Karoo Basin, South Africa: Science, v. 307, p. 709–714.

Ward, P.D., Montgomery, D.R., and Smith, R.M.H., 2000, Altered river morphology in South Africa related to the Permian–Triassic extinction: Science, v. 289, p. 1740–1743.

Ward, P.D., Retallack, G.J., and Smith, R.M.H., 2012, The terrestrial Permian–Triassic boundary event bed is a nonevent: Comment: Geology, v. 40, p. e256.

Wilson, A., Flint, S., Payenberg, T., Tohver, E., and Lanci, L., 2014, Architectural styles and sedimentology of the fluvial lower Beaufort Group, Karoo Basin, South Africa: Journal of Sedimentary Research, v. 84, p. 326–348.

Received 15 February 2019; accepted 12 September 2019.

SUPPLEMENTAL INFORMATION

Gastaldo, R.A., Neveling, J., Geissman, J.W., and Looy, C.V., Testing the *Daptocephalus* and *Lystrosaurus* Assemblage Zones in a Lithostratographic, Magnetostratigraphic, and Palynological Framework in the Free State, South Africa: PALAIOS, v. **, p. ***-***.

METHODS

Assessing vertebrate-collection locality GPS coordinates on the Bethel, Heldenmoed, and Donald 207 (Fairydale) farms

Roger Smith (email communication 2 February 2014; available upon request) provided us his complete data set of vertebrate collections on which the end-Permian extinction and recovery model of Smith and Botha-Brink (2014), and previous reports (Ward et al., 2000, 2005; Smith and Ward, 2001; Smith and Botha, 2005; Botha and Smith, 2005; Smith and Botha-Brink, 2006; and others), is based. We requested all metadata in the database associated with the Smith and Botha-Brink (2014) supplemental data table, but only received the following data fields in the Excel spreadsheet: Accession No, Clade, Family, Genus, Species, m+/-PTB, Locality, District, Latitude (degree, minute, second format), Longitude (degree, minute, second format), Period, and Notes (skeletal element). The geographic coordinate system used in South Africa until 1999 differed from the world standard. Until 1 January 1999, GPS coordinates, depending upon the worker, were recorded using the Cape Datum system. As of the beginning of 1999, South Africa adopted the WGS84 standard. As Smith and Botha-Brink (2014) and Viglietti et al. (2016) note, the latitude and longitude coordinates documented by earlier reports of vertebrate fossils often referred to "farm centroids" without providing a specific set of coordinates for any specimen. However, the data set used to refine the so-called End-Permian model in the Karoo is reportedly based on accurate GPS coordinates for each vertebrate, along with an accurate positioning of each relative to a horizon designated as an "event bed" (Smith and Ward, 2001; Ward et al., 2005; Smith and Botha-Brink, 2014) identified and illustrated on the Bethel farm. The first specimens used to construct that model, according to their accession numbers in the Iziko Museum database, were collected before 1999 (e.g., *Lystrosaurus maccaigi* RS74 [SAM-PK-K09958], collected by Smith in 1998). The first evidence provided to us of RS labeled specimens collected in 1999 begins with RS78 (i.e., *Galesaurus planiceps* [SAM-PK-K09956], collected by Smith on the Donald 207 farm; Supplemental Table 1). There is no information in the queried database of the Museum collections about which coordinate system was used in the field when recording specimen locations (Excel file via email communication S. Kaal, 3 May 2013; Supplemental Table 1 with redacted GPS coordinates, original non-redacted version available upon request). Hence, we have worked on the premise that vertebrates collected prior to 1 January 1999 were recorded under the Cape Datum system, and that no adjustment was implemented;

those collected after 1 January 1999 were recorded using the WGS84 system. Without metadata, we are also unable to comment on whether the instruments used after May 2000 eliminated Selective Availability, increasing spatial resolution for samples collected beginning at that time. Prior to 1 May 2000, Selective Availability added 50 m of error horizontally in any direction to the world standard. It is presumed that the Cape Datum, based on the modified Clarke 1880 ellipsoid, was similarly affected. Hence, we have to take into account that the GPS coordinate system in use at the time of collection will affect the positioning of any specimen on a GoogleEarth plot.

We have undertaken a test of vertebrate collection sites on the Bethel, and Heldenmoed farms, where there is varying topographic relief across the valley, using WGS84 and the Cape Datum systems. Most vertebrates collected from Donald 207 (Fairydale) farm are found across a gentle plateau with little relief, with little impact to their relative positions regardless of the datum in use at the time. Collection sites on the Bethel and Heldenmoed farms, where the topographic relief is greatest, uniformly shift ~55 m to the southwest when te Cape Datum (Supplemental Fig. 1A blue pin) coordinate system is employed versus the WGS84 standard (Supplemental Fig. 1A green balloon). There is essentially no difference in the elevation of specimens collected in areas of low topographic relief when assessed on GoogleEarth (e.g., RS55: Cape Datum elevation 1314 m, WGS elevation 1314 m; RS56: Cape Datum elevation 1312 m, WGS elevation 1313 m). Thus, the stratigraphic position of such pre-1999 specimens, when placed into our stratigraphic framework and the assemblage-zone boundary, as identified by Smith and Botha-Brink (2014, their fig. 3; see Gastaldo et al., 2017), isn't significantly affected. The stratigraphic position of vertebrates relative to the purported boundary is affected more on steeper valley slopes.

We have field checked the position of the majority of specimens on the eastern side of the valley using the WGS84 standard. Those with RS numbers lower than RS78, and collected prior to 1999, differ when coordinates are plotted using the Cape Datum. The positions of pre-1999 collection sites are moved downslope by an elevation of ~10 m (Supplemental Fig. 1B). Vertebrates collected before 1999 include RS63 (*Lystrosaurus maccaigi*), RS64 (*Moschorhinus kitchingi* collected by Smith), and RS65 (*Lystrosaurus maccaigi*) show the greatest divergence in elevational difference when these two coordinate systems are compared. RS63 is reported to be positioned 3 m below the assemblage-zone boundary (Fig. 1B, dashed white line). Our field check of those coordinates using WGS84 placed that collection site more than 10 m above the boundary, whereas the Cape Datum plots below it. RS64 is reported to be positioned exactly on the boundary, and plots at this elevation using the Cape Datum coordinates. Using WGS84 coordinates, the collection site is more than 10 m above the boundary. A similar effect is found with RS65. Hence, we have restricted our analysis to specimens on this part of the farm collected after 1 January 1999 when WGS84 standards were adopted in South Africa and, presumably, used in subsequent collections. We are unable, though, to determine which specimens were collected between 1 January

1999 and 1 May 2000 when selective availability was eliminated. The impact of different coordinate systems on the stratigraphic position for GPS coordinates of collection sites on the western side of the valley is a very different story.

The shift in collection localities of ~55 m to the southwest on the western side of the valley moves specimens up slope several meters. But, in these cases, their shift up slope has no material impact on the discrepancies between our field checked data and their stratigraphic position above the assemblage-zone boundary reported by Smith and Botha-Brink (2014). Five examples, all assigned to the *Lystrosaurus* Assemblage Zone, will suffice–RS183 (*Lystrosaurus declivis*) & SAM-PK-K-10377 (*L. declivis*), SAM-PK-K-10373 (*L. declivis*), RS201 (*L. murrayi*), and SAM-PK-K-10375 (*L. murrayi*; Supplemental Fig. 1C). All of these samples lie within a polygon where we field checked each reported site. All samples were collected post 1 January 1999, based on the RS collection number or the SAM-PK-K acquisition number. RS183 and SAM-PK-K-10377 were collected at the exact same GPS coordinates, but are reported to occur at above the boundary horizon at 92 and 105 m, respectively. WGS84 coordinates plot at an elevation of 1356 m whereas the same coordinates plotted using the Cape Datum are at an elevation of 1363 m. Regardless, of the discrepancy of these lystrosaurids relative to the assemblage-zone boundary, plotting them using the Cape Datum does not move either specimen up slope an additional 70 m which would validate their reported stratigraphic position (compare Figs. 5, 13). There is an elevational difference of < 7 m between the location of SAM-PK-K-10373, reported as 90 m above the boundary, when the WGS84 and Cape Datum coordinate systems are compared. The change in elevation up slope can't account for the additional 75 m required for it to have been collected at that stratigraphic distance above the assemblage-zone boundary (see text). The difference in elevation on the side of the koppie between these coordinate systems, for RS201, is ~8 m, which would, at most, raise its stratigraphic position to ~48 m above the reported turnover (see Figs. 5), which is substantially lower than the position of 120 m above the assemblage-zone boundary reported for this specimen. And, when the elevation of SAM-PK-K-10375 is plotted using both coordinate systems, these spots only differ by 11 m (giving it a maximum stratigraphic distance of 50 m above the biozone boundary); this specimen is reported to have been collected 180 m above the assemblage-zone boundary. Therefore, we are satisfied that any variance we documented between the reported and real stratigraphic position for fossil localities used by Smith and Botha-Brink (2014) and others can not be attributed to differences in coordinate systems in the field. Hence, we have retained all vertebrate locations recorded after 1 January 1999 and used WGS84 coordinates in our analysis. We have omitted all specimens with RS vertebrates with numbers < RS78 and SAM-PK-K samples where the acquisition number is <SAM-PK-K-09956. And, based on the variance in field coordinates of +/-3 to +/-4 m over the course of our investigation, we have retained the upper and lower limits of a 10 m variance between our field locations and those of Smith as relevant to the discussion. It also can be seen that there is a wide discrepancy between the reported position above the

Daptocephalus–Lystrosaurus boundary in collection sites in close proximity to each other across the Donald 207 (Fairydale) farm (supplemental Fig. 3).

Magnetic Polarity Stratigraphy and Rock Magnetism

For most of our study, samples were collected by drilling oriented cores using a portable field drill with a non-magnetic diamond drill bit. Typically, seven to 12+ independently-oriented core samples were obtained from each suitable bed (independent sampling site). In addition, those sampling sites where paleomagnetic contact tests were carried out (sampling of both the Karoo mafic dike and adjacent host rocks) typically involve a larger sample number, with host rocks sampled as a function of distance from the dike contact in a near-perpendicular traverse. Most beds sampled are exposed in the two adjacent dongas (Figs. 3, 5). Sampled lithologies consist of medium- to coarse-grained siltstone and very fine wacke, in addition to some nodular (concretions) horizons in fine siltstone/mudstone. The relatively large number of independently oriented samples obtained allows us to more fully characterize the magnetization in the rocks of this sequence and to robustly assess the homogeneity, or lack thereof, of the remanence at each stratigraphic level. This approach differs from all previous studies of presumably uppermost Permian and lowermost Triassic strata in the Karoo Basin where field evidence suggests that only a single independently oriented sample (core) per horizon was obtained (De Kock and Kirschvink, 2004; Ward et al., 2005). In part, full characterization of the remanence is needed because of the extensive suite of mafic (diabase) intrusions of the Early Jurassic Karoo Large Igneous Province that was emplaced throughout the Eastern Cape Province (e.g., Svenson et al., 2012). On the Bethel farm, six Karoo dikes are well-exposed in the main donga, and all of these also were sampled. It is possible that other sills are present in the Bethel farm area, but simply not exposed. All of the dikes are less than 2 m in width. In terms of general background from a regional perspective, most Karoo Both intrusions exhibit a sill-like geometry and can be tens of meters in thickness and traced laterally for tens of kilometers. Most of these sills in the Free State Province, including the two we sampled at Old Lootsberg Pass, are of normal polarity (Gastaldo et al., 2018; Geissmanet and Ferre, 2019; unpublished). A key to any magnetic polarity stratigraphy study in the Karoo Basin is the need to separate an inferred early acquired, normal polarity remanence in upper Permian and inferred lowermost Triassic strata from a normal polarity Early Jurassic "overprint," which is not necessarily straightforward (Lanci et al., 2013; Maré et al., 2014; Gastaldo et al., 2018). Published paleomagnetic results from such strata in the central Karoo Basin (Free State Province) are associated with limited documentation and, thus, associated with limited viability. For example, there is no evidence, based on the data reported, that reverse polarity magnetozones exist that are defined by consecutive samples exhibiting well-behaved, stable endpoint magnetizations of reverse polarity in any of the reported sections (De Kock andKirschvink, 2004; Ward et al., 2005).

For this study, core samples were processed into standard 2.2 cm high specimens for remanence and rock magnetic measurements. Each specimen was washed in dilute HCl to remove any form of metal contamination after specimen preparation. Specimens were typically stored in the large volume magnetic shield in the laboratory after preparation. For those stratigraphic intervals lacking beds suitable for drilling, samples were collected as oriented blocks of a range of sizes by marking the orientation of any flat surface of a block that could be removed from the outcrop. Typically five to eight oriented blocks were obtained from a single (< 0.5 m) stratigraphic interval. These were re-cut into multiple, 2.0 cm cubical specimens using a non-magnetic diamond saw blade. The nomenclature for our magnetostratigraphic sample collection utilizes a "Bt" prefix (Bethel farm = Bethulie).

Remanence measurements were made on either (1) a 2G Enterprises, DC SQUID, three-axis pulse cooled superconducting rock magnetometer, interfaced with an automated specimen handler, and an on-line alternating field (AF) degausser system, or (2) JR5A or JR6A AGICO spinner magnetometers. All magnetometers and related demagnetization instrumentation are housed inside a large magnetic shield (Version #50 of Lodestar Magnetics) with an ambient field of less than 300 nT over most volume. In addition, specimens were housed in multilayered mu-metal shields, with ambient fields less than 10nT, in between thermal demagnetization steps and measurements. Previous work at, for example, Old (West) Lootsberg Pass (Gastaldo et al., 2018) demonstrate that the principal magnetic phase in siltstone is mainly magnetite, although hematite may carry a substantial fraction of the remanence at some sites. Consequently, a subset of specimens prepared from samples from all sites was subjected to both thermal and alternating field (AF) demagnetization. Thermal demagnetization was carried out using one of three ASC TD48, dual zone thermal demagnetizers, in a progressive fashion involving 20 to 30 steps, sometimes to maximum laboratory unblocking temperatures of 680° C (+/-). AF demagnetization was carried out using the integrated 2G Enterprises AF demagnetization system, typically to peak fields of90 to 120 mT.

Acquisition of isothermal remanent magnetization (IRM) and backfield demagnetization of saturation IRM (SIRM) utilized an ASC multi-coil impulse magnet system. Three-component thermal demagnetization of IRM acquired in different DC fields followed the method of Lowrie (1990). Anisotropy of magnetic susceptibility (AMS) measurements were made using either an AGICO KLY-3S or a MFK1A automated magnetic susceptibility instrument. Measurements of the variation in magnetic susceptibility, as a function of heating and cooling, were carried out on bulk-rock powders or magnetic separates from powders of block samples collected from selected sites using an AGICO CS-4 apparatus interfaced with a MFK1A susceptibility instrument. These measurements were conducted in an argon atmosphere. Results of progressive demagnetization were inspected using orthogonal demagnetization diagrams (Zijderveld, 1967), and the directions of magnetization components identified by the co-linearity of

several demagnetization data points determined using principal components analysis (Kirschvink, 1980). Magnetization directions at the site level were estimated as mean directions using as many independent observations as accepted, following the method of Fischer (1953). These estimated site mean-magnetization directions were transformed into virtual geomagnetic poles (VGPs) and plotted on the cumulative stratigraphic column (Opdyke and Channell, 1996) to reveal the magnetic polarity stratigraphy of our section. Estimated paleomagnetic pole positions (e.g., Muttoni et al., 2013) for Africa during the late Permian to early Triassic time are such that normal polarity magnetizations in these strata in the Karoo Supergroup in the Free State Province of South Africa are expected to have a north-northwest (~ 330 °) declination and moderate to steep negative (~ 60°) inclination magnetization.

MAGNETIC POLARITY STRATIGRAPHY AND ROCK MAGNETISM

A considerable amount of The scope of this paper does not permit detailed presentation of all of the paleomagnetic data has been obtained from the Bethulie stratigraphic section, which includes over 75 discrete sampling sites, most of which are in separate, distinct beds. The nature of this contribution does not permit detailed presentation of all of the results from this section; they are succinctly summarized here in the context of the construction of a preliminary magnetic polarity stratigraphy for the section. Response to progressive demagnetization (either thermal methods, or less common, alternating field methods) is typically quite well-defined in both the sedimentary rocks and the Karoo dikes sampled (Fig. 11; Supplemental Fig. 5). Most demagnetization results are fully interpretable, with principal components analysis (Kirschvink, 1980) providing the resolution of magnetization vectors associated with maximum angular deviation (MAD) values well less than 10°. Several directional responses to progressive demagnetization are recognized, and on this basis we tentatively define a magnetic polarity stratigraphy for the Beathulie section. This polarity stratigraphy consists of a lower magnetozone of normal polarity (north-northwest directed, moderate to steep negative inclination remanence dominates), an interval that has been influenced by Karoo intrusions, a middle magnetozone of reverse polarity (south-southeast directed, moderate to steep positive inclination remanence dominates), an overlying interval that also has been influenced by Karoo dikes, and an upper magnetozone of normal polarity (Supplemental Fig. 4). Based on our knowledge of the paleogeography of southern Africa in the late Permian to early Triassic, a time-averaged geomagnetic field (expected) direction of normal polarity should be ~335°/-65°, with an expected direction of reverse polarity of ~155°/+65°. Notably, for the sites providing data interpreted to be of reverse polarity, it is always the case that a north-northwest directed, moderate to steep negative inclination remanence (normal polarity) is superimposed on this magnetization (Supplemental Fig. 5A). This "overprint" remanence is typically unblocked in the laboratory by about 400°C and the maximum laboratory unblocking temperature of this component may provide clues as to the general

thermal history of the sedimentary sequence comprising the Bethulie section as well as other sequences of sedimentary rocks in the Karoo Basin. The magnetization record of most of the Karoo dikes is, with minor exceptions, internally very uniform, with the magnetization characteristic (ChRM) of the Karoo dikes being of east-southeast declination and shallow positive inclination (Supplemental Fig. 5B; Fig. 11A). The direction of this ChRM in the Karoo dikes is considerably shallower in inclination than, and in fact statistically distinguishable from that recovered from the sites that define the middle stratigraphic interval of interpreted reverse polarity (Fig. 11S, Supplemental Figs. 5A,B). Host strata in immediate contact with Karoo dikes typically yield a magnetization similar in direction of the ChRM of the Karoo dike (e.g., compare results from site Bt29 (Karoo dike) and Bt35 (host strata immediately adjacent and up to about 2 m distant from the southeast contact with the dike ; Fig. 11A, Supplemental Fig. 5B), indicating that the host strata adjacent to the dike have been pervasively remagnetized due to dike intrusion. All specimens from all samples of this Karoo dike (site Bt29) and the host rock in contact (site Bt29) show the first removal, in either progressive thermal or alternating field demagnetization, of a north-northwest directed, moderate to steep negative inclination magnetization. This "overprint" magnetization is, here, demonstrably younger that the Early Jurassic Karoo dike. Sites Bt31, Bt32, and Bt33, some 12 m farther to the northwest up the donga, and stratigraphically above host strata at site Bt35, show no evidence of a thermal remagnetization by the dike in that most of the specimens from samples obtained at these sites only show the isolation of a remanence of north-northwest declination and moderate to steep negative inclination (interpreted to be of normal polarity; Fig. 11B). In addition, most of the demagnetization data from sites toward the base of the section (e.g., sites Bt60 to Bt70) reveal similar north-northwest declination, steep to moderate negative inclination magnetizations. Taken together, it is these kinds of paleomagnetic observations that lead us to construct the tentative magnetic polarity stratigraphy reported here for the Bethulie section (Fig. 5; Supplemental Fig. 4).

Anisotropy of magnetic susceptibility (AMS) data from each site in sedimentary rocks in the Bethulie section are consistent with the preservation of a primary depositional sedimentary fabric, and are typical of previously reported data from fine to very fine sandstones and siltstones (Marton et al., 2010; Dudzisz et al., 2016; Kiss et al., 2016; Lozinski et al., 2017) where undeformed beds are characterized by a well-grouped and sub-vertical to vertical orientation of the least principal susceptibility axis (K_{min}) and the maximum and intermediate susceptibility axes distributed in planar, near horizontal orientation (Supplemental Fig. 6). Furthermore, the AMS fabric is controlled by both fine-grained magnetite/maghemite grains as well as fine phyllosilicate minerals.

Three component IRM thermal demagnetization data (Supplemental Fig. 7) show that the IRM component acquired at the lowest DC field (15 mT) predominates in all of the rocks selected for these experiments and is fully unblocked between about 575 and 620° C. These

results are interpreted to suggest that the predominant magnetic mineral assemblage in the siltstones consists of fine (20-30 micron or less) magnetite/maghemite grains that would be in the fine multidomain to pseudo-single domain grain state.

Plots showing the response of bulk susceptibility vs. continuous heating to elevated temperature and subsequent cooling (Supplemental Fig. 8) reveal the presence of a phase with Curie temperature between about 575 and 625°C, depending on the selected specimen. These results are also consistent with those revealed in progressive thermal demagnetization and also three component thermal demagnetization, regarding the predominant magnetic mineral phases. The heating/cooling curves are not completely reversible, indicating slight changes in the magnetic mineralogy. Notably, the four examples of host rock sampled at site Bt35 (adjacent to Karoo dike at Bt29) have bulk magnetic susceptibilities that are comparable to host rock far removed from any dike (Bt20 and Bt51), suggesting that little change to the magnetic mineralogy took place to the contact rocks at site Bt35, despite the fact that the rocks were completely remagnetized by dike emplacement.

PALYNOLOGICAL COMMENTARY

Botanical Affinities of Recovered Palynomorphs

The botanical affinities of the palynomorphs recovered from Fairydale are similar to those reported elsewhere in South Africa (Prevec et al., 2009, 2010; Barbolini, 2014; Gastaldo et al., 2017). Multitaeniate pollen genera (e.g., *Protohaploxypinus*) have been found *in situ* in the pollen-sac clusters in the southern hemisphere and assigned to *Arberiella*. These pollen-sac clusters that are identical to those produced by a range of glossopterid microsporophylls (e.g., Zavada, 1991; Lindström et al., 1997), and pollen sacs attached to the microsporophyll *Eretmonia* (Ryberg et al, 2012). *Weylandites* has been found *in situ* in the synangium *Rugatheca*, a pollen organ with a possible glossopterid affinity (Pant and Basu, 1977; Balme, 1995). *Marsupipollenites* is known from the *Polytheca elongata*, a Permian pollen organ from India that is found in association with glossopterids (Pant et Nautiyal, 1960). Taeniate bisaccates, including *Lueckisporites*, *Corisaccites*, *Guttulapollenites* and *Lunatisporites*, were likely produced by conifers (Clement-Westerhof, 1974, 1987).

Alete bisaccate pollen assignable to the genera *Falcisporites* and *Alisporites* may represent corystosperms and/or peltasperms. *Falcisporites* has been found *in situ* in the microsporangiate organ *Pteruchus* (e.g. Zavada and Crepet, 1985; Taylor et al., 2006), which is attributed to the corystosperm *Dicroidium*. *Dicroidium* is well known from Triassic Gondwanan floras including South Africa, but also is reported from upper Permian strata of Jordan (Kerp et al., 2006; Abu Hamad et al., 2008; Bloemenkemper et al., 2018) and India (Chandra et al., 2008). *Falcisporites australis* is associated with the peltasperm *Lepidopteris*

(Lower Triassic, Antarctica, Australia; Retallack, 2002; Lindström et al., 1997). *Alisporites* was produced by Euramerican Permian peltasperms (*Autunia conferta*), but it also known from the tentative peltasperm pollen organ *Lelestrobus* (Permian/Triassic, India; Srivastava, 1984) and Corystospermales (Triassic; Osborn and Taylor, 1993). In addition, *Alisporites* is also known from late Permian Euramerican voltzian conifers (Balme, 1995) and has been isolated from the pollen cones of the Triassic voltzian conifer *Telemachus* from Antarctica (Hermsen et al., 2007).The pollen type *Cycadopites* is known to occur in many major plant groups (Balme, 1995), but here probably represents a peltasperm origin. Plants responsible for producing the pollen *Inaperturopollenites*, *Hamiapollenites*, *Scheuringipollenites*, *Pteruchipollenites* and Klausipollenites are, thus far, unknown.

The parent plants of all but the Glossopterid-produced pollen are not represented in the late Permian macrofloras and were likely growing in extrabasinal areas in environments where chances on preservation are limited (Looy et al., 2014; Gastaldo et al., 2017).

Plant groups represented by their spores include lycopsids, sphenopsids, and ferns, as well as *incertae sedis*. *Densoisporites* taxa represent the Pleuromeiaceae and other cormose lycopods (Grauvogel-Stamm and Lugardon, 2004; Looy et al., 2005). The parent plants of *Playfordiaspora* and *Limatulasporites* are unknown, but based on their morphology they were likely produced by lycopods as well (Balme, 1995). Various *Cyclogranisporites* taxa have been found *in situ* in fertile fronds of Marattiales (France, Germany, USA; Pfefferkorn et al., 1971; Zodrow et al., 2006) and the putative Medullosan pollen organ *Potoniea* (Carboniferous, England; Balme, 1995). *Deltoidospora* is known from several Mesozoic fern taxa, but *in situ* spores have not yet been described from Permian representatives (Balme, 1995), based on their morphology the parent plants of *Brevitriletes* spores are also likely ferns. *Verrucosisporites* is known from both ferns and gymnosperms (Balme, 1995) and, hence, cannot be assigned to any specific taxon. *Calamaspora* has been found *in situ* in sporangia of both Equisetales and Sphenophyllales (Balme, 1995).

Phylogenetically diverse assemblages such as these, with high amounts of fern-and-lycopod spores, pollen characteristic for late Permian gymnosperm taxa, along with pollen forms that became dominant in the Early Triassic, are known from the latest Permian records worldwide. In the Gondwanan realm, such assemblages represent the stepwise transition of basinal lowland communities dominated by *Glossopteris* to those characterized by peltasperms, corystosperms, voltzian conifers, and cormose lycopods (e.g., Lindström and McLoughlin, 2007; Fielding et al., 2019).

Late Paleozoic Palynological Zonation in the Karoo Basin

Barbolini (2014) proposed a new palynozonation for the Karoo Basin wherein a latest Permian biozonation was established using indicator taxa to separate the *Daptocephalus*

(=*Dicynodon*) Assemblage Zone of the Palingkloof Member from underlying Elandsberg and Barberskrans members. Index taxa of the Palingkloof Member are *Granulatisporites convexus* and *Limbosporites denmeadii*, based on only two reportedly productive sample sites (Barbolini, 2014, table 3.1). Barbolini et al. (2018) establish a new palynozone, the *Dictyophyllidites mortonii* Interval Zone on these two samples and they note that they both originate from the transition from the *Dicynodon* to the *Lystrosaurus* AZs, equating this turnover to the end-Permian extinction event. We have worked at both of these localities, one of which is detailed in the manuscript, proper (Supplemental Figs. 5, 6), and the other locality deserves attention, here.

The collection site of Palingkloof sample (14) is reported on the R390 between Steynburg and Venterstad (Supplemental Fig. 5A) at the *Dicynodon/Lystrosaurus* Assemblage Zone contact. Hence, the assemblage from this location should document any significant change in palynological assemblage, if present. The location of the GPS coordinates of locality 14 (Barbolini, 2014) on GoogleEarth, and field checked by us on 27 January 2016 (Supplemental Fig. 5D), occurs in the only outcrop along the R58 for more than 10 km. The R58 bisects the rise, with exposures on either side of the road. That rise is a consequence of a Jurassic dolerite intrusion (Supplemental Figs. 5C, D) that has altered all surrounding siltstone lithologies as a consequence of contact metamorphism. We are unsure about how any palynological assemblage was recovered from this outcrop or, if one was recovered, the quality of preservation. In other papers we have documented that the quality of preservation varies with proximity to an intrusive body (e.g., Prevec et al., 2010, Gastaldo et al., 2017) with a darkening and opacity of palynomorphs from samples taken in some proximity to dolerite. A specific assemblage is not figured by Barbolini (2014) or Barbolini et al. (2016), and the maturity of the spores is not mentioned. Hence, we are not sure if the palynolgical data described originated from this exact site.

The second productive palynological assemblage reported by Barbolini (2014) comes from the section we sampled on Donald 207 (Fairydale) farm (Supplemental Fig. 10). In a previous version of this manuscript, an anonymous reviewer commented that s/he had accompanied Barbolini in the field when the sample was collected, and the GPS coordinates of our sample were incorrect. Supplemental Figure 6A, a snippet from Table 3.1 of Barbolini (2014, p. 103), shows the collection site as S30°24.416', E026°14.261'. And, it is noted that the sample also originates from the Permo–Triassic boundary on the Fairydale farm. Supplemental Figure 6B plots those coordinates on Figures 9, 10 of the current contribution, from which we report our palynomorph assemblage, demonstrating congruence. Compare the white polygon outlining the same area as illustrated in Figures 9, 10. We find it curious that the locality is reported to represent the PTB when, in fact, all vertebrates reported from Donald 207 (Fairydale) farm are placed in the *Lystrosaurus* AZ by Smith and Botha-Brink (2014; their supplemental table). As is demonstrated by our manuscript figures, the Donald 207 farm is located nearly 50 m higher in elevation than the

transition from Facies C to Facies D, purported to represent the end-Permian event, by Smith and Botha-Brink (2014; but see Gastaldo et al., 2017). There is no question that the palynomorph assemblage we report, herein, originates from high in the *Lystrosaurus* Assemblage Zone.

Citations

ABU HAMAD, A., KERP, H., VÖRDING, B., AND BANDEL, K., 2008, A Late Permian flora with *Dicroidium* from the Dead Sea region, Jordan: Review of Palaeobotany and Palynology, v. 149, p. 85–130.

BALME, B.E., 1995, Fossil *in situ* spores and pollen grains: an annotated catalogue. Review of Palaeobotany and Palynology, v. 87, p. 81–323.

BARBOLINI, N., 2014. Palynostratigraphy of the South African Karoo Supergroup and Correlations with Coeval Gondwanan Successions: Ph.D. Thesis, University of the Witwatersrand, Johannesburg, South Africa, 386 p.

BARBOLINI, N., RUBIDGE, B., AND BAMFORD, M.K., 2018, A new approach to biostratigraphy in the Karoo retroarc foreland system: Utilizing restricted-range palynomorphs and their first appearance datums for correlation: Journal of African Earth Sciences, v. 140, p. 114-133.

BOTHA, J., AND SMITH, R.M.H., 2006, Rapid vertebrate recuperation in the Karoo Basin of South Africa following the End-Permian extinction: Journal of African Earth Sciences, v. 45, p. 502-514.

CHANDRA, S., SING, K.J., AND JHA, N., 2008, First report of the fertile plant genus *Umkomasia* from Late Permian beds in India and its biostratigraphic significance: Palaeontology, v. 51, p. 817–826.

CLEMENT-WESTERHOF, J.A., 1974, *In situ* pollen from gymnospermous cones from the Upper Permian of the Italian Alps-a preliminary account: Review of Palaeobotany and Palynology, v. 17, p. 63-73.

DE KOCK, M.O. AND KIRSCHVINK, J.L., 2004, Paleomagnetic Constraints on the Permian-Triassic Boundary in Terrestrial Strata of the Karoo Supergroup, South Africa: Implications for Causes of the End-Permian Extinction Event: Gondwana Research, v. 7, p. 175-183.

DUDZISZ, K., SZANIAWKSI, R., MICHALSKI, K., AND MANBY, G., 2016, Applying the anisotropy of magnetic susceptibility technique to the study of the tectonic evolution of the West Spitsbergen Fold-and-thrust belt: Polar Research, v. 35, p. 1-12.

FISHER, R.A., 1953, Dispersion on a sphere: Proceedings of the Royal Society of London, v. A217, p. 295-305.

GASTALDO, R.A., NEVELING, J., LOOY, C.V., BAMFORD, M.K., KAMO, S.L., AND GEISSMAN, J.W., 2017, Paleontology of the Blaauwater 67 Farm, South Africa: Testing the *Daptocephalus/Lystrosaurus* Biozone Boundary in a Stratigraphic Framework: PALAIOS, v. 34, p. 349-366. DOI: http://dx.doi.org/10.2110/palo.2016.106

GASTALDO, R.A., NEVELING, J., GEISSMAN, J.W., AND LI., J.W., 2019, A Multidisciplinary Approach to Review the Vertical and Lateral Facies Relationships of the Purported Vertebrate-defined Terrestrial Boundary Interval at Bethulie, Karoo Basin, South Africa: Earth Science Reviews, v. 189. p. 220-243: doi 10.1016/j.earscirev.2017.08.002
GRAUVOGEL-STAMM, L., AND LUGARDON, B., 2004, The spores of the Triassic lycopsid *Pleuromeia sternbergii* (Munster) Corda: morphology, ultrastructure, phylogenetic implications, and chronostratigraphic inferences: International Journal of Plant Science, v. 165, p. 631–650.
HERMSEN, E.J., Taylor, T.N., AND Taylor E.N, 2007, A voltzialean pollen cone from the Triassic of Antarctica. Review of Palaeobotany and Palynolology, v. 144, p. 113-122.
KERP, H., HAMAD, A.A., VÖRDING, B., AND BANDEL, K., 2006, Typical Gondwanan floral elements in the Upper Permian of the paleotropics: Geology, v. 34, p. 265–268.
KIRSCHVINK, J.L., 1980, The least squares line and plane and the analysis of paleomagnetic data: Geophysical Journal of the Royal Astronomical Society, v. 62, p. 699-718.
KISS, D., MARTON, E., AND TOKARSKI, A.K., 2016, An integrated paleomagnetic and magnetic anisotropy study of the Oligocene flysch from the Dukla nappe, outer Western Carpathians, Poland: Geologica Carpathica, v. 67, p. 595-605.
LANCI, L., TOHVER, E., WILSON, A., AND FLINT, S., 2013, Upper Permian magnetic stratigraphy of the lower Beaufort group, Karoo basin: Earth and Planetary Science Letters, v. 175, v. 123-134.
LINDSTRÖM, S., MCLOUGHLIN, S., AND DRINNAN, A.N., 1997, Intraspecific variation of taeniate bisaccate pollen within Permian glossopterid sporangia, from the Prince Charles Mountains, Antarctica: International Journal of Plant Sciences, v. 158, p. 673–684.
LOOY, C.V., COLLINSON, M.E., VAN KONIJNENBURG-VAN CITTERT, J.H.A., AND VISSCHER, H., 2005, The ultrastructure and botanical affinity of end-Permian spore tetrads: International Journal of Plant Sciences, v. 166, p. 875-887.
LOOY, C.V., KERP, H., DUIJNSTEE, I.A.P., AND DIMICHELE, W.A., 2014, The late Paleozoic ecological evolutionary laboratory, a land-plant fossil record perspective: Sedimentary Record, v. 12, p. 4–9.
LOWRIE, W., 1990, Identification of ferromagnetic minerals in a rock by coercivity and unblocking temperature properties: Geophysical Research Letters, v. 17, p. 159-162.
LOZINSKI, M., ZIOLKOWSKI, P., AND WYSOCKA, A., 2017, Tectono-sedimentary analysis using the anisotropy of magnetic susceptibility: a study of the terrestrial and freshwater Neogene of the Orava Basin: Geologica Carpathica, v. 68, p. 479-500.
MARÉ, L.P., DE KOCK, M.O., CAIRNCROSS, B., AND MOURI, H., 2014, Application of magnetic geothermometers in sedimentary basins: An example from the western Karoo Basin, South Africa: South African Journal of Geology, v. 117, p. 1-14.
MARTON, E., BRADAK, B., RAUCH-WLODARSKA, M., AND TOKARSKI, A.K., 2011, Magnetic anisotropy of clayey and silty members of Tertiary flysch from the Silesian and Skole Nappes (Outer Carpathians): Studies in Geophysics and Geodesy, v. 54, p. 121-134.
MUTTONI, G., DALLANAVE, E., AND CHANNELL, J.E.T., 2013, The drift history of Adria

and Africa from 280 Ma to Present, Jurassic true polar wander, and zonal climate control on Tethyan sedimentary facies: Palaeogeography, Palaeoclimatology, Palaeoecology, v. 386, p. 415-435.
OPDYKE, N.D., AND CHANNEL, J.E.T., 1966, *Magnetic Stratigraphy*: Academic Press, San Diego, 346 pp.
OSBORN, J.M., AND Taylor, T.N., 1993. Pollen morphology and ultrastructure of the Corystospermales: permineralized *in situ* grains from the Triassic of Antarctica. Review of Palaeobotany and Palynology, v. 79, p. 205-219.
PANT, D.D. AND NAUTIYAL, D.D., 1960, Some seeds and sporangia of *Glossopteris* flora from the Raniganj Coalfield, India: Palaeontographica Abteilung B, v. 107, p. 41-64.
PFEFFERKORN, H.W., PEPPERS, R.A., PHILLIPS, T.L., 1971, Some fern-like fructifications and their spores from the Mazon Creek compression flora of Illinois (Pennsylvanian). Illinois State Geological Survey Circ., v. 463, p.1-54.
PREVEC, R., GASTALDO, R.A., NEVELING, J., REID, S.B., AND LOOY, C.V., 2010, An autochthonous glossoperid flora with Latest Permian palynomorphs from the *Dicynodon* Assemblage Zone of the southern Karoo Basin, South Africa: Palaeogeography, Palaeoclimatology, Palaeoecology, v. 292, p. 381-408. doi: 10.1016
RYBERG, P., TAYLOR, E., AND TAYLOR, T., 2012, The first permineralized microsporophyll of the Glossopteridales: *Eretmonia macloughlinii* sp. nov: International Journal of Plant Science, v. 173, p. 812–822.
SMITH, R.M.H., AND WARD, P.D., 2001, Pattern of vertebrate extinctions across an event bed at the Permian–Triassic boundary in the Karoo Basin of South Africa: Geology, v. 29, p. 1147–1150.
SMITH, R.M.H., AND BOTHA, J., 2005, The recovery of terrestrial vertebrate diversity in the South African Karoo Basin after the end-Permian Extinction: Compte Rendu Palevol, v. 4, p. 555-568.
SMITH, R.M.H., AND BOTHA-BRINK, J., 2014, Anatomy of a mass extinction: Sedimentological and taphonomic evidence for drought-induced die-offs at the Permo–Triassic boundary in the main Karoo Basin, South Africa: Palaeogeography, Palaeoclimatology, Palaeoecology, v. 396, p. 99–118.
SRIVASTAVA, S.C., 1984, *Lelestrobus*: a new microsporangiate organ from the Triassic of Nidpur, India. Palaeobotanist, v. 32, p. 86-90.
SVENSEN, H., CORFU, F., POLTEAU, S., HAMMER, Ø., and PLANKE, S., 2012, Rapid emplacement in the Karoo Large Igneous Province: Earth and Planetary Science Letters, v. 325-326, p. 1-9.
TAYLOR, E.L., TAYLOR, T.N., KERP, H., AND HERMSEN, E.J., 2006, Mesozoic seedferns: old paradigms, new discoveries: Journal of the Torrey Botanical Society, v. 133, p. 62–82.
VIGLIETTI, P.A., SMITH, R.M.H., ANGIELCZYK, K.D., KAMMERER, C.F., FRÖBISCH, J., AND RUBIDGE, B.S., 2016, The *Daptocephalus* Assemblage Zone (Lopingian), South Africa: A proposed biostratigraphy based on a new compilation of stratigraphic ranges: Journal of African Earth Sciences, v. 113, p. 153–164.

WARD, P.D., MONTGOMERY, D.R., AND SMITH, R.M.H., 2000, Altered river morphology in South Africa related to the Permian–Triassic extinction: Science, v. 289, p. 1740–1743.
WARD, P.D., BOTHA, J., BUICK, R., DEKOCK, M.O., ERWIN, D.H., GARRISON, G., KIRSCHVINK, J., AND SMITH, R.M.H., 2005, Abrupt and gradual extinction among Late Permian land vertebrates in the Karoo Basin, South Africa: Science, v. 307, p. 709–714.
ZAVADA, M.S., 1991, The ultrastructure of pollen found in dispersed sporangia of *Arberiella* (Glossopteridaceae): Botanical Gazette, v. 152, p. 248–255.
ZAVADA, M.S., AND CREPET, W.L., 1985, Pollen wall ultrastructure of the type material of *Pteruchus africanus*, *P. dubius* and *P. papillatus*: Pollen et Spores, v. 27, p. 271–276.
ZIJDERVELD, J.D.A., 1967, Demagnetization of rocks: Analysis of results: *in* Collinson, D.W., Creer, K.M., and Runcorn, S.K., Eds., *Methods in Palaeomagnetism*, Elsevier, Amsterdam, p. 254, 286.
ZODROW, E.L., ŠIMŮNEK, Z., CLEAL, C.J., BEK, J., PŠENIČKA, J., 2006. Taxonomic revision of the Palaeozoic marattialean fern *Acitheca* Schimper. Review of Palaeobotany and Palynolology, v. 138, p. 239-280.

Figure and Table Captions

Supplemental Figure 1 – Results comparing plots of vertebrate-collection sites using Cape Datum (blue pin) versus WGS84 (green balloon) coordinate systems in three parts of the Bethel farm locality. (A) Change in position of specimens RS55 and RS56, all of which were collected prior to 1 January 1999, in an area of low relief. The position of each shifts ~55 m to the southwest, but the elevation at which each occurs remains consistent. Hence, there is no significant change in their stratigraphic position when placed within measured sections. (B) On steeper gradients on the eastern side of the valley, the location of specimens RS63, RS64, and RS65, all of which were collected prior to 1 January 1999, differs between WGS84 (green ballon) and Cape Datum (blue pin) coordinate systems. Field-checked vertebrates that lie above the assemblage zone boundary using WGS84 shift to below the boundary when the Cape Datum system is used. (C) On the western slope below the Swartberg Member of the Katberg Formation, application of the Cape Datum coordinate system to specimens collected after 1 January 1999, shifts their position up slope. The extent of elevational change, though, can not account for the discrepancies between their field-checked positions and those reported by Smith and Botha-Brink (2014) as distance above the assemblage-zone boundary.

Supplemental Figure 2–Graphical plot of a subset of fossil vertebrates from Bethel farm illustrating their reported vs. field-checked stratigraphic position relative to the upper contact of Smith and Botha-Brink's (2014) Facies C, their proposed biozone boundary, marked as 0. Specimen numbers of the taxa identified by black shapes are plotted relative to their reported position either below or above the biozone boundary as provided by R.H.M.

Smith (pers. Comm., 2014; Smith and Botha-Brink, 2014, supplemental data table) in an Excel file including GPS coordinates of each vertebrate in the database. Note, only vertebrates with collection dates after 1 January 1999 are considered (see supplemental information). Colored circles indicate the stratigraphic position of these taxa, relative to the *Daptocephalus–Lystrosaurus* AZ boundary, as determined in the field and correlated into our measured stratigraphic framework (Fig. 5). The color of the circle indicates the magnitude of discrepancy between the reported and field-checked position of each specimen in 10 m increments. The transect along the X-axis conforms to the LAD of taxa reported in the Phase 2 and the Recovery phase of the Karoo extinction model.

Supplemental Figure 3– Plot of collection sites of other *Lystrosaurus* Assemblage Zone vertebrates on the Donald 207 (Fairydale), Heldenmoed, and Bethel farms with the reported stratigraphic distance above the *Lystrosaurus–Daptocephalus* Assemblage Zone contact as identified by Smith and Botha-Brink (2014) on the adjoining Bethel farm. Note the discrepancies in reported distance above the boundary for vertebrates collected in close physical proximity to one another. This analysis complements the one presented in Figure 10 of the manuscript.

Supplemental Figure 4–Composite lithostratigraphic column of measured sections in which samples for magnetic properties were collected and analyzed. All magnetic polarity stratigraphy (paleomagnetism) sampling sites in sedimentary rocks, as well as sites in cross-cutting Karoo dikes, are shown, along with an interpretive magnetic polarity stratigraphy.

Supplemental Figure 5– Examples of orthogonal progressive demagnetization digrams. (A, B) Orthogonal progressive demagnetization diagrams showing the end point of the magnetization vector plotted onto the horizontal (filled symbols) and vertical (open symbols) planes (NS-EW, EW-Up/Dn) for individual specimens from samples from sites Bt21 (A) and Bt35/Bt29 (B) ,with all samples at essentially the same stratigraphic interval, that have been subjected to progressive thermal demagnetization or alternating field demagnetization followed by thermal demagnetization, demonstrating the within site consistency of the demagnetization behavior. Demagnetization steps in temperatures (°C) or in milliTesla (mT) are given alongside selected vertical projection data points. Also shown are normalized intensity decay plots showing response to progressive demagnetization treatment (abscissa is either demagnetizing temperature or peak alternating field, mT) and equal area stereographic projections of the magnetization vector measured at each step. Note that the coordinate axes for each and every diagram are identical in orientation. Site Bt21 is in a light green-gray siltstone, exposed in the main donga (location in Supplemental Figure 4) and within our inferred stratigraphically thick reverse polarity magnetozone. Site Bt35 is in light green siltstone exposed immediately southeast of the contact with a Karoo mafic dike (sampled as site Bt29). All samples from the host rock at site

Bt35 show very similar response to demagnetization and yield a magnetization that is statistically indistinguishable from the Karoo dike. Positions of sites Bt35/Bt29 shown in Supplemental Figure 4). All data are shown in geographic coordinates.

Supplemental Figure 6–Examples of anisotropy of magnetic susceptibility (AMS) data from selected sites in the Bethulie section. (A,B) Sites arearranged in stratigraphic order from uppermost site selected (Bt33) to lowermost (Bt64). For each site, the stereographic projection shows the principal susceptibility axes for each specimen (typically two specimens per sample measured; lower hemisphere projections). In addition, the anisotropy parameter P, where $P = K_{max}/K_{min}$, is plotted vs. bulk susceptibility for each specimen measured and the anisotropy parameter T, where T, the shape parameter (= $([2\ln K_{int} - \ln K_{max} - \ln K_{min}]/[\ln K_{max} - \ln K_{min}]$) is plotted vs. P. T values close to 1.0 are associated with strong oblate fabrics. The data from all sites, show a fabric that is typical of very fine grained detrital sedimentary rocks, with the minimum susceptibility axis (circles) essential vertical and well-grouped. Some sites display a moderately -defined imbrication fabric, with the minimum susceptibility axis canted from the vertical. Site Bt25was established in several 0.5 m + diameter concretions confined to a specific stratigraphic datum.

Supplemental Figure 7–Plots showing the response to progressive thermal demagnetization by isothermal remanent magnetizations (IRM) acquired in three orthogonal orientations at three different field strengths for specimens from samples from representative sites in sedimentary rocks sampled in the Bethulie section. The method follows that of Lowrie (1990), with data normalized to initial total magnetization (M_{total}) prior to demagnetization. For all of these experiments, the IRM acquisition fields are 2.97T, 300mT, and 15mT. Note that in many cases the IRM component acquired at 15 mT (last to be acquired) is nearly identical to the total magnetization (M_{total}) of the specimen.

Supplemental Figure 8–Plots showing the change in bulk susceptibility during heating and cooling (X vs. temperature experiments). Experiments conducted on crushed but not ground whole rock fragments of samples from selected sites in the Bethulie sedimentary sequence. In each of these diagrams, the red curve is the heating curve of the sample; blue curve is the cooling. Heating and cooling cycles are carried out with the sample flushed with argon gas.

Supplemental Figure 9– Location of reported palynological assemblage at the contact between the *Dicynodon* (=*Daptocephalus*) and *Lystrosaurus* AZs southwest of Bethulie, Free State. (A) Snippet of Table 3.1 from Barbolini (2014) in which the GPS coordinates for sample 14, reported to have been collected at the Permian–Triassic boundary at the contact of the *Dicynodon* (=*Daptocephalus*) AZ are highlighted. (B) Barbolini (2014) reports the locality on the R390; the coordinates plot on the R58, 3.4 km from Schalkwykskraal on the shore of Garip Dam. Vertebrates collected from Schalkwykskraal are used by Viglietti et al.

(2016) to circumscribe the *Daptocephalus* Assemblage Zone. (C) GoogleEarth street view of the outcrop sampled by Barbolini (2014) showing exposure on either side of the R58. (D) Panoramic image of the southeast roadside where a dolerite intrusive dike crosscuts the outcrop, resulting in contact metamorphism of surrounding siltstone. J. Geissman, atop dolerite dike, and J. Neveling for scale (27 January 2016).

Supplemental Figure 10–Palynological assemblage from Donald 207 (Fairydale) farm. (A) Snippet of Table 3.1 from Barbolini (2014) in which the GPS coordinates for sample 15, reported to have been collected at the Permian–Triassic boundary at the top of the *Dicynodon* (=*Daptocephalus*) AZ on Fairydale farm, are highlighted. (B) The coordinates of Barbolini (2014) exactly match those we used to resample the locality, plotted on GoogleEarth.

Supplemental Table 1 – Iziko Museum query of vertebrate collections made by S. Kaal, 3 May 2013, after field work around Lootsberg Pass, Eastern Cape Province. Note that GPS coordinates identifying the site from which each vertebrate was collected are redacted to preserve the integrity of the fossil record. The museum database indicates that specimens given an RS assignment lower than RS74 were collected prior to 1 January 1999. In contrast, vertebrates given RS assigned number beginning with RS78 were collected after 1 January 1999. GPS coordinates for specimens with numbers lower than RS74 are considered to have been located using the Cape Datum system, and omitted from consideration in our analysis. Specimens collected after 1 January 1999 are presumed to have been located using the WGS84 coordinate system. Vertebrates collected in October 2000 in the area around Lootsberg Pass are assigned numbers of RS124 (SAM-PK-K-10685). There is no indication in any published report documenting vertebrate biostratigraphy, other than our work, about which coordinate system was in use at any point in time.

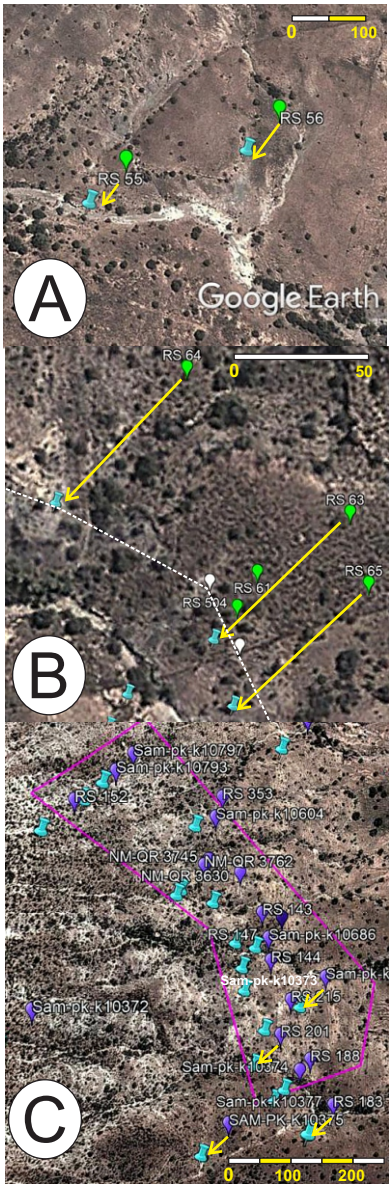

Gastaldo et al. Supplemental Fig. 1

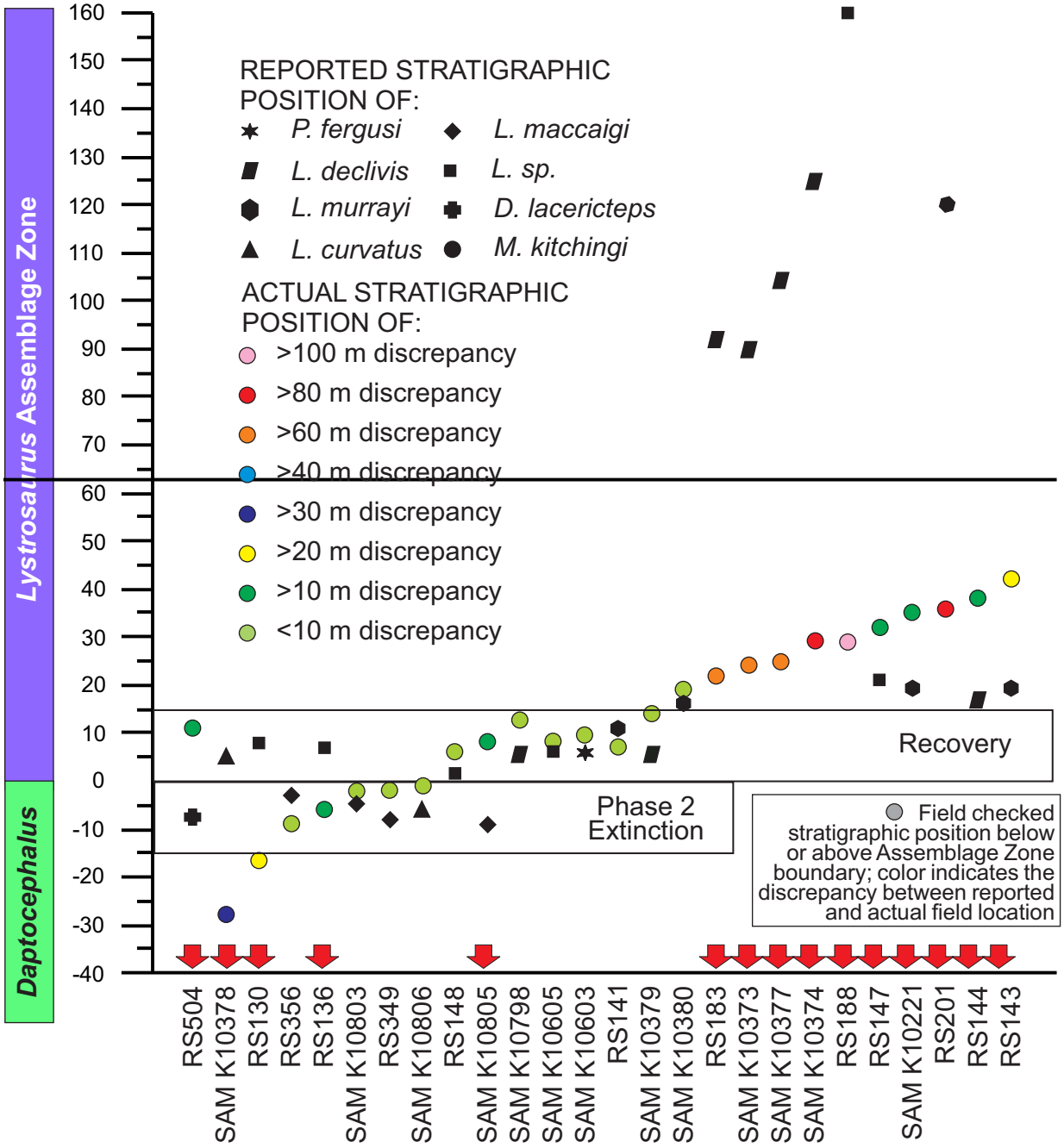

Gastaldo et al. Supplemental Fig. 2

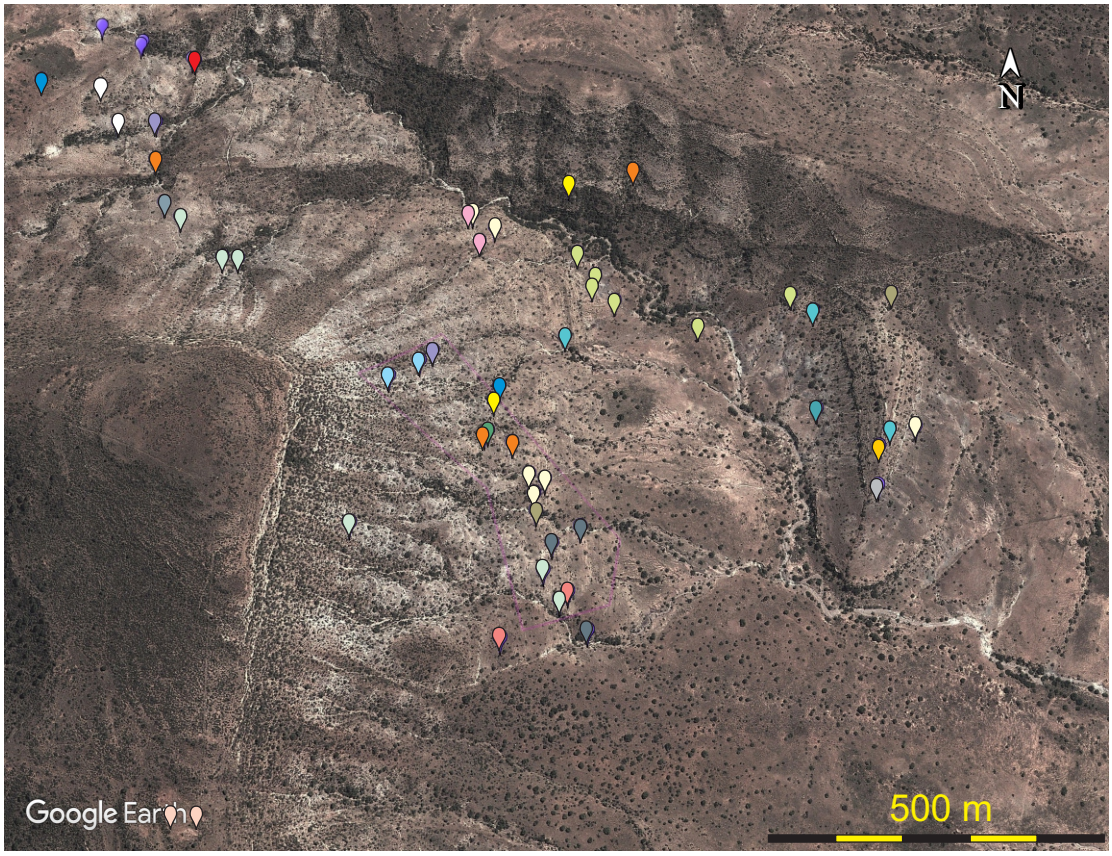

Reported Positions Above the *Daptocephalus/Lystrosaurus* Assemblage Zone Boundary

20-24 m	40-44 m	60-64 m	80-89 m	>160 m
15-19 m	35-39 m	55-59 m	75-79 m	130-159 m
10-14 m	30-34 m	50-54 m	70-74 m	100-129 m
<10 m	25-29 m	45-49 m	65-69 m	90-99 m

Gastaldo et al. Supplemental Fig. 3

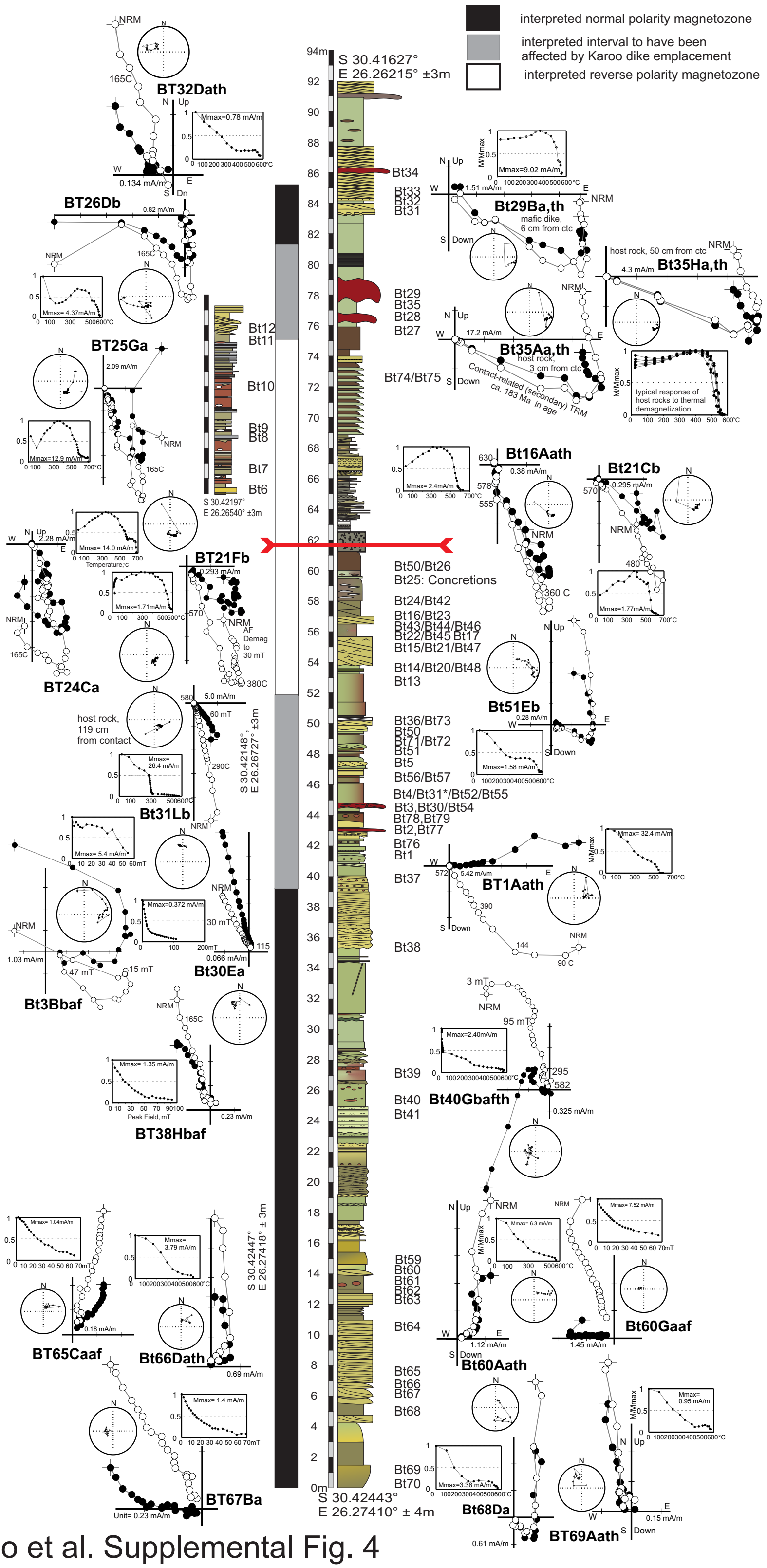

Gastaldo et al. Supplemental Fig. 4

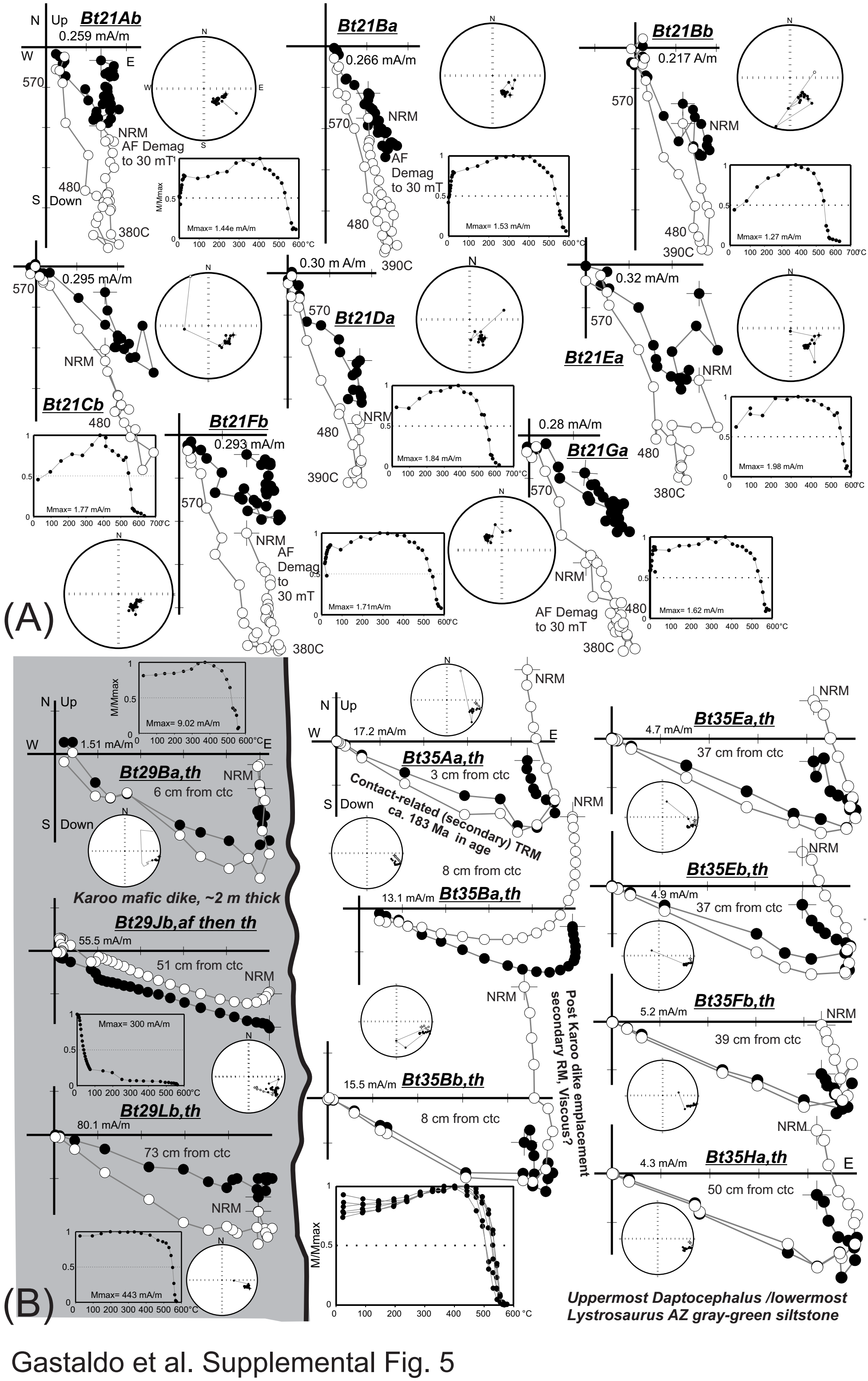

Gastaldo et al. Supplemental Fig. 5

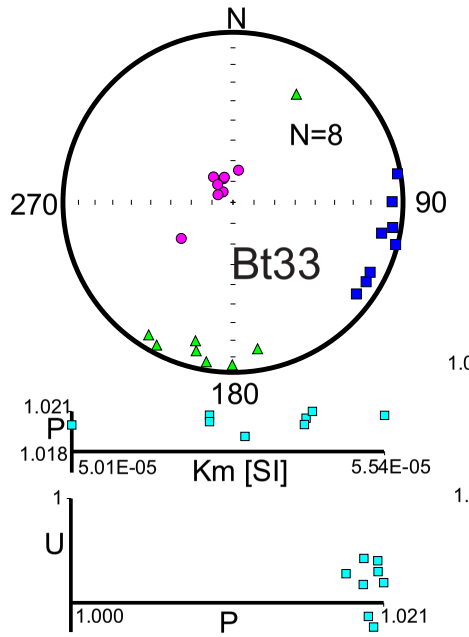

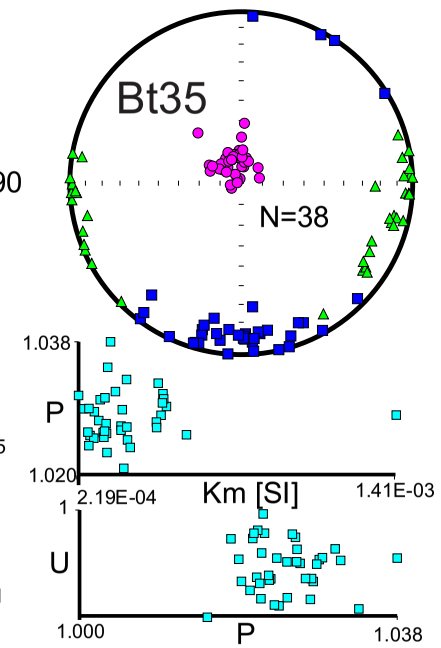

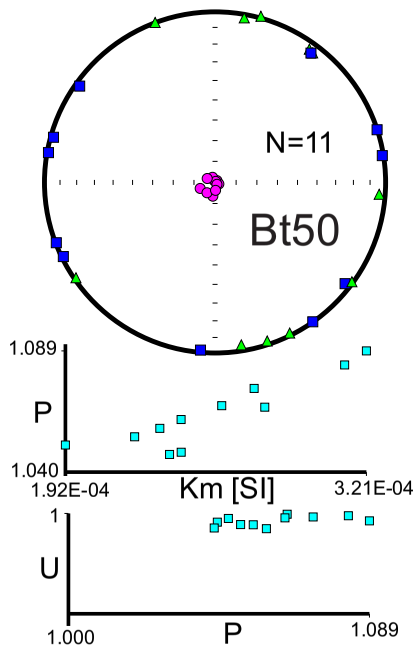

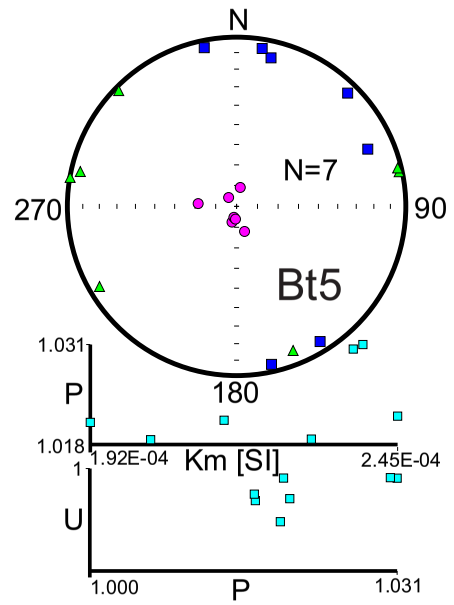

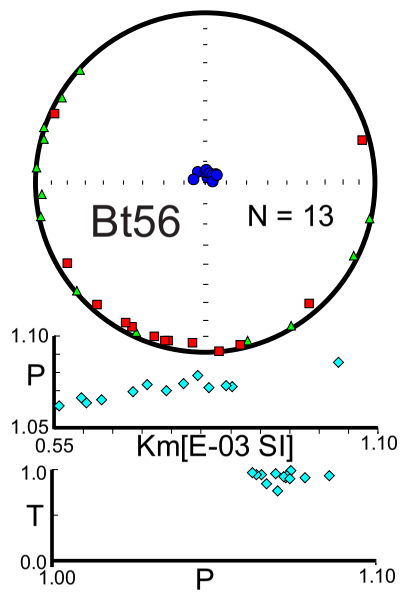

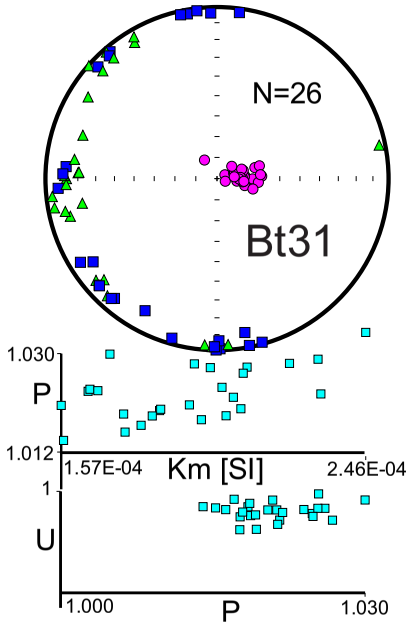

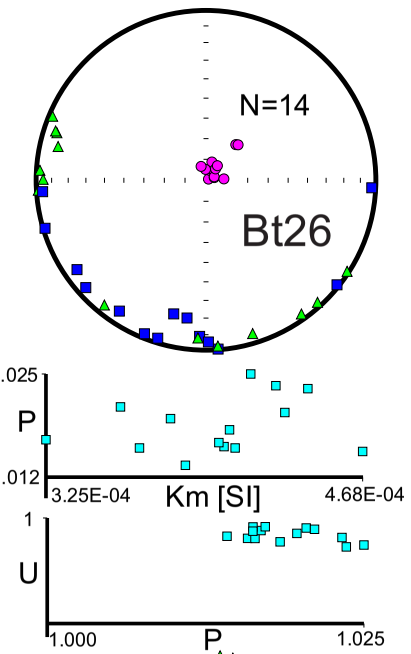

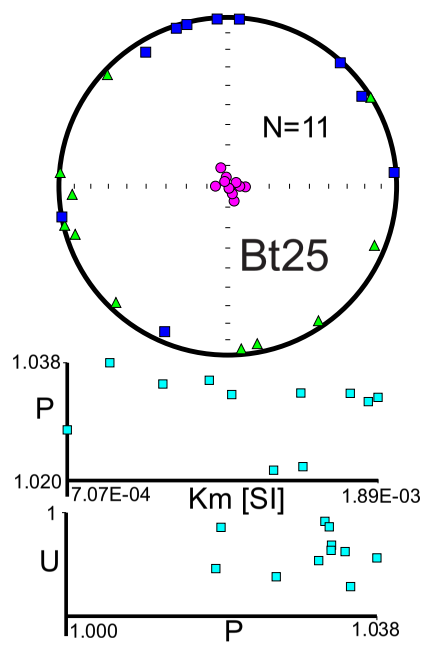

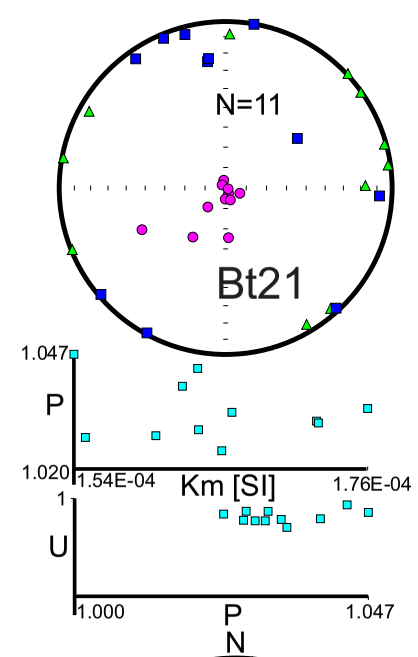

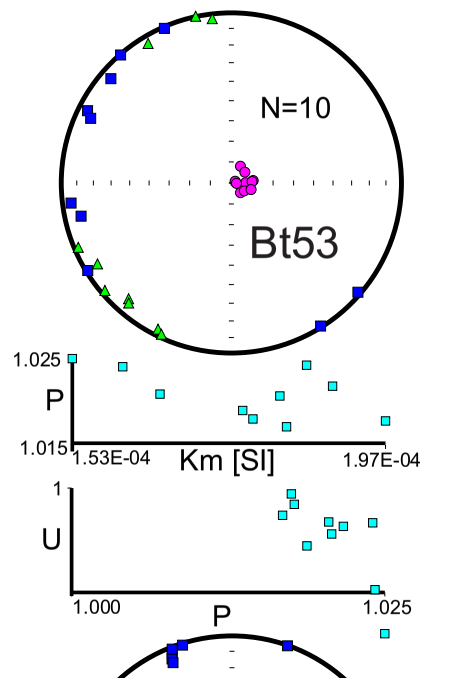

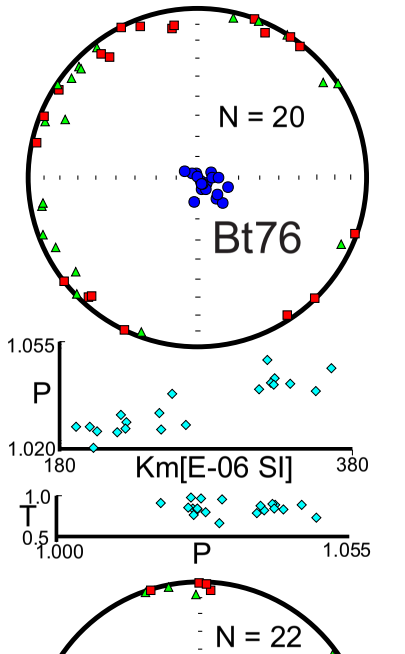

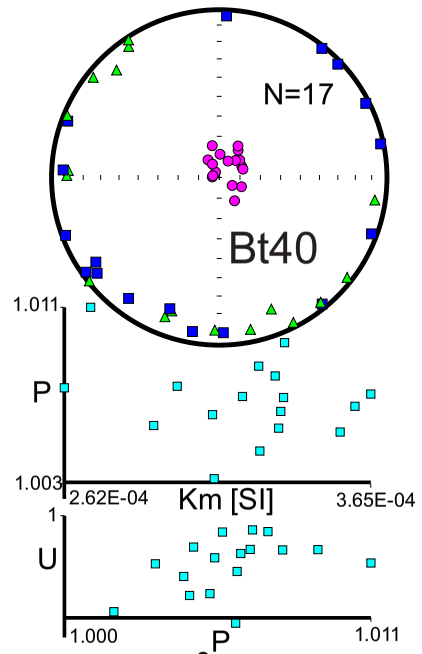

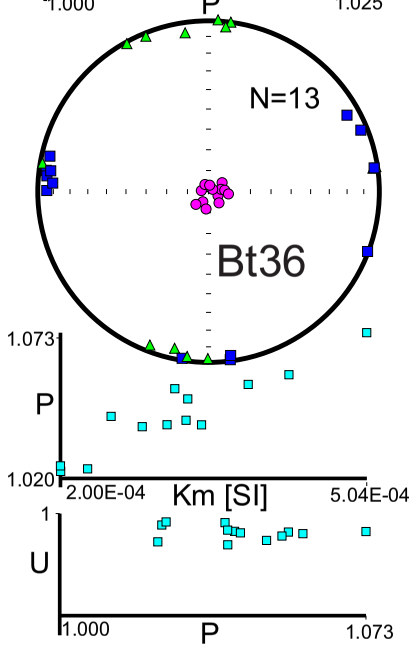

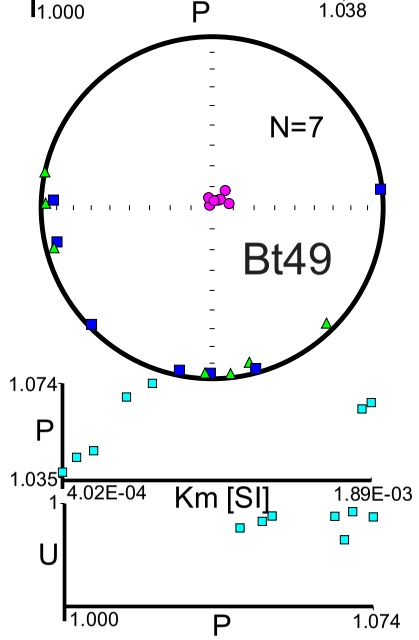

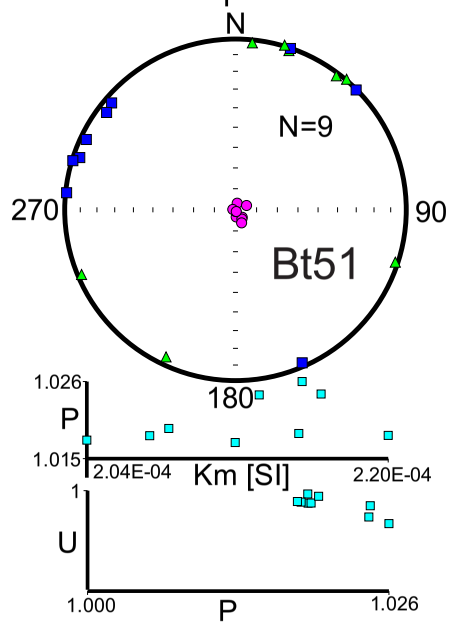

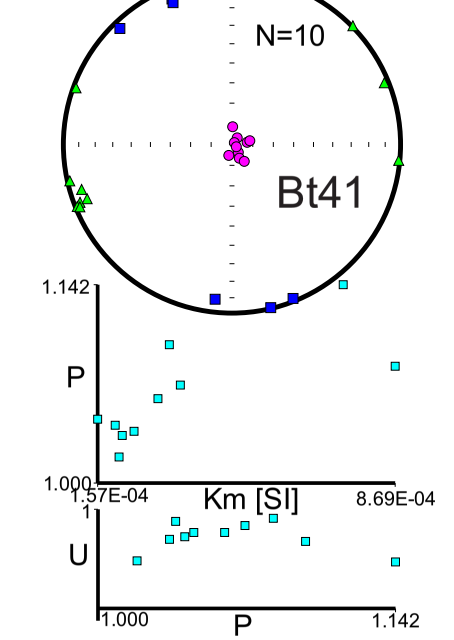

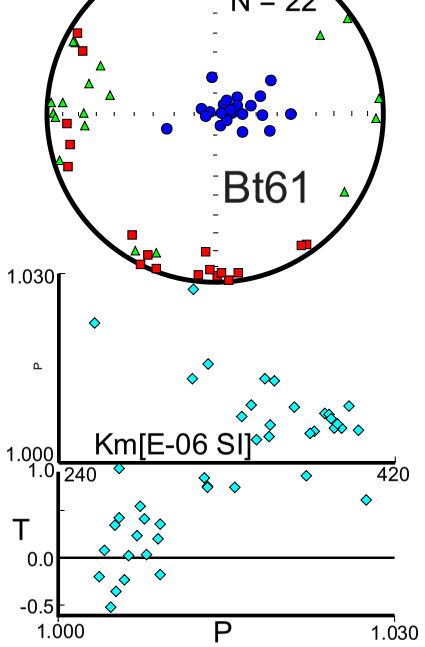

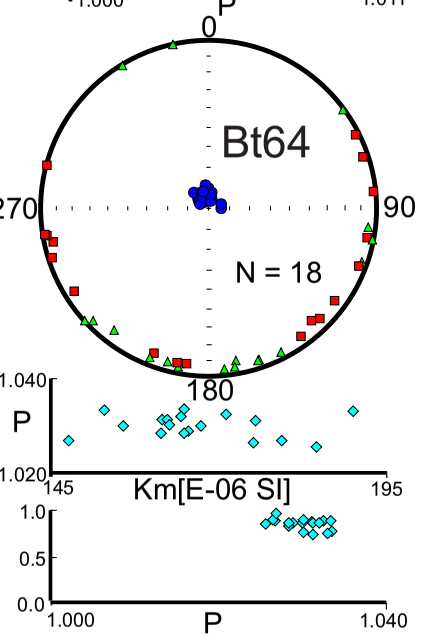

Gastaldo et al. Supplemental Fig. 6

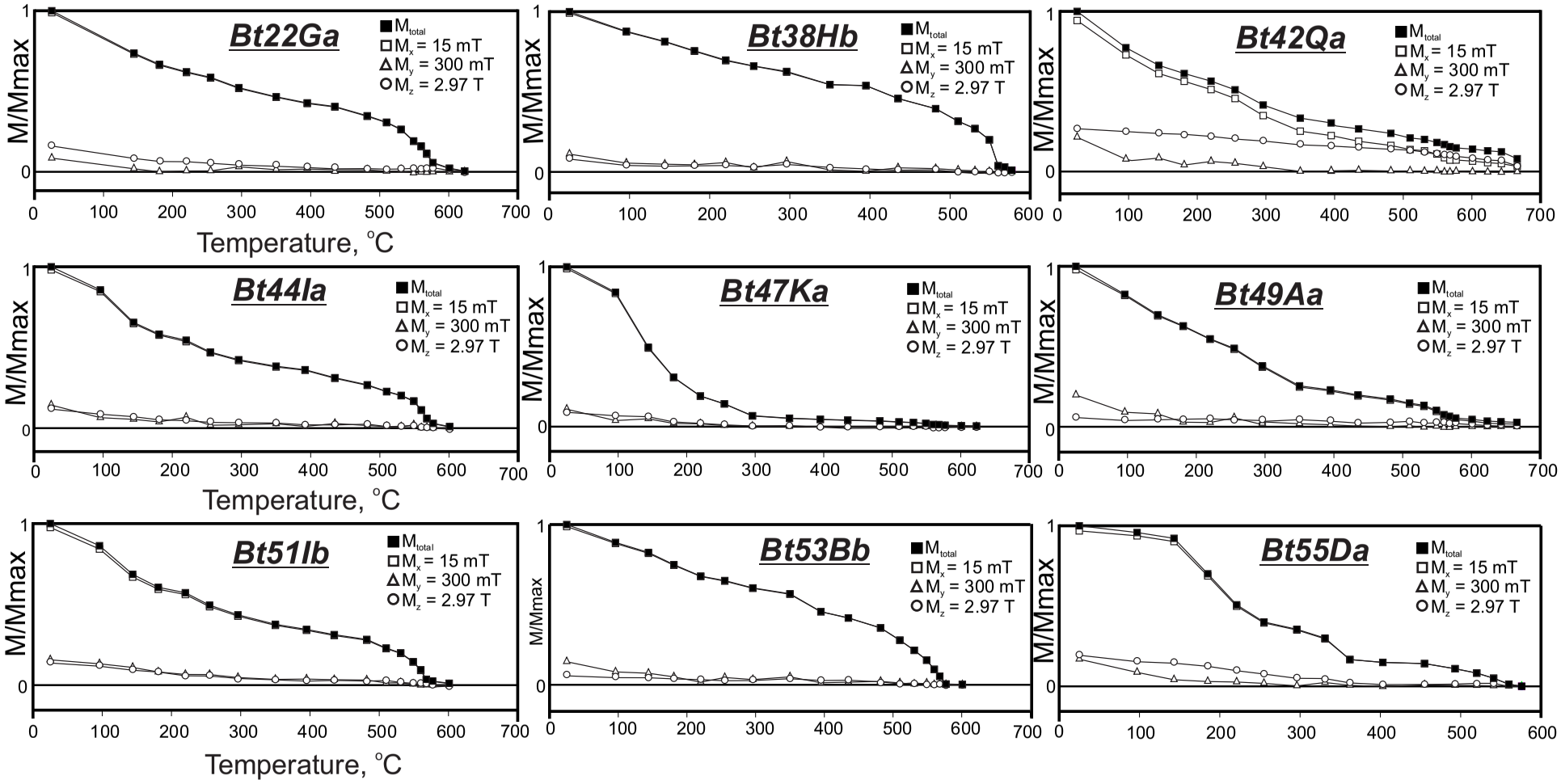

Gastaldo et al. Supplemental Fig. 7

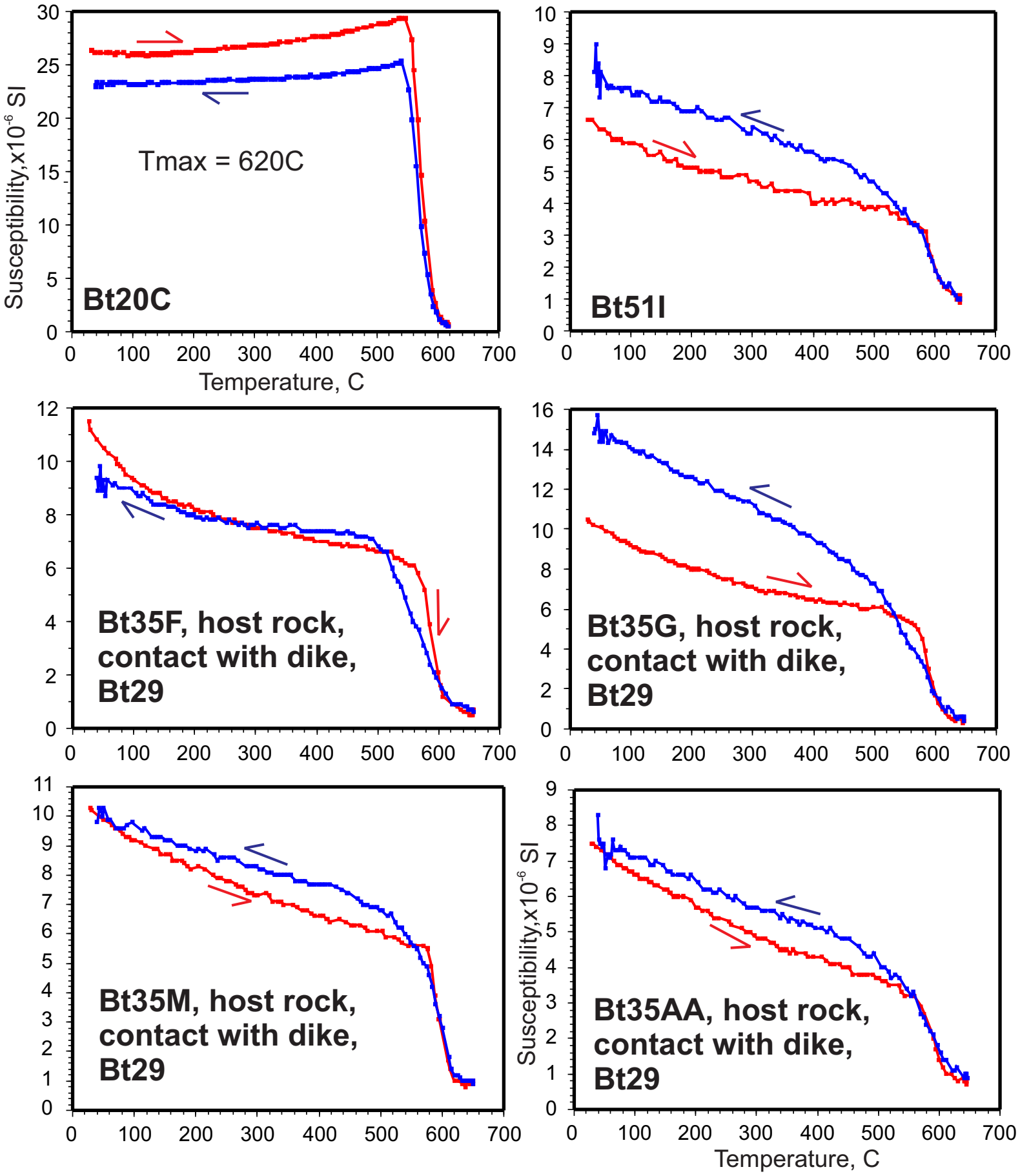

Gastaldo et al. Supplemental Fig. 8

A

E.Katberg Fm 13	S32°20.701' E026°54.315'	*Lystrosaurus* AZ	Road cutting	R67 Whittlesea, Fort Beaufort District
E.Palingkloof M. 14	S30°44.384' E025°39.494'	*Dicynodon* - *Lystrosaurus* AZ Contact	Road cutting	Road from Steynsburg to Venterstad, R390

Gastaldo et al. Supplemental Fig. 9

RS NUMBERS:

Accession Number	Other Number	Genus	Species	Cranial Elements	District	Gov Farm & Number	Farm Name/Place	Latitude	Longitude	Formation	Member	Assemblage Zone	Epoch	Period	Collector 1 Surname	Date Collected
SAM-PK-K09953	RS6	Moschorhinus	sp.	Skull	Graaff-Reinet	Lucerne 70	Lootsberg Pass					Lystrosaurus	Early	Triassic	Smith	00/03/1999
SAM-PK-K09954	RS11	Progalesaurus	lootsbergensis	Skull with lower jaw	Graaff-Reinet	Lucerne 70	Lootsberg Pass				Palingkloof	Lystrosaurus	Early	Triassic	Smith	00/11/1998
SAM-PK-K09955	RS43	Dicynodon	lacerticeps	Skull	Rouxville	Caledon Draai 877	Caledon Draai					Dicynodon	Late	Permian	Ward	00/11/1998
SAM-PK-K09949	RS51	Dicynodon	lacerticeps	Skull	Rouxville	Caledon Draai 877	Caledon Draai					Dicynodon	Late	Permian	Stummer	00/11/1998
SAM-PK-K10684	RS64	Moschorhinus	kitchingi	Pieces of anterior skull	Smithfield	Bethel 763	Bethal				Palingkloof	Dicynodon	Latest	Permian	Smith	00/11/1998
SAM-PK-K09957	RS66	Proterosuchus	fergusi	Incomplete skull	Smithfield	Heldenmoed 677	Heldemoed					Lystrosaurus		Permian/Triassic Boundary	Ward	00/11/1998
SAM-PK-K09950	RS68	Lystrosaurus	sp.	Skulls	Rouxville	Caledon Draai 877	Caledon Draai					Lystrosaurus	Early	Triassic	October	00/11/1998
SAM-PK-K09951	RS71	Lystrosaurus	sp.	Skull	Rouxville	Caledon Draai 877	Caledon Draai					Lystrosaurus	Early	Triassic	Smith	00/11/1998
SAM-PK-K10370	RS72	Micropholis	stowi	Skulls, some with lower jaws	Rouxville	Caledon Draai 877	Caledon Draai					Lystrosaurus	Early	Triassic	Smith	00/11/1998
SAM-PK-K09958	RS74	Lystrosaurus	maccaigi	Skull with lower jaw	Smithfield	Bethel 763	Bethal					Dicynodon		Permian/Triassic Boundary	Smith	00/11/1998
SAM-PK-K09956	RS78	Galesaurus	planiceps	Skull with lower jaw	Bethulie	Donald 207	Donald 207					Lystrosaurus	Early	Triassic	Smith	00/11/1999
SAM-PK-K10022	RS88	Daptocephalus	leoniceps	Skull	Graaff-Reinet	Farm 80	Wapadsberg Pass					Dicynodon	Late	Permian	Smith	00/11/1999
SAM-PK-K10021	RS89	Rhinesuchid		Partial skull	Graaff-Reinet	Lucerne 70	Lucerne 70					Dicynodon	Late	Permian	Ward	00/10/1999
SAM-PK-K10698	RS91	Moschorhinus		Partial lower jaw	Graaff-Reinet	Lucerne 70	Lucerne 70					Lystrosaurus	Early	Triassic	Smith	26/10/1999
SAM-PK-K10697	RS100	Promoschorhynchus		Partial maxilla and lower jaw	Graaff-Reinet	Zeekoegat 77	Zeekoegat 77				Palingkloof	Uppermost Dicynodon		Permian/Triassic Boundary	October	27/10/1999
SAM-PK-K10617	RS101	Akidnognathid			Graaff-Reinet	Zeekoegat 77	Zeekoegat 77					Lystrosaurus	Early	Triassic	Smith	26/10/1998
SAM-PK-K11045	RS109	Lystrosaurus		Anterior skull	Graaff-Reinet	Zeekoegat 77	Zeekoegat 77				Palingkloof	Uppermost Dicynodon		Permian/Triassic Boundary	Smith	30/10/1999
SAM-PK-K10685	RS124	Lystrosaurus	maccaigi	Skull	Smithfield	Bethel 763	Bethal				Palingkloof	Dicynodon	Late	Permian	Smith	04/10/2000
SAM-PK-K10014	RS129	Promoschorhynchus	aff.platyrhinus	Skull	Smithfield	Bethel 763	Bethal				Palingkloof	Lystrosaurus	Late	Permian	Smith	00/10/2000
SAM-PK-K10015	RS137	Moschorhinus	sp.	Skulls	Smithfield	Bethel 763	Bethal				Palingkloof	Lystrosaurus	Late	Permian	Smith	00/11/2000
SAM-PK-K10221	RS145	Lystrosaurus	murrayi	Skull with lower jaw	Smithfield	Bethel 763	Bethal					Lystrosaurus	Early	Triassic	Smith	09/10/2000
SAM-PK-K10686	RS146	Lystrosaurus	murrayi	Skull with incomplete lower jaw	Smithfield	Bethel 763	Bethal					Lystrosaurus	Early	Triassic	Smith	09/10/2000
SAM-PK-K10185	RS149	Lystrosaurus	curvatus	Skull with lower jaw	Smithfield	Bethel 763	Bethal				Palingkloof	Dicynodon		Permian/Triassic Boundary	Stummer	12/10/2000
SAM-PK-K10023	RS158	Scaloposaurus	constrictus	Skull with lower jaw	Bethulie	Straat Drift 395	Tussen Die Riviere Game Reserve					Lystrosaurus	Early	Triassic	Ward	14/10/2000
SAM-PK-K10687	RS161	Lystrosaurus	murrayi	Skull with lower jaw	Bethulie	Straat Drift 395	Tussen Die Riviere Game Reserve					Lystrosaurus	Early	Triassic	Smith	14/10/2000
SAM-PK-K10016	RS166	Thrinaxodon	liorhinus	Skull	Graaff-Reinet	Zeekoegat 77	Zeekoegat 77					Lystrosaurus	Early	Triassic	Smith	00/11/2000
SAM-PK-K10017	RS167	Thrinaxodon	liorhinus	Skulls with lower jaws	Graaff-Reinet	Zeekoegat 77	Zeekoegat 77					Lystrosaurus	Early	Triassic	Smith	00/11/2000
SAM-PK-K10220	RS168	Dinanomodon		Skull with lower jaw	Graaff-Reinet	Farm 79	Old Wapadsberg Pass					Dicynodon	Late	Permian	Stummer	18/10/2000
SAM-PK-K10094	RS176	Therapsid			Noupoort	Naauw Poort 1	Carlton Heights					Lystrosaurus	Early	Triassic	Smith	22/11/2001
SAM-PK-K10095	RS177	Lystrosaurus	sp.	Skull	Noupoort	Naauw Poort 1	Carlton Heights Pass					Dicynodon	Late	Permian	Crean	22/11/2001
SAM-PK-K10092	RS178	Lystrosaurus	sp.	Skull	Noupoort	Naauw Poort 1	Carlton Heights					Lystrosaurus	Early	Triassic	Smith	22/11/2001
SAM-PK-K10093	RS179	Dicynodon	lacerticeps	Incomplete skull	Noupoort	Naauw Poort 1	Carlton Heights					Dicynodon	Late	Permian	Crean	23/11/2001
SAM-PK-K10371	RS182	Lystrosaurus	maccaigi	Lower jaw	Smithfield	Bethel 763	Bethal				Palingkloof	Dicynodon	Latest	Permian	Smith	12/03/2004
SAM-PK-K10372	RS184	Lystrosaurus	murrayi	Skull	Smithfield	Bethel 763	Bethal					Lystrosaurus	Early	Triassic	Smith	12/03/2004
SAM-PK-K10373	RS185	Lystrosaurus	declivis	Skull with lower jaw	Smithfield	Bethel 763	Bethal					Lystrosaurus	Early	Triassic	Crean	12/03/2004
SAM-PK-K10374	RS186	Lystrosaurus	declivis	Skull	Smithfield	Bethel 763	Bethal					Lystrosaurus	Early	Triassic	Stummer	12/03/2004
SAM-PK-K10375	RS187	Lystrosaurus	murrayi	Skull with lower jaw	Smithfield	Bethel 763	Bethal					Lystrosaurus	Early	Triassic	Crean	12/03/2004
SAM-PK-K10376	RS189	Lystrosaurus	maccaigi	Skull	Bethulie	Mooidraai 513	Mooidraai					Dicynodon	Late	Permian	Stummer	13/03/2004
SAM-PK-K10377	RS190	Lystrosaurus	declivis	Skull	Smithfield	Bethel 763	Bethal					Lystrosaurus	Early	Triassic	Crean	13/03/2004
SAM-PK-K10378	RS191	Lystrosaurus	curvatus	Skull	Smithfield	Heldenmoed 677	Heldemoed					Lystrosaurus	Early	Triassic	Smith	14/03/2004
SAM-PK-K10379	RS192	Lystrosaurus	declivis	Skull	Smithfield	Heldenmoed 677	Heldemoed					Lystrosaurus	Early	Triassic	Smith	14/03/2004
SAM-PK-K10380	RS193	Lystrosaurus	murrayi	Skull	Smithfield	Heldenmoed 677	Heldemoed					Lystrosaurus	Early	Triassic	Stummer	14/03/2004
SAM-PK-K10381	RS194	Lystrosaurus	sp.		Smithfield	Heldenmoed 677	Heldemoed					Lystrosaurus	Early	Triassic	Smith	15/03/2004
SAM-PK-K10382	RS196	Scaloposaurus	sp.	Skull with lower jaw	Bethulie	Donald 207	Donald 207					Lystrosaurus	Early	Triassic	Smith	18/03/2004
SAM-PK-K10383	RS198	Lystrosaurus	murrayi	Skull with lower jaw	Bethulie	Donald 207	Donald 207					Lystrosaurus	Early	Triassic	Smith	18/03/2004
SAM-PK-K10384	RS199	Lystrosaurus	declivis	Skull with lower jaw	Bethulie	Donald 207	Donald 207					Lystrosaurus	Early	Triassic	Smith	18/03/2004
SAM-PK-K10385	RS201	Lystrosaurus	murrayi	Skull with lower jaw	Smithfield	Bethel 763	Bethal					Lystrosaurus	Early	Triassic	October	12/03/2004
SAM-PK-K10386	RS202	Lystrosaurus	declivis	Skull with lower jaw	Bethulie	Donald 207	Donald 207					Lystrosaurus	Early	Triassic	Stummer	17/03/2004

SAM-PK-K10387	RS204	Micropholis	stowi	Partial skull with lower jaw	Bethulie	Donald 207	Donald 207				Lystrosaurus	Early	Triassic	Smith	19/03/2004
SAM-PK-K10388	RS205	Vertebrate	indet.		Bethulie	Donald 207	Donald 207				Lystrosaurus	Early	Triassic	Smith	19/03/2004
SAM-PK-K10389	RS206	Lystrosaurus	murrayi	Skull	Bethulie	Donald 207	Donald 207				Lystrosaurus	Early	Triassic	Smith	19/03/2004
SAM-PK-K10390	RS207	Lystrosaurus	sp.	Skulls with lower jaws	Bethulie	Donald 207	Donald 207				Lystrosaurus	Early	Triassic	Erasmus	19/03/2004
SAM-PK-K10391	RS208	Vertebrate	indet.		Bethulie	Donald 207	Donald 207				Lystrosaurus	Early	Triassic	Crean	19/03/2004
SAM-PK-K10218	RS209	Tetracynodon	sp.	Skull with lower jaw	Graaff-Reinet	Zeekoegat 77	Zeekoegat 77				Lystrosaurus	Early	Triassic	Stummer	09/06/2003
SAM-PK-K10392	RS210	Proterosuchus	fergusi		Graaff-Reinet	Zeekoegat 77	Zeekoegat 77				Lystrosaurus	Early	Triassic	Stummer	27/03/2004
SAM-PK-K10403	RS211	Scaloposaurus	constrictus	Skull with lower jaw	Graaff-Reinet	Zeekoegat 77	Zeekoegat 77				Lystrosaurus	Early	Triassic	Smith	27/03/2004
SAM-PK-K10216	RS212	Owenetta		Skull with lower jaw	Graaff-Reinet	Zeekoegat 77	Zeekoegat 77				Lystrosaurus	Earliest	Triassic	Smith	09/06/2003
SAM-PK-K10217	RS213	Dicynodon	lacerticeps	Skull	Graaff-Reinet	Farm 79	Old Wapadsberg Pass	Balfour		Palingkloof	Dicynodon	Latest	Permian	Smith	10/06/2003
SAM-PK-K10406	RS214	Sauropareian		Skulls and lower jaw	Graaff-Reinet	Lucerne 70	Lucerne 70	Katberg			Lystrosaurus	Earliest	Triassic	Smith	
SAM-PK-K10415	RS216	Diictodon	sp.	Skull and disarticulated lower jaw	Graaff-Reinet	Rust 126	Doornplaats	Balfour	2		Upper Cistecephalus	Late	Permian	Erasmus	05/10/2004
SAM-PK-K10416	RS217	Oudenodon	sp.	Two skulls	Graaff-Reinet	Rust 126	Doornplaats	Balfour			Upper Cistecephalus	Late	Permian	Smith	05/10/2004
SAM-PK-K10417	RS218	Gorgonopsian		Snout	Graaff-Reinet	Rust 126	Doornplaats	Balfour			Dicynodon	Late	Permian	Smith	05/10/2004
SAM-PK-K10418	RS219	Oudenodon	sp.	Skull	Graaff-Reinet	Rust 126	Doornplaats	Balfour			Dicynodon	Late	Permian	Botha	06/10/2004
SAM-PK-K10419	RS220	Cistecephalus	sp.	Skull with anterior lower jaw	Graaff-Reinet	Rust 126	Doornplaats	Balfour			Cistecephalus	Late	Permian	Botha	05/10/2004
SAM-PK-K10420	RS221	Diictodon	sp.	Skulls, one with lower jaw	Graaff-Reinet	Rust 126	Doornplaats	Balfour			Cistecephalus/Dicynodon	Late	Permian	Smith	05/10/2004
SAM-PK-K10421	RS222	Dicynodon	lacerticeps	Snout	Graaff-Reinet	Rust 126	Doornplaats	Balfour			Cistecephalus/Dicynodon	Late	Permian	Smith	06/10/2004
SAM-PK-K10422	RS223	Diictodon	sp.	Skull with lower jaw	Graaff-Reinet	Rust 126	Doornplaats	Balfour			Dicynodon	Late	Permian	Smith	08/10/2004
SAM-PK-K10423	RS224	Ictidosuchoides	longiceps	Snout with lower jaw	Graaff-Reinet	Rust 126	Doornplaats	Balfour			Dicynodon	Late	Permian	Smith	08/10/2004
SAM-PK-K10424	RS225	Diictodon	sp.	Skull with lower jaw	Graaff-Reinet	Rust 126	Doornplaats	Balfour			Dicynodon	Late	Permian	Smith	08/10/2004
SAM-PK-K10425	RS226	Emydops	sp.	Skull	Graaff-Reinet	Rust 126	Doornplaats	Balfour			Dicynodon	Late	Permian	Botha	08/10/2004
SAM-PK-K10426	RS227	Emydops	sp.	Skull	Graaff-Reinet	Rust 126	Doornplaats	Balfour			Dicynodon	Late	Permian	Smith	08/10/2004
SAM-PK-K10496	RS228	Aelurognathus		Anterior skull with lower jaw	Graaff-Reinet	Rust 126	Doornplaats	Balfour		Daggaboersnek	Lower Dicynodon	Late	Permian	Smith	08/10/2004
SAM-PK-K10427	RS229	Vertebrate	indet.		Graaff-Reinet	Rust 126	Doornplaats	Balfour			Dicynodon	Late	Permian	Smith	08/10/2004
SAM-PK-K10428	RS231	Cyonosaurus	longiceps	Skull with lower jaw	Graaff-Reinet	Rust 126	Doornplaats	Balfour			Dicynodon	Late	Permian	Smith	10/10/2004
SAM-PK-K10429	RS232	Theriognathus	sp.	Skull	Graaff-Reinet	Rust 126	Doornplaats	Balfour			Dicynodon	Late	Permian	Botha	09/10/2004
SAM-PK-K10430	RS233	Diictodon	sp.	Skull	Graaff-Reinet	Rust 126	Doornplaats	Balfour			Dicynodon	Late	Permian	Erasmus	09/10/2004
SAM-PK-K10431	RS235	Rhinesuchus	sp.	Left side of snout with accompanying lower jaw	Graaff-Reinet	Rust 126	Doornplaats	Balfour			Cistecephalus/Dicynodon	Late	Permian	Smith	11/10/2004
SAM-PK-K10454	RS237	Lystrosaurus	declivis	Skull	Bethulie	Donald 207	Donald 207	Lower	Katberg		Lystrosaurus	Early	Triassic	Smith	19/04/2005
SAM-PK-K10459	RS237(b)	Lystrosaurus	sp.	Snout	Bethulie	Donald 207	Donald 207	Lower	Katberg		Lystrosaurus	Early	Triassic	Smith	19/04/2005
SAM-PK-K10455	RS238	Lystrosaurus	sp.		Bethulie	Donald 207	Donald 207	Lower	Katberg		Lystrosaurus	Early	Triassic	Smith	19/04/2005
SAM-PK-K10456	RS241	Lystrosaurus	declivis	Skull with lower jaw	Bethulie	Donald 207	Donald 207	Lower	Katberg		Lystrosaurus	Early	Triassic	October	19/04/2005
SAM-PK-K10457	RS242	Lystrosaurus	declivis	Skull with lower jaw	Bethulie	Donald 207	Donald 207	Lower	Katberg		Lystrosaurus	Early	Triassic	October	19/04/2005
SAM-PK-K10458	RS242	Lystrosaurus	declivis	Partial skull with complete lower jaw	Bethulie	Donald 207	Donald 207	Lower	Katberg		Lystrosaurus	Early	Triassic	October	19/04/2005
SAM-PK-K10460	RS243	Lystrosaurus	declivis	Skull	Bethulie	Donald 207	Donald 207	Lower	Katberg		Lystrosaurus	Early	Triassic	Erasmus	20/04/2005
SAM-PK-K10461	RS244	Lystrosaurus	murrayi	Skull	Bethulie	Donald 207	Donald 207	Lower	Katberg		Lystrosaurus	Early	Triassic	Erasmus	20/04/2005
SAM-PK-K10462	RS246	Lystrosaurus	sp.	Skull with lower jaw	Bethulie	Donald 207	Donald 207	Lower	Katberg		Lystrosaurus	Early	Triassic	October	20/04/2005
SAM-PK-K10463	RS247	Procolophon	sp.	Skull with lower jaw	Bethulie	Donald 207	Donald 207	Lower	Katberg		Lystrosaurus	Early	Triassic	October	20/04/2005
SAM-PK-K10464	RS248	Lystrosaurus	sp.	Snout	Smithfield	Heldenmoed 677	Heldemoed	Lower	Katberg		Lystrosaurus	Early	Triassic	Smith	20/04/2005
SAM-PK-K10465	RS249	Galesaurus	planiceps	Skull with lower jaw	Bethulie	Donald 207	Donald 207	Lower	Katberg	Palingkloof	Lystrosaurus	Early	Triassic	Smith	20/04/2005
SAM-PK-K10466	RS250	Lystrosaurus	murrayi	Skull with lower jaw	Bethulie	Donald 207	Donald 207	Lower	Katberg		Lystrosaurus	Early	Triassic	Smith	20/04/2005
SAM-PK-K10467	RS255	Lystrosaurus	declivis	Skull with lower jaw	Bethulie	Donald 207	Donald 207	Lower	Katberg		Lystrosaurus	Early	Triassic	Smith	20/04/2005
SAM-PK-K10468	RS256	Galesaurus	planiceps	Skull with lower jaw	Bethulie	Donald 207	Donald 207	Lower	Katberg	Palingkloof	Lystrosaurus	Early	Triassic	Smith	20/04/2005
SAM-PK-K10469	RS257	Lystrosaurus	sp.		Bethulie	Donald 207	Donald 207	Lower	Katberg		Lystrosaurus	Early	Triassic	Smith	21/04/2005
SAM-PK-K10470	RS258	Lystrosaurus	declivis	Partial skull with lower jaw	Bethulie	Donald 207	Donald 207	Lower	Katberg		Lystrosaurus	Early	Triassic	Smith	21/04/2005
SAM-PK-K10471	RS259	Lystrosaurus	murrayi	Skull with lower jaw	Bethulie	Donald 207	Donald 207	Lower	Katberg		Lystrosaurus	Early	Triassic	Botha	21/04/2005
SAM-PK-K10472	RS262	Lystrosaurus	sp.	Skull with lower jaw	Bethulie	Donald 207	Donald 207	Lower	Katberg		Lystrosaurus	Early	Triassic	Smith	24/04/2005
SAM-PK-K10473	RS263	Lystrosaurus	declivis	Skull	Bethulie	Donald 207	Donald 207	Lower	Katberg		Lystrosaurus	Early	Triassic	Smith	24/04/2005
SAM-PK-K10474	RS264	Lystrosaurus	declivis	Skull with lower jaw	Bethulie	Donald 207	Donald 207	Lower	Katberg		Lystrosaurus	Early	Triassic	Wolvaardt	25/04/2005
SAM-PK-K10475	RS266	Micropholis	stowi	Skull with lower jaw	Bethulie	Donald 207	Donald 207	Lower	Katberg		Lystrosaurus	Early	Triassic	Smith	25/04/2005

SAM-PK-K10476	RS267	Fish		Fish head plates	Bethulie	Donald 207	Donald 207			Lower Katberg		Lystrosaurus	Early	Triassic		Wolvaardt	25/04/2005
SAM-PK-K10477	RS276	Cynodont		Skull with lower jaw	Bethulie	Grootfontein 339	Tussen Die Riviere Game Reserve			Lower Katberg		Lystrosaurus	Early	Triassic		Smith	27/04/2005
SAM-PK-K10478	RS277	Procolophon	sp.	Skull with lower jaw	Bethulie	Grootfontein 339	Tussen Die Riviere Game Reserve			Lower Katberg		Lystrosaurus	Early	Triassic		Wolvaardt	27/04/2005

BALFOUR FORMATION:

Accession Number	Other Number	Genus	Species	Cranial Elements	District	Gov Farm & Number	Farm Name/Place	Latitude	Longitude	Formation	Member	Assemblage Zone	Epoch		Period	Collector 1 Surname	Date Collected
SAM-PK-K08617	DOORN-1	Diictodon	sp.	Skull	Graaff-Reinet	Rust 126	Doornplaats			Balfour		Dicynodon	Late	Permian		Smith	00/04/1998
SAM-PK-K08618	DOORN-2	Oudenodon	sp.	Lower jaw	Graaff-Reinet	Rust 126	Doornplaats			Balfour		Dicynodon	Late	Permian		Smith	00/04/1998
SAM-PK-K08619	DOORN-3	Dicynodon	lacerticeps	Skull with lower jaw	Graaff-Reinet	Rust 126	Doornplaats			Balfour		Dicynodon	Late	Permian		Smith	00/04/1998
SAM-PK-K08620	DOORN-4	Kingoria	sp.	Skull	Graaff-Reinet	Rust 126	Doornplaats			Balfour		Dicynodon	Late	Permian		Skinner	00/04/1998
SAM-PK-K08621	DOORN-5	Oudenodon	sp.	Skull	Graaff-Reinet	Rust 126	Doornplaats			Balfour		Dicynodon	Late	Permian		Stummer	00/04/1998
SAM-PK-K08622	DOORN-6	Gorgonopsian		Skull with lower jaw	Graaff-Reinet	Rust 126	Doornplaats			Balfour		Dicynodon	Late	Permian		Stummer	00/04/1998
SAM-PK-K08623	DOORN-7	Gorgonopsian		Skull element	Graaff-Reinet	Rust 126	Doornplaats			Balfour		Dicynodon	Late	Permian		Stummer	00/04/1998
SAM-PK-K08624	DOORN-8	Diictodon	sp.	Skull with lower jaw	Graaff-Reinet	Rust 126	Doornplaats			Balfour		Dicynodon	Late	Permian		Skinner	00/04/1998
SAM-PK-K08625	BLAAU-1	Pelanomodon	sensulato	Partial skull	Graaff-Reinet	Blaauwewater 67	Blaauwewater			Balfour		Dicynodon	Late	Permian		October	00/04/1998
SAM-PK-K08626	BLAAU-2	Dicynodon	sp.	Snout	Graaff-Reinet	Blaauwewater 67	Blaauwewater			Balfour		Dicynodon	Late	Permian		Skinner	00/04/1998
SAM-PK-K08627	TWEE-1	Dicynodon	sp.	Skull with lower jaw	Graaff-Reinet	Tweefontein 68	Tweefontein			Balfour		Dicynodon	Late	Permian		Skinner	00/04/1998
SAM-PK-K10036	DOORN-9	Pareiasaurus	serridens	Skull with lower jaw	Graaff-Reinet	Farm 127	Farm 127			Balfour	Daggaboersnek	Dicynodon	Late	Permian		Smith	00/06/1998
SAM-PK-K10393	F1	Cistecephalus	sp.	Skull	Graaff-Reinet	Rust 126	Doornplaats			Balfour		Cistecephalus	Late	Permian		Myburgh	24/03/2004
SAM-PK-K10394	F2	Procynosuchus	delaharpeae	Skull with lower jaw	Graaff-Reinet	Rust 126	Doornplaats			Balfour		Upper Cistecephalus	Late	Permian		Smith	24/03/2004
SAM-PK-K10395	F3/RS236	Oudenodon	sp.	Skulls and lower jaws	Graaff-Reinet	Rust 126	Doornplaats			Balfour	Oudeberg	Cistecephalus/Dicynodon	Late	Permian		Smith	24/03/2004
SAM-PK-K10396	F4	Diictodon	sp.	Skull with lower jaw	Graaff-Reinet	Rust 126	Doornplaats			Balfour	Oudeberg	Cistecephalus	Late	Permian		Harvey	24/03/2004
SAM-PK-K10397	F5	Cistecephalus	sp.	Skull with lower jaw	Graaff-Reinet	Steilkrans 96	Steilkrans			Balfour	Oudeberg	Cistecephalus	Late	Permian		Van Zyl	25/03/2004
SAM-PK-K10398	F6	Cistecephalus	sp.	Skull	Graaff-Reinet	Steilkrans 96	Steilkrans			Balfour		Cistecephalus	Late	Permian		Smith	25/03/2004
SAM-PK-K10399	F7	Diictodon	sp.	Skull	Graaff-Reinet	Steilkrans 96	Steilkrans			Balfour		Cistecephalus/Dicynodon	Late	Permian		Botha	25/03/2004
SAM-PK-K10400	F8	Cistecephalus	sp.	Skull	Graaff-Reinet	Steilkrans 96	Steilkrans			Balfour		Cistecephalus	Late	Permian		Botha	25/03/2004
SAM-PK-K10401	F9	Oudenodon	sp.	Skull	Graaff-Reinet	Steilkrans 96	Steilkrans			Balfour		Cistecephalus/Dicynodon	Late	Permian		Joachim	25/03/2004
SAM-PK-K10402		Temnospondyl		Lower jaw	Graaff-Reinet	Farm 356	Petersburg			Balfour		Cistecephalus	Late	Permian		Harvey	26/03/2004
SAM-PK-K10494		Daptocephalus	leoniceps	Nearly complete lower jaw	Graaff-Reinet	Rust 126	Doornplaats			Balfour		Cistecephalus/Dicynodon	Late	Permian		Smith	00/04/1998

KATBERG FORMATION

Accession Number	Other Number	Genus	Species	Cranial Elements	District	Gov Farm & Number	Farm Name/Place	Longitude	Formation	Member	Assemblage Zone	Epoch		Period	Collector 1 Surname	Date Collected
SAM-PK-K08002	25/10/2	Lystrosaurus	declivis	Skull with lower jaw	Smithfield	Heldenmoed 677	Heldemoed		Katberg		Lystrosaurus	Early	Triassic		Smith	00/10/1992
SAM-PK-K08004	23/10/1	Thrinaxodon	sp.	Skull with lower jaw	Bethulie	Donald 207	Donald 207		Katberg		Lystrosaurus	Early	Triassic		Smith	00/10/1992
SAM-PK-K08010	25/10/4	Lydekkerinid			Smithfield	Heldenmoed 677	Heldemoed		Katberg		Lystrosaurus	Early	Triassic		Crean	00/00/1992
SAM-PK-K08011	27/10/6	Lystrosaurus	sp.	Skull	Smithfield	Heldenmoed 677	Heldemoed		Katberg		Lystrosaurus	Early	Triassic		Smith	00/10/1992
SAM-PK-K08012	24/10/2	Lystrosaurus	murrayi	Skull with lower jaw	Bethulie	Donald 207	Donald 207		Katberg		Lystrosaurus	Early	Triassic		Crean	00/00/1992
SAM-PK-K08013	30/10/1	Lystrosaurus	declivis	Skull with lower jaw	Smithfield	Heldenmoed 677	Heldemoed		Katberg		Lystrosaurus	Early	Triassic		Crean	00/00/1992
SAM-PK-K08017	26/10/1	Lystrosaurus	murrayi	Skull with lower jaw	Smithfield	Heldenmoed 677	Heldemoed		Katberg		Lystrosaurus	Early	Triassic		Smith	00/10/1992
SAM-PK-K08019	25/10/5	Lystrosaurus	declivis	Skull with lower jaw	Smithfield	Heldenmoed 677	Heldemoed		Katberg		Lystrosaurus	Early	Triassic		Crean	00/00/1992
SAM-PK-K08020	25/10/3	Lystrosaurus	murrayi	Skull with lower jaw	Smithfield	Heldenmoed 677	Heldemoed		Katberg		Lystrosaurus	Early	Triassic		Smith	00/10/1992
SAM-PK-K08021	25/10/6	Lystrosaurus	sp.	Skull with lower jaw	Smithfield	Heldenmoed 677	Heldemoed		Katberg		Lystrosaurus	Early	Triassic		Smith	00/10/1992
SAM-PK-K08038	26/10/1	Lystrosaurus	declivis	Skull with lower jaw	Smithfield	Heldenmoed 677	Heldemoed		Katberg		Lystrosaurus	Early	Triassic		Smith	00/10/1992
SAM-PK-K08518		Thrinaxodon	sp.		Bethulie	Donald 207	Donald 207		Katberg		Lystrosaurus	Early	Triassic		Crean	00/00/1996
SAM-PK-K08519		Lystrosaurus	sp.	Skulls and lower jaw	Bethulie	Donald 207	Donald 207		Katberg		Lystrosaurus	Early	Triassic		Crean	00/00/1996
SAM-PK-K08520		Lystrosaurus	murrayi	Skull with lower jaw	Bethulie	Donald 207	Donald 207		Katberg		Lystrosaurus	Early	Triassic		Crean	00/00/1996
SAM-PK-K08521		Lystrosaurus	sp.	Skull with lower jaw	Bethulie	Donald 207	Donald 207		Katberg		Lystrosaurus	Early	Triassic		October	00/00/1996
SAM-PK-K08522		Lystrosaurus	declivis	Part of skull	Bethulie	Donald 207	Donald 207		Katberg		Lystrosaurus	Early	Triassic		Smith	00/04/1996

SAM-PK-K08523	Lystrosaurus	sp.	Skull with lower jaw	Smithfield	Heldenmoed 677	Heldemoed	Katberg	Lystrosaurus	Early	Triassic	Smith	00/04/1996
SAM-PK-K08524	Lystrosaurus	sp.	Skull with lower jaw	Smithfield	Heldenmoed 677	Heldemoed	Katberg	Lystrosaurus	Early	Triassic	Smith	00/04/1996
SAM-PK-K08525	Lystrosaurus	sp.	Skull with lower jaw	Smithfield	Heldenmoed 677	Heldemoed	Katberg	Lystrosaurus	Early	Triassic	Smith	00/04/1996
SAM-PK-K08526	Lystrosaurus	sp.	Skull with lower jaw	Smithfield	Heldenmoed 677	Heldemoed	Katberg	Lystrosaurus	Early	Triassic	Smith	00/04/1996
SAM-PK-K08527	Lystrosaurus	sp.	Skull with lower jaw	Smithfield	Heldenmoed 677	Heldemoed	Katberg	Lystrosaurus	Early	Triassic	Crean	00/00/1996
SAM-PK-K08528	Thrinaxodon	sp.		Bethulie	Donald 207	Donald 207	Katberg	Lystrosaurus	Early	Triassic	Crean	00/00/1996
SAM-PK-K08548	Lystrosaurus	sp.		Bethulie	Donald 207	Donald 207	Katberg	Lystrosaurus	Early	Triassic	Smith	00/05/1996
SAM-PK-K08549	Galesaurus	planiceps	Skull and hyoid?	Bethulie	Donald 207	Donald 207	Katberg	Lystrosaurus	Early	Triassic	Crean	00/00/1996
SAM-PK-K08550	Micropholis	stowi	Skull with lower jaw	Bethulie	Donald 207	Donald 207	Katberg	Lystrosaurus	Early	Triassic	Crean	00/00/1996
SAM-PK-K08551	Lystrosaurus	declivis	Skulls and lower jaws	Bethulie	Donald 207	Donald 207	Katberg	Lystrosaurus	Early	Triassic	Crean	00/05/1996
SAM-PK-K08566	Lystrosaurus	declivis	Skull with lower jaw	Smithfield	Heldenmoed 677	Heldemoed	Katberg	Lystrosaurus	Early	Triassic	Smith	00/03/1996
SAM-PK-K08567	Lystrosaurus	murrayi	Skull with lower jaw	Bethulie	Donald 207	Donald 207	Katberg	Lystrosaurus	Early	Triassic	Smith	00/03/1996
SAM-PK-K10583	Lystrosaurus	declivis	Skull with lower jaw	Graaff-Reinet	Lucerne 70	Lucerne 70	Katberg	Lystrosaurus	Early	Triassic	Smith	00/11/1999

Supplemental Table 1

Iziko Museum query of vertebrate collections made by S. Kaal, 3 May 2013, preserve the integrity of the fossil record.
after field work around Lootsberg Pass, Eastern Cape Province. Note that GPS coordinates identifying the site from
which each vertebrate was collected are redacted to 'preserve the integrity of the fossil record.
The museum database indicates that specimens given an RS assignment lower than RS74 were collected prior to 1 January 1999.